

Global warming in the pipeline

James E. Hansen^{1*}, Makiko Sato¹, Leon Simons², Larissa S. Nazarenko^{3,4}, Isabelle Sangha¹, Pushker Kharecha¹, James C. Zachos⁵, Karina von Schuckmann⁶, Norman G. Loeb⁷, Matthew B. Osman⁸, Qinjian Jin⁹, George Tselioudis³, Eunbi Jeong¹⁰, Andrew Lacis³, Reto Ruedy^{3,11}, Gary Russell³, Junji Cao¹², Jing Li¹³

¹Climate Science, Awareness and Solutions, Columbia University Earth Institute, New York, NY, USA

²The Club of Rome Netherlands, 's-Hertogenbosch, The Netherlands

³NASA Goddard Institute for Space Studies, New York, NY, USA

⁴Center for Climate Systems Research, Columbia University Earth Institute, New York, NY, USA

⁵Earth and Planetary Science, University of CA, Santa Cruz, CA, USA

⁶Mercator Ocean International, Ramonville St., -Agne, France

⁷NASA Langley Research Center, Hampton, VA, USA

⁸Department of Geosciences, University of AZ, Tucson, AZ, USA

⁹Department of Geography and Atmospheric Science, University of KS, Lawrence, KS, USA

¹⁰CSAS KOREA, Goyang, Gyeonggi-do, South Korea

¹¹Business Integra, Inc, New York, NY, USA

¹²Institute of Atmospheric Physics, Chinese Academy of Sciences, Beijing, China

¹³Department of Atmospheric and Oceanic Sciences, School of Physics, Peking University, Beijing, China

*Correspondence address. Director of Climate Science, Awareness and Solutions, Earth Institute, Columbia University, 475 Riverside Drive, Ste. 401-O, New York, NY 10115, USA. E-mail: jeh1@columbia.edu

Abstract

Improved knowledge of glacial-to-interglacial global temperature change yields Charney (fast-feedback) equilibrium climate sensitivity $1.2 \pm 0.3^\circ\text{C}$ (2σ) per W/m^2 , which is $4.8^\circ\text{C} \pm 1.2^\circ\text{C}$ for doubled CO_2 . Consistent analysis of temperature over the full Cenozoic era—including ‘slow’ feedbacks by ice sheets and trace gases—supports this sensitivity and implies that CO_2 was 300–350 ppm in the Pliocene and about 450 ppm at transition to a nearly ice-free planet, exposing unrealistic lethargy of ice sheet models. Equilibrium global warming for today’s GHG amount is 10°C , which is reduced to 8°C by today’s human-made aerosols. Equilibrium warming is not ‘committed’ warming; rapid phaseout of GHG emissions would prevent most equilibrium warming from occurring. However, decline of aerosol emissions since 2010 should increase the 1970–2010 global warming rate of 0.18°C per decade to a post 2010 rate of at least 0.27°C per decade. Thus, under the present geopolitical approach to GHG emissions, global warming will exceed 1.5°C in the 2020s and 2°C before 2050. Impacts on people and nature will accelerate as global warming increases hydrologic (weather) extremes. The enormity of consequences demands a return to Holocene-level global temperature. Required actions include: (1) a global increasing price on GHG emissions accompanied by development of abundant, affordable, dispatchable clean energy, (2) East-West cooperation in a way that accommodates developing world needs, and (3) intervention with Earth’s radiation imbalance to phase down today’s massive human-made ‘geo-transformation’ of Earth’s climate. Current political crises present an opportunity for reset, especially if young people can grasp their situation.

Keywords: Aerosols; Climate Sensitivity; Paleoclimate; Global Warming; Energy Policy; Cenozoic

Background information and structure of paper

It has been known since the 1800s that infrared-absorbing (greenhouse) gases (GHGs) warm Earth’s surface and that the abundance of GHGs changes naturally as well as from human actions [1, 2].¹ Roger Revelle wrote in 1965 that we are conducting a ‘vast geophysical experiment’ by burning fossil fuels that accumulated in Earth’s crust over hundreds of millions of years [3]. Carbon dioxide (CO_2) in the air is now increasing and already has reached levels that have not existed for millions of years, with consequences that have yet to be determined. Jule Charney led a study in 1979 by the United States National Academy of Sciences that concluded that doubling of atmospheric CO_2 was likely to cause global warming of $3 \pm 1.5^\circ\text{C}$ [4]. Charney added: ‘However, we believe it is quite possible that the capacity of the

intermediate waters of the ocean to absorb heat could delay the estimated warming by several decades.’

After U.S. President Jimmy Carter signed the 1980 Energy Security Act, which included a focus on unconventional fossil fuels such as coal gasification and rock fracturing ('fracking') to extract shale oil and tight gas, the U.S. Congress asked the National Academy of Sciences again to assess potential climate effects. Their massive *Changing Climate* report had a measured tone on energy policy—amounting to a call for research [5]. Was not enough known to caution lawmakers against taxpayer subsidy of the most carbon-intensive fossil fuels? Perhaps the unanimity was due in part to a major error: the report assumed that the delay of global warming caused by the ocean’s thermal inertia is 15 years, independent of climate sensitivity. With that assumption, they concluded that climate sensitivity for $2 \times \text{CO}_2$ is near or below the low end of Charney’s $1.5\text{--}4.5^\circ\text{C}$ range. If climate

Received: December 08, 2022. Revised: August 22, 2023. Accepted: September 15, 2023

© The Author(s) 2023. Published by Oxford University Press.

This is an Open Access article distributed under the terms of the Creative Commons Attribution License (<https://creativecommons.org/licenses/by/4.0/>), which permits unrestricted reuse, distribution, and reproduction in any medium, provided the original work is properly cited.

sensitivity was low and the lag between emissions and climate response was only 15 years, climate change would not be nearly the threat that it is.

Simultaneous with preparation of *Changing Climate*, climate sensitivity was addressed at the 1982 Ewing Symposium at the Lamont Doherty Geophysical Observatory of Columbia University on 25–27 October, with papers published in January 1984 as a monograph of the American Geophysical Union [6]. Paleoclimate data and global climate modeling together led to an inference that climate sensitivity is in the range 2.5–5°C for $2 \times \text{CO}_2$ and that climate response time to a forcing is of the order of a century, not 15 years [7]. Thus, the concept that a large amount of additional human-made warming is already ‘in the pipeline’ was introduced. E.E. David, Jr, President of Exxon Research and Engineering, in his keynote talk at the symposium insightfully noted [8]: ‘The critical problem is that the environmental impacts of the CO_2 buildup may be so long delayed. A look at the theory of feedback systems shows that where there is such a long delay, the system breaks down, unless there is anticipation built into the loop.’

Thus, the danger caused by climate’s delayed response and the need for anticipatory action to alter the course of fossil fuel development was apparent to scientists and the fossil fuel industry 40 years ago.² Yet industry chose to long deny the need to change energy course [9], and now, while governments and financial interests connive, most industry adopts a ‘greenwash’ approach that threatens to lock in perilous consequences for humanity. Scientists will share responsibility if we allow governments to rely on goals for future global GHG levels, as if targets had meaning in the absence of policies required to achieve them.

The Intergovernmental Panel on Climate Change (IPCC) was established in 1988 to provide scientific assessments on the state of knowledge about climate change [10] and almost all nations agreed to the 1992 United Nations Framework Convention on Climate Change [11] with the objective to avert ‘dangerous anthropogenic interference with the climate system’. The current IPCC Working Group 1 report [12] provides a best estimate of 3°C for equilibrium global climate sensitivity to $2 \times \text{CO}_2$ and describes shutdown of the overturning ocean circulations and large sea level rise on the century time scale as ‘high impact, low probability’ even under extreme GHG growth scenarios. This contrasts with ‘high impact, high probability’ assessments reached in a paper [13]—hereafter abbreviated Ice Melt—that several of us published in 2016. Recently, our paper’s first author (JEH) described a long-time effort to understand the effect of ocean mixing and aerosols on observed and projected climate change, which led to a conclusion that most climate models are unrealistically insensitive to freshwater injected by melting ice and that ice sheet models are unrealistically lethargic in the face of rapid, large climate change [14].

Eelco Rohling, editor of Oxford Open Climate Change, invited a perspective article on these issues. Our principal motivation in this paper is concern that IPCC has underestimated climate sensitivity and understated the threat of large sea level rise and shutdown of ocean overturning circulations, but these issues, because of their complexity, must be addressed in two steps. Our present paper addresses climate sensitivity and warming in the pipeline, concluding that these exceed IPCC’s best estimates. Response of ocean circulation and ice sheet dynamics to global warming—already outlined in the Ice Melt paper—will be addressed further in a later paper.

The structure of our present paper is as follows. Climate sensitivity section makes a fresh evaluation of Charney’s equilibrium

climate sensitivity (ECS) based on improved paleoclimate data and introduces Earth system sensitivity (ESS), which includes the feedbacks that Charney held fixed. Climate response time section explores the fast-feedback response time of Earth’s temperature and energy imbalance to an imposed forcing, concluding that cloud feedbacks buffer heat uptake by the ocean, thus increasing the delay in surface warming and making Earth’s energy imbalance an underestimate of the forcing reduction required to stabilize climate. Cenozoic era section analyzes temperature change of the past 66 million years and infers the Cenozoic history of CO_2 , thus providing insights about climate change. Aerosols section addresses the absence of aerosol forcing data via inferences from paleo data and modern global temperature change, and we point out potential information in ‘the great inadvertent aerosol experiment’ provided by recent restrictions on fuels in international shipping. Summary section discusses policy implications of high climate sensitivity and the delayed response of the climate system. Warming in the pipeline need not appear. We can take actions that slow and reverse global warming; indeed, we suggest that such actions are needed to avoid disastrous consequences for humanity and nature. Reduction of greenhouse gas emissions as rapidly as practical has highest priority, but that policy alone is now inadequate and must be complemented by additional actions to affect Earth’s energy balance. The world is still early in this ‘vast geophysical experiment’—as far as consequences are concerned—but time has run short for the ‘anticipation’ that E.E. David recommended.

Climate sensitivity (ECS and ESS)

This section gives a brief overview of the history of ECS estimates since the Charney report and uses glacial-to-interglacial climate change to infer an improved estimate of ECS. We discuss how ECS and the more general Earth system sensitivity (ESS) depend on the climate state.

Charney defined ECS as the eventual global temperature change caused by doubled CO_2 if ice sheets, vegetation and long-lived GHGs are fixed (except the specified CO_2 doubling). Other quantities affecting Earth’s energy balance—clouds, aerosols, water vapor, snow cover and sea ice—change rapidly in response to climate change. Thus, Charney’s ECS is also called the ‘fast-feedback’ climate sensitivity. Feedbacks interact in many ways, so their changes are calculated in global climate models (GCMs) that simulate such interactions. Charney implicitly assumed that change of the ice sheets on Greenland and Antarctica—which we categorize as a ‘slow feedback’—was not important on time scales of most public interest.

ECS defined by Charney is a gedanken concept that helps us study the effect of human-made and natural climate forcings. If knowledge of ECS were based only on models, it would be difficult to narrow the range of estimated climate sensitivity—or have confidence in any range—because we do not know how well feedbacks are modeled or if the models include all significant real-world feedbacks. Cloud and aerosol interactions are complex, e.g. and even small cloud changes can have a large effect. Thus, data on Earth’s paleoclimate history are essential, allowing us to compare different climate states, knowing that all feedbacks operated.

Climate sensitivity estimated at the 1982 Ewing Symposium

Climate sensitivity was addressed in our paper [7] for the Ewing Symposium monograph using the feedback framework implied

by E.E. David and employed by electrical engineers [15]. The climate forcing caused by $2 \times \text{CO}_2$ —the imposed perturbation of Earth's energy balance—is $\sim 4 \text{ W/m}^2$. If there were no climate feedbacks and Earth radiated energy to space as a perfect black surface, Earth's temperature would need to increase $\sim 1.2^\circ\text{C}$ to increase radiation to space 4 W/m^2 and restore energy balance. However, feedbacks occur in the real world and in GCMs. In our GCM the equilibrium response to $2 \times \text{CO}_2$ was 4°C warming of Earth's surface. Thus, the fraction of equilibrium warming due directly to the CO_2 change was 0.3 ($1.2^\circ\text{C}/4^\circ\text{C}$) and the feedback 'gain', g , was 0.7 ($2.8^\circ\text{C}/4^\circ\text{C}$). Algebraically, ECS and feedback gain are related by

$$\text{ECS} = 1.2^\circ\text{C}/(1 - g) \quad (1)$$

We evaluated contributions of individual feedback processes to g by inserting changes of water vapor, clouds, and surface albedo (reflectivity, literally whiteness, due to sea ice and snow changes) from the $2 \times \text{CO}_2$ GCM simulation one-by-one into a one-dimensional radiative-convective model [16], finding $g_{\text{wv}} = 0.4$, $g_{\text{cl}} = 0.2$, $g_{\text{sa}} = 0.1$, where g_{wv} , g_{cl} , and g_{sa} are the water vapor, cloud and surface albedo gains. The 0.2 cloud gain was about equally from a small increase in cloud top height and a small decrease in cloud cover. These feedbacks all seemed reasonable, but how could we verify their magnitudes or the net ECS due to all feedbacks?

We recognized the potential of emerging paleoclimate data. Early data from polar ice cores revealed that atmospheric CO_2 was much less during glacial periods and the CLIMAP project [17] used proxy data to reconstruct global surface conditions during the Last Glacial Maximum (LGM), which peaked about 20 000 years ago. A powerful constraint was the fact that Earth had to be in energy balance averaged over the several millennia of the LGM. However, when we employed CLIMAP boundary conditions including sea surface temperatures (SSTs), Earth was out of energy balance, radiating 2.1 W/m^2 to space, i.e. Earth was trying to cool off with an enormous energy imbalance, equivalent to half of $2 \times \text{CO}_2$ forcing.

Something was wrong with either assumed LGM conditions or our climate model. We tried CLIMAP's maximal land ice—this only reduced the energy imbalance from 2.1 to 1.6 W/m^2 . Moreover, we had taken LGM CO_2 as 200 ppm and did not know that CH_4 and N_2O were less in the LGM than in the present interglacial period; accurate GHGs and CLIMAP SSTs produce a planetary energy imbalance close to 3 W/m^2 . Most feedbacks in our model were set by CLIMAP. Sea ice is set by CLIMAP. Water vapor depends on surface temperature, which is set by CLIMAP SSTs. Cloud feedback is uncertain, but ECS smaller than 2.4°C for $2 \times \text{CO}_2$ would require a negative cloud gain. $g_{\text{cl}} \sim 0.2$ from our GCM increases ECS from 2.4°C to 4°C (Equation 1) and accounts for almost the entire difference of sensitivities of our model (4°C for $2 \times \text{CO}_2$) and the Manabe and Stouffer model [18] (2°C for $2 \times \text{CO}_2$) that had fixed cloud cover and cloud height. Manabe suggested [19] that our higher ECS was due to a too-large sea ice and snow feedback, but we noted [7] that sea ice in our control run was less than observed, so we likely understated sea ice feedback. Amplifying feedback due to high clouds increasing in height with warming is expected and is found in observations, large-eddy simulations and GCMs [20]. Sherwood et al. [21] conclude that negative low-cloud feedback is 'neither credibly suggested by any model, nor by physical principles, nor by observations.' Despite a wide spread among models, GCMs today show an amplifying cloud feedback due to increases in cloud height and decreases in

cloud amount, despite increases in cloud albedo [22]. These cloud changes are found in all observed cloud regimes and locations, implying robust thermodynamic control [23].

CLIMAP SSTs were a more likely cause of the planetary energy imbalance. Co-author D. Peteet used pollen data to infer LGM tropical and subtropical cooling $2\text{--}3^\circ\text{C}$ greater than in a GCM forced by CLIMAP SSTs. D. Rind and Peteet found that montane LGM snowlines in the tropics descended 1 km in the LGM, inconsistent with climate constrained by CLIMAP SSTs. CLIMAP assumed that tiny shelled marine species migrate to stay in a temperature zone they inhabit today. But what if, instead, these species partly adapt over millennia to changing temperature? Based on the work of Rind and Peteet, later published [24], we suspected but could not prove that CLIMAP SSTs were too warm.

Based on GCM simulations for $2 \times \text{CO}_2$, on our feedback analysis for the LGM, and on observed global warming in the past century, we concluded that ECS was in the range $2.5\text{--}5^\circ\text{C}$ for $2 \times \text{CO}_2$. If CLIMAP SSTs were accurate, ECS was near the low end of that range. In contrast, our analysis implied that ECS for $2 \times \text{CO}_2$ was in the upper half of the $2.5\text{--}5^\circ\text{C}$ range, but our analysis depended in part on our GCM, which had sensitivity 4°C for $2 \times \text{CO}_2$. To resolve the matter, a paleo thermometer independent of biologic adaptation was needed. Several decades later, such a paleo thermometer and advanced analysis techniques exist. We will use recent studies to infer our present best estimates for ECS and ESS. First, however, we will comment on other estimates of climate sensitivity and clarify the definition of climate forcings that we employ.

IPCC and independent climate sensitivity estimates

Reviews of climate sensitivity are available, e.g. Rohling et al. [25], which focuses on the physics of the climate system, and Sherwood et al. [26], which adds emphasis on probabilistic combination of multiple uncertainties. Progress in narrowing the uncertainty in climate sensitivity was slow in the first five IPCC assessment reports. The fifth assessment report [26] (AR5) in 2014 concluded only—with 66% probability—that ECS was in the range $1.5\text{--}4.5^\circ\text{C}$, the same as Charney's report 35 years earlier. The broad spectrum of information on climate change—especially constraints imposed by paleoclimate data—at last affected AR6 [12], which concluded with 66% probability that ECS is $2.5\text{--}4^\circ\text{C}$, with 3°C as their best estimate (Supplementary Fig. TS.6).

Sherwood et al. [21] combine three lines of evidence: climate feedback studies, historical climate change, and paleoclimate data, inferring $S = 2.6\text{--}3.9^\circ\text{C}$ with 66% probability for $2 \times \text{CO}_2$, where S is an 'effective sensitivity' relevant to a 150-year time scale. They find ECS only slightly larger: $2.6\text{--}4.1^\circ\text{C}$ with 66% probability. Climate feedback studies, inherently, cannot yield a sharp definition of ECS, as we showed in the cloud feedback discussion above. Earth's climate system includes amplifying feedbacks that push the gain, g , closer to unity than zero, thus making ECS sensitive to uncertainty in any feedback; the resulting sensitivity of ECS to g prohibits precise evaluation from feedback analysis. Similarly, historical climate change cannot define ECS well because the aerosol climate forcing is unmeasured. Also, forced and unforced ocean dynamics give rise to a pattern effect: [27] the geographic pattern of transient and equilibrium temperature changes differ, which affects ECS inferred from transient climate change. These difficulties help explain how Sherwood et al. [21] could estimate ECS as only 6% larger than S , an implausible result in view of the ocean's great thermal inertia. An intercomparison of GCMs run for millennial time scales, LongRunMIP [28],

includes 14 simulations of 9 GCMs with runs of 5000 years (or close enough for extrapolation to 5000 years). Their global warmings at 5000 years range from 30% to 80% larger than their 150-year responses.

Our approach is to compare glacial and interglacial equilibrium climate states. The change of atmospheric and surface forcings can be defined accurately, thus leading to a sharp evaluation of ECS for cases in which equilibrium response is assured. With this knowledge in hand, additional information can be extracted from historical and paleo climate changes.

Climate forcing definitions

Attention to climate forcing definitions is essential for quantitative analysis of climate change. However, readers uninterested in radiative forcings may skip this section with little penalty. We describe our climate forcing definition and compare our forcings with those of IPCC. Our total GHG forcing matches that of IPCC within a few percent, but this close fit hides larger differences in individual forcings that deserve attention.

Equilibrium global surface temperature change is related to ECS by

$$\Delta T_S \sim F \times ECS = F \times \lambda, \quad (2)$$

where λ is a widely used abbreviation of ECS, ΔT_S is the global mean equilibrium surface temperature change in response to climate forcing F , which is measured in W/m^2 averaged over the entire planetary surface. There are alternative ways to define F , as discussed in Chapter 8 [29] of AR5 and in a paper [30] hereafter called *Efficacy*. Objectives are to find a definition of F such that different forcing mechanisms of the same magnitude yield a similar global temperature change, but also a definition that can be computed easily and reliably. The first four IPCC reports used adjusted forcing, F_a , which is Earth's energy imbalance after stratospheric temperature adjusts to presence of the forcing agent. F_a usually yields a consistent response among different forcing agents, but there are exceptions such as black carbon aerosols; F_a exaggerates their impact. Also, F_a is awkward to compute and depends on definition of the tropopause, which varies among models. F_s , the fixed SST forcing (including fixed sea ice), is more robust than F_a as a predictor of climate response [30, 31], but a GCM is required to compute F_s . In *Efficacy*, F_s is defined as

$$F_s = F_o + \frac{\delta T_o}{\lambda}, \quad (3)$$

where F_o is Earth's energy imbalance after atmosphere and land surface adjust to the presence of the forcing agent with SST fixed. F_o is not a full measure of the strength of a forcing, because a portion (δT_o) of the equilibrium warming is already present as F_o is computed. A GCM run of about 100 years is needed to accurately define F_o because of unforced atmospheric variability. That GCM run also defines δT_o , the global mean surface air temperature change caused by the forcing with SST fixed. λ is the model's ECS in $^{\circ}C$ per W/m^2 . $\delta T_o/\lambda$ is the portion of the total forcing (F_s) that is 'used up' in causing the δT_o warming; radiative flux to space increases by $\delta T_o/\lambda$ due to warming of the land surface and global air. The term $\delta T_o/\lambda$ is usually, but not always, less than 10% of F_o . Thus, it is better not to neglect $\delta T_o/\lambda$. IPCC AR5 and AR6 define effective radiative forcing as $ERF = F_o$. Omission of $\delta T_o/\lambda$ was intentional [29] and is not an issue if the practice is followed consistently. However, when the forcing is used to calculate global surface temperature response, the forcing to use is

F_s , not F_o . It would be useful if both F_o and δT_o were reported for all climate models.

A further refinement of climate forcing is suggested in *Efficacy*: effective forcing (F_e) defined by a long GCM run with calculated ocean temperature. The resulting global surface temperature change, relative to that for equal CO_2 forcing, defines the forcing's efficacy. Effective forcings, F_e , were found to be within a few percent of F_s for most forcing agents, i.e. the results confirm that F_s is a robust forcing. This support is for F_s , not for $F_o = ERF$, which is systematically smaller than F_s . The Goddard Institute for Space Studies (GISS) GCM [32, 33] used for CMIP6 [34] studies, which we label the GISS (2020) model,³ has higher resolution ($2^{\circ} \times 2.5^{\circ}$ and 40 atmospheric layers) and other changes that yield a moister upper troposphere and lower stratosphere, relative to the GISS model used in *Efficacy*. GHG forcings reported for the GISS (2020) model [32, 33] are smaller than in prior GISS models, a change attributed [33] to blanketing by high level water vapor. However, part of the change is from comparison of F_o in GISS (2020) to F_s in earlier models. The $2 \times CO_2$ fixed SST simulation with the GISS (2020) model yields $F_o = 3.59 W/m^2$, $\delta T_o = 0.27^{\circ}C$ and $\lambda = 0.9^{\circ}C$ per W/m^2 . Thus $F_s = 3.59 + 0.30 = 3.89 W/m^2$, which is only 5.4% smaller than the $F_s = 4.11 W/m^2$ for the GISS model used in *Efficacy*.

Our GHG effective forcing, F_e , was obtained in two steps. Adjusted forcings, F_a , were calculated for each gas for a large range of gas amount with a global-mean radiative-convective model that incorporated the GISS GCM radiation code, which uses the correlated k-distribution method [35] and high spectral resolution laboratory data [36]. The F_a are converted to effective forcings (F_e) via efficacy factors (E_a ; [Table 1](#) of *Efficacy*) based on GCM simulations that include the 3-D distribution of each gas. The total GHG forcing is

$$F_e = F_a(CO_2) + 1.45F_a(CH_4) + 1.04F_a(N_2O) + 1.32F_a(MPTGs+OTGs) + 0.45F_a(O_3) \quad (4)$$

The CH_4 coefficient (1.45) includes the effect of CH_4 on O_3 and stratospheric H_2O , as well as the efficacy (1.10) of CH_4 *per se*. We assume that CH_4 is responsible for 45% of the O_3 change [37]. Forcing caused by the remaining 55% of the O_3 change is based on IPCC AR6 O_3 forcing ($F_a = 0.47 W/m^2$ in 2019); we multiply this AR6 O_3 forcing by $0.55 \times 0.82 = 0.45$, where 0.82 is the efficacy of O_3 forcing from [Table 1](#) of *Efficacy*. Thus, the non- CH_4 portion of the O_3 forcing is $0.21 W/m^2$ in 2019. MPTGs and OTGs are Montreal Protocol Trace Gases and Other Trace Gases [38]. A list of these gases and a table of annual forcings since 1992 are [available](#) as well as the [earlier data](#) [39].

The climate forcing from our formulae is slightly larger than IPCC AR6 forcings ([Fig. 1](#)). In 2019, the final year of AR6 data, our GHG forcing is $4.00 W/m^2$; the AR6 forcing is $3.84 W/m^2$. Our forcing should be larger, because IPCC forcings are F_o for all gases except O_3 , for which they provide F_a (AR6 section 7.3.2.5). [Table 1](#) in

Table 1. Greenhouse gas radiative forcings

Gas	Radiative Forcing
CO_2	$F = f(c) - f(c_o)$, where $f(c) = 4.996 \ln(c + 0.0005c^2)$
CH_4	$F = 0.0406(\sqrt{m} - \sqrt{m_o}) - [g(m, n_o) - g(m_o, n_o)]$
N_2O	$F = 0.136(\sqrt{n} - \sqrt{n_o}) - [g(m_o, n) - g(m_o, n_o)]$ where $g(m, n) = 0.5 \ln[1 + 2 \times 10^{-5}(mn)^{0.75}]$
CFC-11	$F = 0.264(x - x_o)$
CFC-12	$F = 0.323(y - y_o)$

c, CO_2 (ppm); m, CH_4 (ppb); n, N_2O (ppb); x/y, CFC-11/12 (ppb).

Efficacy allows accurate comparison: δT_o for $2 \times CO_2$ for the GISS model used in Efficacy is $0.22^\circ C$, λ is $0.67^\circ C$ per W/m^2 , so $\delta T_o/\lambda = 0.33 W/m^2$. Thus, the conversion factor from F_o to F_e (or F_s) is $4.11/(4.11-0.33)$. The non- O_3 portion of AR6 2019 forcing ($3.84-0.47 = 3.37$) W/m^2 increases to $3.664 W/m^2$. The O_3 portion of the AR6 2019 forcing ($0.47 W/m^2$) decreases to $0.385 W/m^2$ because the efficacy of $F_a(O_3)$ is 0.82. The AR6 GHG forcing in 2019 is thus $\sim 4.05 W/m^2$, expressed as $F_e \sim F_s$, which is $\sim 1\%$ larger than follows from our formulae. This precise agreement is not indicative of the true uncertainty in the GHG forcing, which IPCC AR6 estimates as 10%, thus about $0.4 W/m^2$. We concur with their error estimate and employ it in our ECS uncertainty analysis (Equilibrium climate sensitivity section).

We conclude that the GHG increase since 1750 already produces a climate forcing equivalent to that of $2 \times CO_2$ (our formulae yield $F_e \sim F_s = 4.08 W/m^2$ for 2021 and $4.13 W/m^2$ for 2022; IPCC AR6 has $F_s = 4.14 W/m^2$ for 2021). The human-made $2 \times CO_2$ climate forcing imagined by Charney, Tyndall and other greenhouse giants is no longer imaginary. Humanity is now taking its first steps into the period of consequences. Earth's paleoclimate history helps us assess the potential outcomes.

Glacial-to-interglacial climate oscillations

In this section we describe how ice core data help us assess ECS for climate states from glacial conditions to interglacial periods such as the Holocene, the interglacial period of the past 12 000 years. We discuss climate sensitivity in warmer climates in Genozoic era section.

Air bubbles in Antarctic ice cores—trapped as snow piled up and compressed into ice—preserve a record of long-lived GHGs for at least 800 000 years. Isotopic composition of the ice provides a measure of temperature in and near Antarctica [40]. Changes of temperature and CO_2 are highly correlated (Fig. 2). This does

not mean that CO_2 is the primal cause of the climate oscillations. Hays et al. [42] showed that small changes of Earth's orbit and the tilt of Earth's spin axis are pacemakers of the ice ages. Orbital changes alter the seasonal and geographical distribution of insolation, which affects ice sheet size and GHG amount. Long-term climate is sensitive because ice sheets and GHGs act as amplifying feedbacks: [43] as Earth warms, ice sheets shrink, expose a darker surface, and absorb more sunlight; also, as Earth warms, the ocean and continents release GHGs to the air. These amplifying feedbacks work in the opposite sense as Earth cools. Orbital forcings oscillate slowly over tens and hundreds of thousands of years [44]. The picture of how Earth orbital changes drive millennial climate change was painted in the 1920s by Milutin Milankovitch, who built on 19th century hypotheses of James Croll and Joseph Adhémar. Paleoclimate changes of ice sheets and GHGs are sometimes described as slow feedbacks [45], but their slow change is paced by the Earth orbital forcing; their slow change does not mean that these feedbacks cannot operate more rapidly in response to a rapid climate forcing.

We evaluate ECS by comparing stable climate states before and after a glacial-to-interglacial climate transition. GHG amounts are known from ice cores and ice sheet sizes are known from geologic data. This empirical ECS applies to the range of global temperature covered by ice cores, which we will conclude is about $-7^\circ C$ to $+1^\circ C$ relative to the Holocene. The Holocene is an unusual interglacial. Maximum melt rate was at 13.2 kyBP, as expected [45] and GHG amounts began to decline after peaking early in the Holocene, as in most interglacials. However, several ky later, CO_2 and CH_4 increased, raising a question of whether humans were affecting GHGs. Ruddiman [46] suggests that deforestation began to affect CO_2 6500 years ago and rice irrigation began to affect CH_4 5000 years ago. Those possibilities complicate use of LGM-Holocene warming to estimate ECS. However, sea level, and thus the size of the ice sheets, had stabilized by 7000 years ago (Evidence of aerosol forcing in the Holocene section). Thus, the millennium centered on 7 kyBP provides a good period to compare with the LGM. Comparison of the Eemian interglacial (Fig. 2) with the prior glacial maximum (PGM) has potential for independent assessment.

LGM-Holocene and PGM-Eemian evaluation of ECS

In this section we evaluate ECS by comparing neighboring glacial and interglacial periods when Earth was in energy balance within less than $0.1 W/m^2$ averaged over a millennium. Larger imbalance would cause temperature or sea level change that did not occur [48].⁴ Thus, we can assess ECS from knowledge of atmospheric and surface forcings that maintained these climates.

Recent advanced analysis techniques allow improved estimate of paleo temperatures. Tierney et al. [49] exclude microbiology fossils whose potential to adapt makes them dubious thermometers. Instead, they use a large collection of geochemical (isotope)

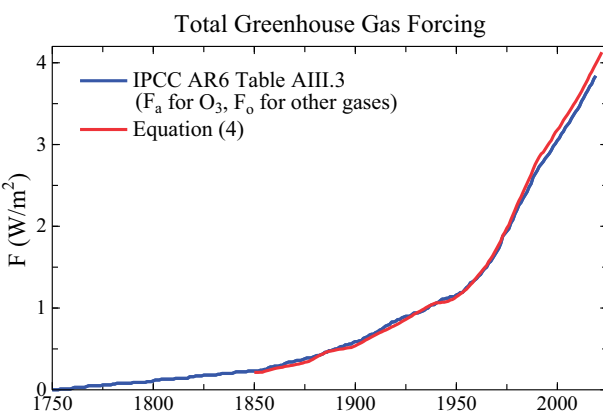


Figure 1. IPCC AR6 Annex III greenhouse gas forcing [12], which employs F_a for O_3 and F_o for other GHGs, compared with the effective forcing, F_e , from Equation (4). See discussion in text.

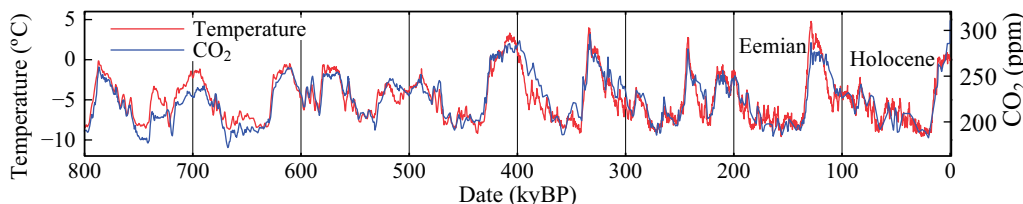


Figure 2. Antarctic Dome C temperature for past 800 ky from Jouzel et al. [40] relative to the mean of the last 10 ky and Dome C CO_2 amount from Lüthi et al. [41] (kyBP is kiloyears before present).

proxies for SST in an analysis constrained by climate change patterns defined by GCMs. They find cooling of 6.1°C (95% confidence:

$5.7\text{--}6.5^{\circ}\text{C}$) for the interval 23–19 kyBP. A similarly constrained global analysis by Osman et al. [50] finds LGM cooling at 21–18 kyBP of $7.0 \pm 1^{\circ}\text{C}$ (95% confidence). Tierney (priv. comm.) attributes the difference between the two studies to the broader time interval of the former study, and concludes that peak LGM cooling was near 7°C .

Seltzer et al. [51] use the temperature-dependent solubility of dissolved noble gases in ancient groundwater to show that land areas between 45°S and 35°N cooled $5.8 \pm 0.6^{\circ}\text{C}$ in the LGM. This cooling is consistent with 1 km lowering of alpine snowlines found by Rind and Peteet [24]. Land response to a forcing exceeds ocean response, but polar amplification makes the global response as large as the low latitude land response in GCM simulations with fixed ice sheets (Supplementary Material Fig. S3). When ice sheet growth is added, cooling amplification at mid and high latitudes is greater [7], making 5.8°C cooling of low latitude land consistent with global cooling of $\sim 7^{\circ}\text{C}$.

LGM CO_2 , CH_4 and N_2O amounts are known accurately with the exception of N_2O in the PGM when N_2O reactions with dust in the ice core corrupt the data. We take PGM N_2O as the mean of the smallest reported PGM amount and the LGM amount; potential error in the N_2O forcing is $\sim 0.01 \text{ W/m}^2$. We calculate CO_2 , CH_4 , and N_2O forcings using Equation (4) and formulae for each gas in Supplementary Material for the periods shown by green bars in Fig. 3. The Eemian period avoids early CO_2 and temperature spikes, assuring that Earth was in energy balance. Between the LGM (19–21 kyBP) and Holocene (6.5–7.5 kyBP), GHG forcing increased 2.25 W/m^2 with 77% from CO_2 . Between the PGM and Eemian, GHG forcing increased 2.30 W/m^2 with 79% from CO_2 .

Glacial-interglacial aerosol changes are not included as a forcing. Natural aerosol changes, like clouds, are fast feedbacks. Indeed, aerosols and clouds form a continuum and distinction is arbitrary as humidity approaches 100%. There are many aerosol types, including VOCs (volatile organic compounds) produced by trees, sea salt produced by wind and waves, black and organic carbon produced by forest and grass fires, dust produced by wind and drought, and marine biologic dimethyl sulfide and its secondary aerosol products, all varying geographically and in response to climate change. We do not know, or need to know, natural aerosol properties in prior eras because their changes are feedbacks included in the climate response. However, human-made aerosols are a climate forcing (an imposed perturbation of Earth's energy balance). Humans may have begun to affect gases and aerosols in the latter Holocene (Aerosols section), but we minimize that issue by using the 6.5–7.5 kyBP window to evaluate climate sensitivity.

Earth's surface change is the other forcing needed to evaluate ECS: (1) change of surface albedo (reflectivity) and topography by

ice sheets, (2) vegetation change, e.g. boreal forests replaced by brighter tundra, and (3) continental shelves exposed by lower sea level. Forcing by all three can be evaluated at once with a GCM. Accuracy requires realistic clouds, which shield the surface. Clouds are the most uncertain feedback [52]. Evaluation is ideal for CMIP [53] (Coupled Model Intercomparison Project) collaboration with PMIP [54] (Paleoclimate Modelling Intercomparison Project); a study of LGM surface forcing could aid GCM development and assessment of climate sensitivity. Sherwood et al. [21] review studies of LGM ice sheet forcing and settle on $3.2 \pm 0.7 \text{ W/m}^2$, the same as IPCC AR4 [55]. However, some GCMs yield efficacies as low as ~ 0.75 [56] or even ~ 0.5 [57], likely due to cloud shielding. We found [7] a forcing of -0.9 W/m^2 for LGM vegetation by using the Koppen [58] scheme to relate vegetation to local climate, but we thought the model effect was exaggerated as real-world forests tends to shake off snow albedo effects. Kohler et al. [59] estimate a continental shelf forcing of -0.67 W/m^2 . Based on an earlier study [60] (hereafter Target CO_2), our estimate of LGM-Holocene surface forcing is $3.5 \pm 1 \text{ W/m}^2$. Thus, LGM (18–21 kyBP) cooling of 7°C relative to mid-Holocene (7 kyBP), GHG forcing of 2.25 W/m^2 , and surface forcing of 3.5 W/m^2 yield an initial ECS estimate $7/(2.25 + 3.5) = 1.22^{\circ}\text{C}$ per W/m^2 . We discuss uncertainties in Equilibrium climate sensitivity section.

PGM-Eemian global warming provides a second assessment of ECS, one that avoids concern about human influence. PGM-Eemian GHG forcing is 2.3 W/m^2 . We estimate surface albedo forcing as 0.3 W/m^2 less than in the LGM because sea level was about 10 m higher during the PGM [61]. North American and Eurasian ice sheet sizes differed between the LGM and PGM [62], but division of mass between them has little effect on the net forcing (Supplementary Fig. S4 [60]). Thus, our central estimate of PGM-Eemian forcing is 5.5 W/m^2 . Eemian temperature reached about $+1^{\circ}\text{C}$ warmer than the Holocene [63], based on Eemian SSTs of $+0.5 \pm 0.3^{\circ}\text{C}$ relative to 1870–1889 [64], or $+0.65 \pm 0.3^{\circ}\text{C}$ SST and $+1^{\circ}\text{C}$ global (land plus ocean) relative to 1880–1920. However, the PGM was probably warmer than the LGM; it was warmer at Dome C (Fig. 2), but cooler at Dronning Maud Land [65]. Based on deep ocean temperatures (Cenozoic Era section), we estimate PGM-Eemian warming as 0.5°C greater than LGM-Holocene warming, that is 7.5°C . The resulting ECS is $7.5/5.5 = 1.36^{\circ}\text{C}$ per W/m^2 . Although PGM temperature lacks quantification comparable to that of Seltzer et al. [51] and Tierney et al. [49] for the LGM, the PGM-Eemian warming provides support for the high ECS inferred from LGM-Holocene warming.

We conclude that ECS for climate in the Holocene-LGM range is $1.2^{\circ}\text{C} \pm 0.3^{\circ}\text{C}$ per W/m^2 , where the uncertainty is the 95% confidence range. The uncertainty estimate is inherently subjective, as it depends mainly on the ice age surface albedo forcing. The GHG forcing and glacial-interglacial temperature change are well-defined, but the efficacy of ice age surface forcing varies among GCMs. This variability is likely related to cloud shielding

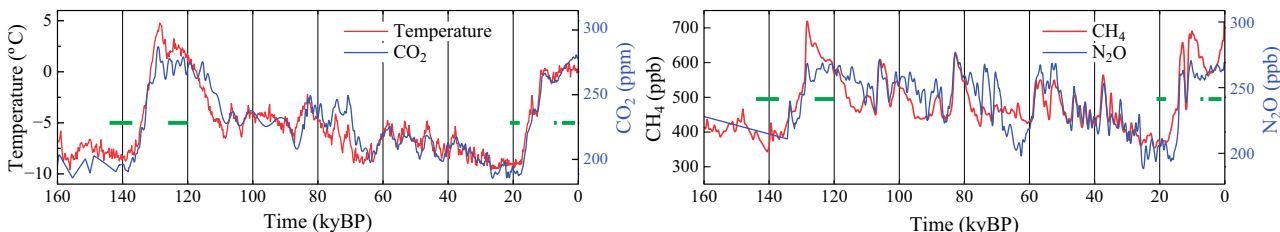


Figure 3. Dome C temperature (Jouzel et al. [40]) and multi-ice core GHG amounts (Schilt et al. [47]). Green bars (1–5, 6.5–7.5, 18–21, 120–126, 137–144 kyBP) are periods of calculations.

of surface albedo, which reaffirms the need for a focus on precise cloud observations and modeling.

State dependence of climate sensitivity

ECS based on glacial-interglacial climate is an average for global temperatures -7°C to $+1^{\circ}\text{C}$ relative to the Holocene and in general differs for other climate states because water vapor, aerosol-cloud and sea ice feedbacks depend on the initial climate. However, ECS is rather flat between today's climate and warmer climate, based on a study [66] covering a range of 15 CO₂ doublings using an efficient GCM developed by Gary Russell [67]. Toward colder climate, ice-snow albedo feedback increases nonlinearly, reaching snowball Earth conditions—with snow and ice on land reaching sea level in the tropics—when CO₂ declines to a quarter to an eighth of its 1950 abundance (Fig. 7 of the study) [66]. Snowball Earth occurred several times in Earth's history, most recently about 600 million years ago [68] when the Sun was 6% dimmer [69] than today, a forcing of about -12 W/m^2 . Toward warmer climate, the water vapor feedback increases as the tropopause rises [70], the tropopause cold trap disappearing at $32 \times \text{CO}_2$ (Fig. 7) [66]. However, for the range of ECS of practical interest—say from half preindustrial CO₂ to $4 \times \text{CO}_2$ —state dependence of ECS is small compared to state dependence of ESS.

Earth system sensitivity (ESS) includes amplifying feedbacks of GHGs and ice sheets [71]. When we consider CO₂ change as a known forcing, other GHGs provide a feedback that is smaller than the ice sheet feedback, but not negligible. Ice core data on GHG amounts show that non-CO₂ GHGs—including O₃ and stratospheric H₂O produced by changing CH₄—provide about 20% of the total GHG forcing, not only on average for the full glacial-interglacial change, but as a function of global temperature right up to $+1^{\circ}\text{C}$ global temperature relative to the Holocene (Supplementary Fig. S5). Atmospheric chemistry modeling suggests that non-CO₂ GHG amplification of CO₂ forcing by about a quarter continues into warmer climate states [72]. Thus, for climate change in the Cenozoic era, we approximate non-CO₂ GHG forcing by increasing the CO₂ forcing by one-quarter.

Ice sheet feedback, in contrast to non-CO₂ GHG feedback, is highly nonlinear. Preindustrial climate was at most a few halvings of CO₂ from runaway snowball Earth and LGM climate was even closer to that climate state. The ice sheet feedback is reduced as Earth heads toward warmer climate today because already two-thirds of LGM ice has been lost. Yet remaining ice on Antarctica and Greenland constitutes a powerful feedback, which humanity is about to bring into play. We can illuminate that feedback and the climate path Earth is now on by examining data on the Cenozoic era—which includes CO₂ levels comparable to today's amount—but first we must consider climate response time.

Climate response time

In this section we define response functions for global temperature and Earth's energy imbalance that help reveal the physics of climate change. Cloud feedbacks amplify climate sensitivity and thus increase eventual heat uptake by the ocean, but cloud feedbacks also have the potential to buffer the rate at which the ocean takes up heat, thus increasing climate response time.

Climate response time was surprisingly long in our climate simulations [7] for the 1982 Ewing Symposium. The e-folding time—the time for surface temperature to reach 63% of its equilibrium response—was about a century. The only published atmosphere-ocean GCM—that of Bryan and Manabe [73]—had a

response time of 25 years, while several simplified climate models referenced in our Ewing paper had even faster responses. The longer response time of our climate model was largely a result of high climate sensitivity—our model had an ECS of 4°C for $2 \times \text{CO}_2$ while the Bryan and Manabe model had an ECS of 2°C .

The physics is straightforward. If the delay were a result of a fixed source of thermal inertia, say the ocean's well-mixed upper layer, response time would increase linearly with ECS because most climate feedbacks come into play in response to temperature change driven by the adjusted forcing, not in direct response to the forcing. Thus, a model with ECS of 4°C takes twice as long to reach full response as a model with ECS of 2°C , if the mixed layer provides the only heat capacity. However, while the mixed layer is warming, there is exchange of water with the deeper ocean, which slows the mixed layer warming. The longer response time with high ECS allows more of the ocean to come into play. If mixing into the deeper ocean is approximated as diffusive, surface temperature response time is proportional to the square of climate sensitivity [74].

Slow climate response accentuates need for the ‘anticipation’ that E.E. David, Jr spoke about. If ECS is 4.8°C (1.2°C per W/m^2), more warming is in the pipeline than widely assumed. GHG forcing today already exceeds 4 W/m^2 . Aerosols reduce the net forcing to about 3 W/m^2 , based on IPCC estimates (Aerosols section), but warming still in the pipeline for 3 W/m^2 forcing is 2.4°C , exceeding warming realized to date (1.2°C). Slow feedbacks increase the equilibrium response even further (Summary section). Large warmings can be avoided via a reasoned policy response, but definition of effective policies will be aided by an understanding of climate response time.

Temperature response function

In the Bjerknes lecture [75] at the 2008 American Geophysical Union meeting, JEH argued that the ocean in many⁵ GCMs had excessive mixing, and he suggested that GCM groups all report the response function of their models—the global temperature change versus time in response to instant CO₂ doubling with the model run long enough to approach equilibrium. The response function characterizes a climate model and enables a rapid estimate of the global mean surface temperature change in response to any climate forcing scenario:

$$T_G(t) = \int [dT_G(t)/dt] dt = \int \lambda \times R(t) [dF_e/dt] dt. \quad (5)$$

T_G is the Green's function estimate of global temperature at time t, λ ($^{\circ}\text{C}$ per W/m^2) the model's equilibrium sensitivity, R the dimensionless temperature response function (% of equilibrium response), and dF_e the forcing change per unit time, dt. Integration over time begins when Earth is in near energy balance, e.g. in pre-industrial time. The response function yields an accurate estimate of global temperature change for a forcing that does not cause reorganization of ocean circulation. Accuracy of this approximation for temperature for one climate model is shown in Chart 15 in the Bjerknes presentation and wider applicability has been demonstrated [76].

We study ocean mixing effects by comparing two GCMs: GISS (2014) [77] and GISS (2020) [33], both models⁶ described by Kelley et al. [32]. Ocean mixing is improved in GISS (2020) by use of a high-order advection scheme [78], finer upper-ocean vertical resolution (40 layers), updated mesoscale eddy parameterization, and correction of errors in the ocean modeling code [32]. The GISS (2020) model has improved variability, including the

Madden-Julian Oscillation (MJO), El Niño Southern Oscillation (ENSO) and Pacific Decadal Oscillation (PDO), but the spectrum of ENSO-like variability is unrealistic and its amplitude is excessive, as shown by the magnitude of oscillations in Fig. 4a. Ocean mixing in GISS (2020) may still be excessive in the North Atlantic, where the model's simulated penetration of CFCs is greater than observed [79].

Despite reduced ocean mixing, the GISS (2020) model surface temperature response is no faster than in the GISS (2014) model (Fig. 4b): it takes 100 years to reach within 1/e of the equilibrium response. Slow response is partly explained by the larger ECS of the GISS (2020) model, which is 3.5°C versus 2.7°C for the GISS (2014) model, but something more is going on in the newer model, as exposed by the response function of Earth's energy imbalance.

Earth's energy imbalance (EEI)

When a forcing perturbs Earth's energy balance, the imbalance drives warming or cooling to restore balance. Observed EEI is now of order +1 W/m² (more energy coming in than going out) [80]. High accuracy of EEI is obtained by tracking ocean warming—the main repository for excess energy—and adding heat

stored in warming continents and heat used in net ice melt [80]. Heat storage in air adds a small amount. Radiation balance measured from Earth-orbiting satellites cannot by itself define the absolute imbalance, but, when anchored to an in situ EEI value for a sufficient interval (e.g. 10 years), satellite Earth radiation budget observations [81] provide invaluable EEI data on finer temporal and spatial scales than the in situ data.

After a step-function forcing is imposed, EEI and global surface temperature must each approach a new equilibrium, but EEI does so more rapidly, especially for the GISS (2020) model (Fig. 5). EEI in GISS (2020) needs only a decade to reach within 1/e of full response (Fig. 5b), but global surface temperature requires a century (Fig. 4b). Rapid decline of EEI—to half the forcing in 5 years (Fig. 5a)—has practical implications. First, EEI defines the rate heat is pumped into the ocean, so if EEI is reduced, ocean warming is slowed. Second, rapid EEI decline implies that it is wrong to assume that global warming can be stopped by a reduction of climate forcing by the amount of EEI. Instead, the required reduction of forcing is larger than EEI. The difficulty in finding additional reduction in climate forcing of even a few tenths of a W/m² is substantial [63]. Calculations that help quantify this matter are discussed in Supplementary Material section SM8.

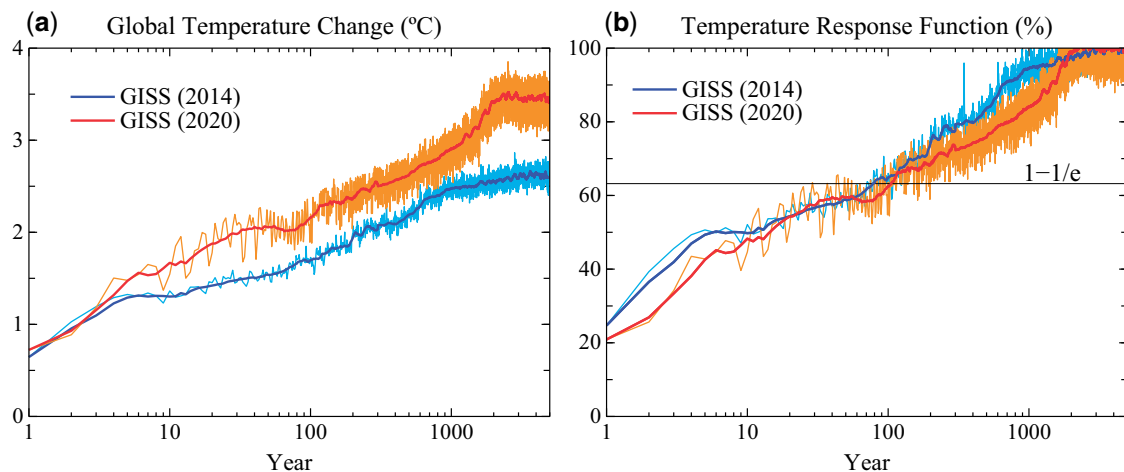


Figure 4. (a) Global mean surface temperature response to instant CO₂ doubling and (b) normalized response function (percent of final change). Thick lines in Figs 4 and 5 are smoothed (yr1 no smoothing; yr2 3-yr mean; yr3–12 5-yr mean; yr13–300 25-yr mean; yr301–5000 101-yr mean).

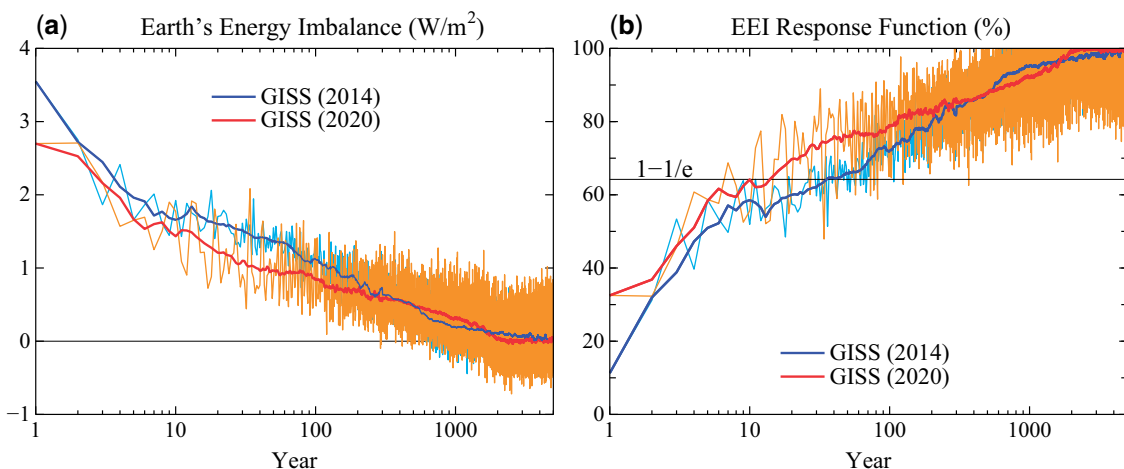


Figure 5. (a) Earth's energy imbalance (EEI) for 2 × CO₂, and (b) EEI normalized response function.

What is the physics behind the fast response of EEI? The $2 \times \text{CO}_2$ forcing and initial EEI are both nominally 4 W/m^2 . In the GISS (2014) model, the decline of EEI averaged over the first year is 0.5 W/m^2 (Fig. 5a), a moderate decline that might be largely caused by warming continents and thus increased heat radiation to space. In contrast, EEI declines 1.3 W/m^2 in the GISS (2020) model (Fig. 5a). Such a huge, immediate decline of EEI implies existence of an ultrafast climate feedback. Climate feedbacks are the heart of climate change and warrant discussion.

Slow, fast and ultrafast feedbacks

Charney et al. [4] described climate feedbacks without discussing time scales. At the 1982 Ewing Symposium, water vapor, clouds and sea ice were described as ‘fast’ feedbacks [7] presumed to change promptly in response to global temperature change, as opposed to ‘slow’ feedbacks or specified boundary conditions such as ice sheet size, vegetation cover, and atmospheric CO_2 amount, although it was noted that some specified boundary conditions, e.g. vegetation, in reality may be capable of relatively rapid change [7].

The immediate EEI response (Fig. 5a) implies a third feedback time scale: ultrafast. Ultrafast feedbacks are not a new concept. When CO_2 is doubled, the added infrared opacity causes the stratosphere to cool. Instant EEI upon CO_2 doubling is only $F_i = +2.5 \text{ W/m}^2$, but stratospheric cooling quickly increases EEI to $+4 \text{ W/m}^2$ [82]. All models calculate a similar radiative effect, so it is useful to define an adjusted forcing, F_a , which is superior to F_i as a measure of climate forcing. In contrast, if cloud change—the likely cause of the present ultrafast change—is lumped into the adjusted forcing, each climate model has its own forcing, losing the merit of a common forcing.

Kamae et al. [83] review rapid cloud adjustment distinct from surface temperature-mediated change. Clouds respond to radiative forcing, e.g. via effects on cloud particle phase, cloud cover, cloud albedo and precipitation [84]. The GISS (2020) model alters glaciation in stratiform mixed-phase clouds, which increases supercooled water in stratus clouds, especially over the Southern Ocean [Fig. 1 in the GCM description [32]]. The portion of supercooled cloud water drops goes from too little in GISS (2014) to too much in GISS (2020). Neither model simulates well stratocumulus clouds, yet the models help expose real-world physics that affects climate sensitivity and climate response time. Several models in CMIP6 comparisons find high ECS [84]. For the sake of revealing the physics, it would be useful if the models defined their temperature and EEI response functions. Model runs of even a decade can define the important part of Figs 4a and 5a. Many short (e.g. 2-year) $2 \times \text{CO}_2$ climate simulations with each run beginning at a different point in the model’s control run, can define cloud changes to an arbitrary accuracy.

Cenozoic era

In this section, we use ocean sediment core data to explore climate change in the past 66 million years. This allows us to study warmer climates that are relevant to human-made climate forcing.

High equilibrium climate sensitivity that we have inferred, $\text{ECS} = 1.2^\circ\text{C} \pm 0.3^\circ\text{C}$ per W/m^2 , may affect interpretation of warmer climates. GCMs have difficulty in producing Pliocene warmth [85], especially in the Arctic, without large—probably unrealistic— CO_2 amounts. In addition, a coupled GCM/ice sheet model needs 700–840 ppm CO_2 for transition between glaciated and unglaciated Antarctica [86]. Understanding of these climate

states is hampered by uncertainty in the forcings that maintained the climate, as proxy measures of CO_2 have large uncertainty.

Theory informs us that CO_2 is the principal control knob on global temperature [87]. Climate of the past 800 000 years demonstrates (Fig. 2) the tight control. Our aim here is to extract Cenozoic surface temperature history from the deep ocean oxygen isotope $\delta^{18}\text{O}$ and infer Cenozoic CO_2 history. Oxygen isotope data has high temporal resolution for the entire Cenozoic, which aids understanding of Cenozoic climate change and resulting implications for future climate. Our CO_2 analysis is a complement to proxy CO_2 measurements. Despite progress in estimating CO_2 via carbon isotopes in alkenones and boron isotopes in planktic foraminifera [88], there is wide scatter among results and fossil plant stomata suggest smaller CO_2 amounts [89].

Deep ocean temperature and sea level from $\delta^{18}\text{O}$

Glacial-interglacial CO_2 oscillations (Fig. 2) involve exchange of carbon among surface carbon reservoirs: the ocean, atmosphere, soil and biosphere. Total CO_2 in the reservoirs also can vary, mainly on longer time scales, as carbon is exchanged with the solid Earth. CO_2 then becomes a primary agent of long-term climate change, leaving orbital effects as ‘noise’ on larger climate swings. Oxygen isotopic composition of benthic (deep ocean dwelling) foraminifera shells provides a starting point for analysis of Cenozoic temperature. Figure 6 includes the recent high-resolution record of Westerhold et al. [90] and data of Zachos et al. [44] that have been used for many studies in the past quarter century. When Earth has negligible ice sheets, $\delta^{18}\text{O}$ (^{18}O amount relative to a standard), provides an estimate of deep ocean temperature (right scale in Fig. 6) [44].

$$T_{\text{do}}(\text{°C}) = -4 \delta^{18}\text{O} + 12. \quad (6)$$

This equation is used for the early Cenozoic, up to the large-scale glaciation of Antarctica at ~ 34 MyBP (O1-in Fig. 6). At larger $\delta^{18}\text{O}$ (colder climate), lighter ^{16}O evaporates preferentially from the ocean and accumulates in ice sheets. In Zachos data, $\delta^{18}\text{O}$ increases by 3 between O1 and the LGM. Half of this $\delta^{18}\text{O}$ change is due to the 6°C change of deep ocean temperature between O1 (5°C) and the LGM (-1°C) [92]. The other 1.5 of $\delta^{18}\text{O}$ change is presumed to be due to the ~ 180 m sea level (SL) change between ice-free Earth and the LGM, with ~ 60 m from Antarctic ice and 120 m from Northern Hemisphere ice. Thus, as an approximation to extract both SL and T_{do} from $\delta^{18}\text{O}$, Hansen et al. [66] assumed that SL rose linearly by 60 m as $\delta^{18}\text{O}$ increased from 1.75 to 3.25 and linearly by 120 m as $\delta^{18}\text{O}$ increased from 3.25 to 4.75.

The Zachos (Z) and Westerhold (W) $\delta^{18}\text{O}$ time series differ (Fig. 6) mainly because of different sites of the sediment cores and the way multiple sites are stacked to obtain a time series for the full Cenozoic. For example, mid-Holocene (6–8 kyBP) values of $\delta^{18}\text{O}$ in the Z and W data sets are $\delta^{18}\text{O}_{\text{H}}^{\text{Z}} = 3.32$ and $\delta^{18}\text{O}_{\text{H}}^{\text{W}} = 3.88$. Thus, the Z and W $\delta^{18}\text{O}$ time series require separate equations for sea level (SL) and deep ocean temperature (T_{do}) [66]:

$$\text{SL}^{\text{Z}}(\text{m}) = 60 - 38.2 (\delta^{18}\text{O} - 1.75) \quad (7)$$

$(\delta^{18}\text{O} < 3.32, \text{maximum SL} = +60 \text{ m}),$

$$\text{SL}^{\text{W}}(\text{m}) = 60 - 25.2 (\delta^{18}\text{O} - 1.5) \quad (8)$$

$(\delta^{18}\text{O} < 3.88, \text{maximum SL} = +60 \text{ m}),$

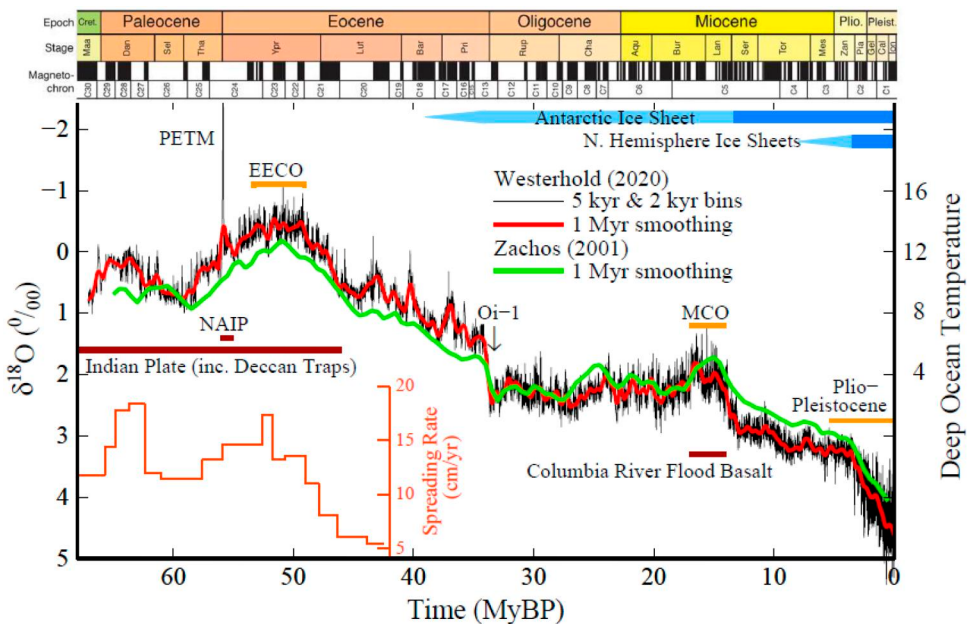


Figure 6. Global deep ocean $\delta^{18}\text{O}$. Black line: Westerhold *et al.* [90] data in 5 kyr bins until 34 MyBP and subsequently 2 kyr bins. Green line: Zachos *et al.* [44] data at 1 Myr resolution. Lower left: velocity [91] of Indian tectonic plate. PETM = Paleocene Eocene Thermal Maximum; EECO = Early Eocene Climatic Optimum; Oi-1 marks the transition to glaciated Antarctica; MCO = Miocene Climatic Optimum; NAIP = North Atlantic Igneous Province.

$$\text{SL}^Z(\text{m}) = -\frac{120(\delta^{18}\text{O} - 3.32)}{1.58} \quad (\delta^{18}\text{O} > 3.32), \quad (9)$$

$$\text{SL}^W(\text{m}) = -\frac{120(\delta^{18}\text{O} - 3.88)}{1.42} \quad (\delta^{18}\text{O} > 3.88), \quad (10)$$

where 1.75 and 1.5 are $\delta^{18}\text{O}$ midpoints at the Oi-1 transition for the Z and W data sets. Equations (9) and (10) are based on $\delta^{18}\text{O}_{\text{LGM}}^Z = 4.9$ and $\delta^{18}\text{O}_{\text{LGM}}^W = 5.3$ with SL = 0 today. T_{do} equations are based on specified Holocene and LGM T_{do} of 1°C [93] and -1°C [92], respectively. Coefficients in the T_{do} equations are calculated as shown by the Equation (12) example.

$$T_{\text{do}}^Z(\text{°C}) = 5 - 2.55 (\delta^{18}\text{O} - 1.75) \quad (1.75 < \delta^{18}\text{O} < 3.32), \quad (11)$$

$$\begin{aligned} T_{\text{do}}^Z(\text{°C}) &= 1 - 2 (\delta^{18}\text{O} - 3.32)/(4.9 - 3.32) \\ &= 1 - 1.27 (\delta^{18}\text{O} - 3.32) \quad (3.32 < \delta^{18}\text{O}), \end{aligned} \quad (12)$$

$$T_{\text{do}}^W(\text{°C}) = 6 - 2.10 (\delta^{18}\text{O} - 1.5) \quad (1.5 < \delta^{18}\text{O} < 3.88), \quad (13)$$

$$T_{\text{do}}^W(\text{°C}) = 1 - 1.41 (\delta^{18}\text{O} - 3.88) \quad (3.88 < \delta^{18}\text{O}). \quad (14)$$

Zachos and Westerhold $\delta^{18}\text{O}$, SL and T_{do} for the full Cenozoic, Pleistocene, and the past 800 000 years are graphed in Supplementary Material and sea level is compared to data of Rohling *et al.* [94]. We focus on the finer resolution W data. Differences between the W and Z data and interpretation of those differences are discussed in Paleocene Eocene Thermal Maximum section.

Cenozoic T_s

In this section we combine the rich detail in T_{do} provided by benthic $\delta^{18}\text{O}$ with constraints on the range of Cenozoic T_s from surface proxies to produce an estimated history of Cenozoic T_s .

We expect T_{do} change, which derives from sea surface temperature (SST) at high latitudes where deepwater forms, to approximate T_s change when T_{do} is not near the freezing point. Global SST change understates global T_s (land plus ocean) change because land temperature response to a forcing exceeds SST response [95], e.g. the equilibrium global SST response of the GISS (2020) GCM to $2 \times \text{CO}_2$ is 70.6% of the global (land plus ocean) response. However, polar amplification of the SST response tends to compensate for SST undershoot of global T_s change. Compensation is nearly exact at latitudes of North Atlantic deepwater formation for $2 \times \text{CO}_2$ climate change in the GISS (2020) climate model (Fig. 7a), but Southern Hemisphere polar amplification does not fully cover the 60–75°S latitudes where Antarctic bottom water forms.

As T_{do} nears the freezing point, ice forms, adhering to the Antarctic continent, extending today to a depth of about 2 km, and also forming floating ice shelves. From the Holocene toward colder climate, the effect on temperature change is large: T_s declines 7°C between the Holocene and LGM, but T_{do} declines only 2°C (from 1°C to -1°C). From the Holocene toward hotter climate, we expect a smaller effect that we quantify by first neglecting the effect and finding how far we underestimate EECO temperature. Thus, as an initial approximation we assume $\Delta T_s = \Delta T_{\text{do}}$:

$$T_s \sim T_{\text{do}} - T_{\text{doH}} + 14^\circ\text{C} = T_{\text{do}} + 13^\circ\text{C}, \quad (\delta^{18}\text{O} < \delta^{18}\text{O}_{\text{H}}) \quad (15)$$

where we take Holocene T_s as 14°C and T_{doH} as 1°C . In this initial approximation, we interpolate linearly for climate colder than the Holocene, the LGM being $\sim 7^\circ\text{C}$ cooler than the Holocene:

$$\begin{aligned} T_s &= 14^\circ\text{C} - 7^\circ\text{C} \times (\delta^{18}\text{O} - \delta^{18}\text{O}_{\text{H}}) \\ &\quad / (\delta^{18}\text{O}_{\text{LGM}} - \delta^{18}\text{O}_{\text{H}}) \quad (\delta^{18}\text{O} > \delta^{18}\text{O}_{\text{H}}) \end{aligned} \quad (16)$$

Resulting EECO (Early Eocene Climatic Optimum) T_s is $\sim 27^\circ\text{C}$ (Fig. 8a). As expected, this initial approximation undershoots EECO T_s , which Zhu *et al.* [96] infer to be 29°C from a proxy-constrained full-field analysis using a GCM to account for the pattern of

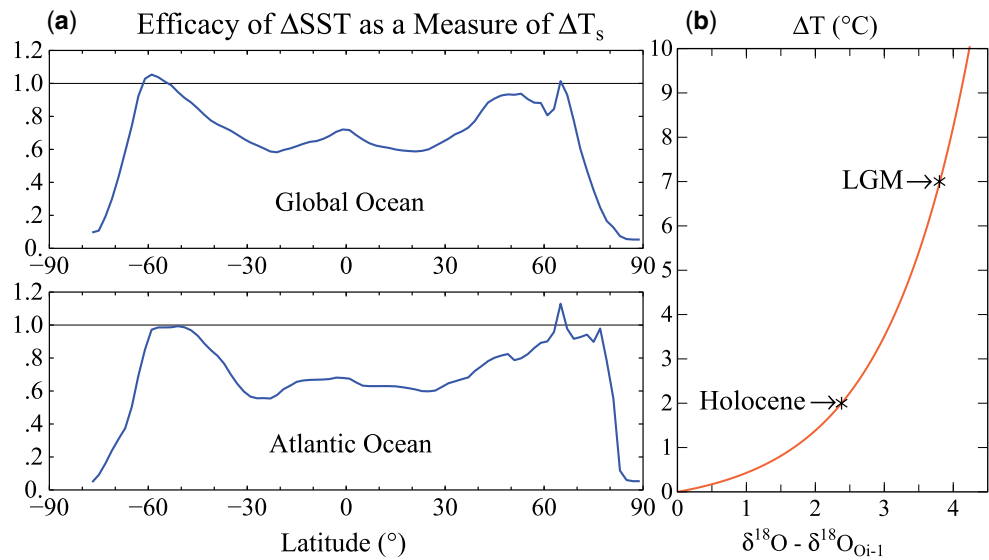


Figure 7. (a) Ratio of ΔS_{ST} (latitude) to global T_s change for all ocean and the Atlantic Ocean, based on equilibrium response (years 4001–4500) in $2 \times \text{CO}_2$ simulations of GISS (2020) model. (b) ΔT , the amount by which T_s change exceeds T_{do} change, based on an exponential fit to the two data points provided by the Holocene and LGM (see text).

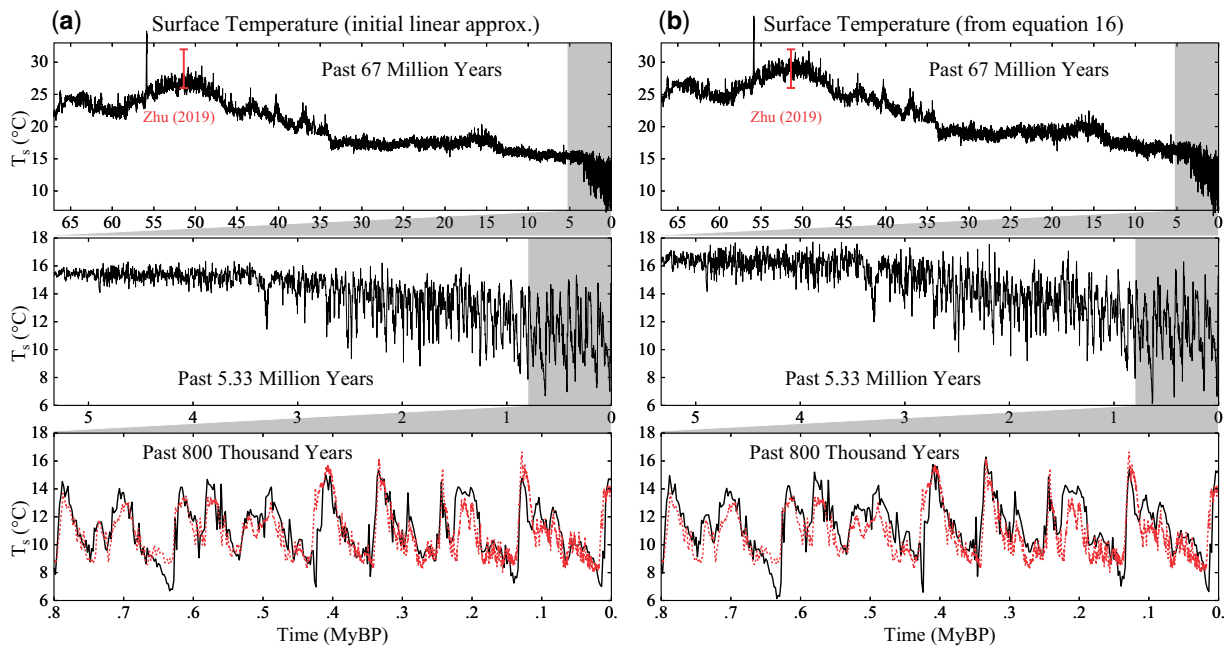


Figure 8. Cenozoic temperature based on linear (Equations 15 and 16) and nonlinear (Equation 17) analyses. Antarctic Dome C data [40] (red) relative to last 1000 years are multiplied by 0.6 to account for polar amplification and 14°C is added for absolute scale.

temperature change. Moderate undershoot ($\Delta T = 2^\circ\text{C}$) of EECO T_s is consistent with expectation that global warming of a few degrees would remove Antarctic ice shelves and allow polar amplification to fully cover regions of deepwater formation. Moreover, ΔT of 2°C at the Holocene and 5°C more between the Holocene and LGM are fit well by an exponential function between Antarctic glaciation and the LGM, as needed for ΔT to asymptote at the freezing point (Fig. 7b). Thus, we take T_s as

$$T_s = T_{\text{do}} - \Delta T + 15^\circ\text{C} = T_{\text{do}} - 0.35(e^{0.8X} - 1) + 15^\circ\text{C}, \quad (17)$$

where $X = \delta^{18}\text{O} - \delta^{18}\text{O}_{\text{O}_i-1}$ and T_s is normalized to 14°C in the Holocene.

The result is a consistent analysis of global T_s for the entire Cenozoic (Fig. 8b). Oxygen isotope $\delta^{18}\text{O}$ of deep ocean foraminifera reproduces glacial-interglacial temperature change well; more detailed agreement is not expected as Antarctic ice core data are for a location that moves, especially in altitude. Our interest is in warmer global climate and its relevance to upcoming human-caused climate change. For that purpose, we want to know the forcing that drove Cenozoic climate change. With the assumption that non- CO_2 GHG forcings provide 20% of the total GHG forcing, it is not difficult to infer the CO_2 abundance required to cause the Cenozoic temperature history in Fig. 8b. Considering the large disagreement among proxy CO_2 measures, this indirect measure of

CO_2 via global T_S may provide the most accurate Cenozoic CO_2 history.

Cenozoic CO_2

We obtain the CO_2 history required to yield the Cenozoic T_S history from the relation

$$\Delta F(t) = [T_S(t) - 14^\circ\text{C}] / \text{ECS}, \quad (18)$$

where $\Delta F(t)$ (0 at 7 kyBP) includes changing solar irradiance and amplification of CO_2 forcing by non- CO_2 GHGs and ice sheets. The GHG amplification factor is taken as 1.25 throughout the Cenozoic (State dependence of climate sensitivity section). The amplification applies to solar forcing as well as CO_2 forcing because it is caused by temperature change, not by CO_2 . Solar irradiance is increasing 10% per billion years [69]; thus solar forcing (240 W/m^2 today) increases 2.4 W/m^2 per 100 million years. Thus,

$$\Delta F(t) = 1.25 \times [\Delta F_{\text{CO}_2}(t) + \Delta F_{\text{Sol}}(t)] \times A_S. \quad (\delta^{18}\text{O} > \delta^{18}\text{O}_H) \quad (19)$$

A_S , surface albedo amplification, is smaller in moving from the Holocene to warmer climate—when the main effect is shrinking of Antarctic ice—than toward colder climate. For $\delta^{18}\text{O} > \delta^{18}\text{O}_H$, we take A_S as its average value over the period from the Holocene to the LGM:

$$A_S = \frac{F_{\text{Ice}} + F_{\text{GHG}}}{F_{\text{GHG}}} = \frac{3.5 + 2.25}{2.25} = 2.55. \quad (\delta^{18}\text{O} > \delta^{18}\text{O}_H) \quad (20)$$

Thus, for climate colder than the Holocene,

$$\Delta F(t) = 3.19 \times [\Delta F_{\text{CO}_2}(t) + \Delta F_{\text{Sol}}(t)]. \quad (\delta^{18}\text{O} > \delta^{18}\text{O}_H) \quad (21)$$

For climate warmer than the Holocene up to Oi-1, i.e. for $\delta^{18}\text{O}_{\text{Oi-1}} < \delta^{18}\text{O} < \delta^{18}\text{O}_H$,

$$\Delta F(t) = 1.25 \times \left[\Delta F_{\text{CO}_2}(t) + \Delta F_{\text{Sol}}(t) + F_{\text{IceH}} \times \frac{\delta^{18}\text{O}_H - \delta^{18}\text{O}}{\delta^{18}\text{O}_H - \delta^{18}\text{O}_{\text{Oi-1}}} \right]. \quad (22)$$

F_{IceH} , the (Antarctic plus Greenland) ice sheet forcing between the Holocene and Oi-1, is estimated to be 2 W/m^2 (Supplementary Fig. S4, Target CO_2). For climate warmer than Oi-1

$$\Delta F(t) = 1.25 \times [\Delta F_{\text{CO}_2}(t) + \Delta F_{\text{Sol}}(t) + \Delta F_{\text{IceH}}] \quad (23)$$

All quantities are known except $\Delta F_{\text{CO}_2}(t)$, which is thus defined. Cenozoic CO_2 (t) for specified ECS is obtained from $T_S(t)$ using the CO_2 radiative forcing equation (Table 1, Supplementary Material). Resulting CO_2 (Fig. 9) is about 1,200 ppm at the EECO, 450 ppm at Oi-1, and 325 ppm in the Pliocene for $\text{ECS} = 1.2^\circ\text{C}$ per W/m^2 . For $\text{ECS} = 1^\circ\text{C}$ —about as low as we believe plausible—Pliocene CO_2 is near 350 ppm, rising only to ~ 500 ppm at Oi-1 and ~ 1500 ppm at EECO.

Assumed Holocene CO_2 amount is also a minor factor. We tested two cases: 260 and 278 ppm (Fig. 9). These were implemented as the CO_2 values at 7 kyBP, but Holocene-mean values are similar—a few ppm less than CO_2 at 7 kyBP. Holocene = 278 ppm increases CO_2 about 20 ppm between today and Oi-1, and about 50 ppm at the EECO. However, Holocene CO_2 278 ppm causes the amplitude of inferred glacial-interglacial CO_2 oscillations to be less than reality (Fig. 9b), providing support for the Holocene 260 ppm level and for the interpretation that high late-Holocene CO_2 was due to human influence. Proxy measures of Cenozoic CO_2 yield a notoriously large range. A recent review [88] constructs a CO_2 history with Loess-smoothed $\text{CO}_2 \sim 700$ –1100

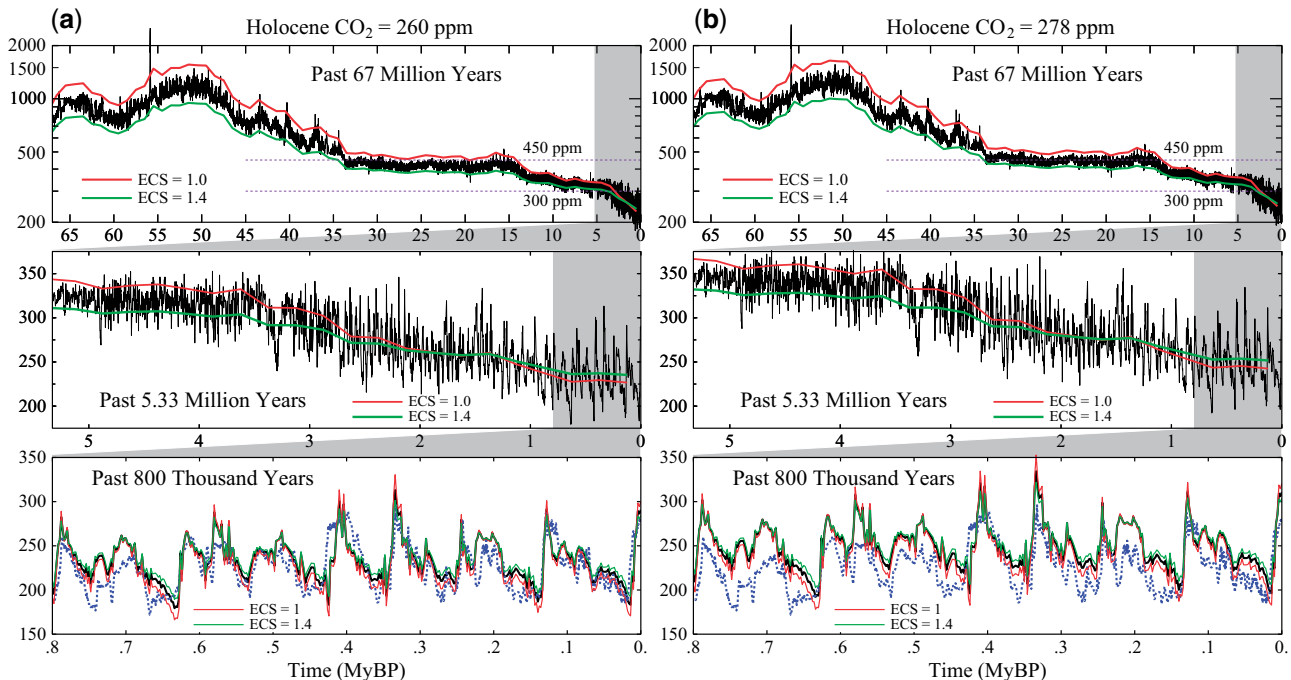


Figure 9. Cenozoic CO_2 estimated from $\delta^{18}\text{O}$ of Westerhold et al. (see text). Black lines are for $\text{ECS} = 1.2^\circ\text{C}$ per W/m^2 ; red and green curves ($\text{ECS} = 1.0$ and 1.4°C per W/m^2) are 1 My smoothed. Blue curves (last 800,000 years) are Antarctica ice core data [41].

ppm at Oi-1. That high Oi-1 CO₂ amount is not plausible without overthrowing the concept that global temperature is a response to climate forcings. More generally, we conclude that actual CO₂ during the Cenozoic was near the low end of the range of proxy measurements.

Interpretation of Cenozoic T_S and CO₂

In this section we consider Cenozoic T_S and CO₂ histories, which are rich in insights about climate change with implications for future climate.

In Target CO₂ [60] and elsewhere [98] we argue that the broad sweep of Cenozoic temperature is a result of plate tectonic (particularly ‘continental drift’) effects on CO₂. Solid Earth sources and sinks of CO₂ are not balanced at any given time. CO₂ is removed from surface reservoirs by: (1) chemical weathering of rocks with deposition of carbonates on the ocean floor, and (2) burial of organic matter [99, 100]. CO₂ returns via metamorphism and volcanic outgassing at locations where oceanic crust is subducted beneath moving continental plates. The interpretation in Target CO₂ was that the main Cenozoic source of CO₂ was associated with the Indian plate (Fig. 10), which separated from Pangea in the Cretaceous [101, 102] and moved through the Tethys (now Indian) Ocean at a rate exceeding 10 cm/year until collision with the Eurasian plate at circa 50 MyBP. Associated CO₂ emissions include those from formation of the Deccan Traps⁷ in western India (a large igneous province, LIP, formed by repeated deposition of large-scale flood basalts), the smaller Rajahmundry Traps [103] in eastern India, and metamorphism and vulcanism associated with the moving Indian plate. The Indian plate slowed circa 60 Mya (inset, Fig. 6) before resuming high speed [91], leaving an indelible signature in the Cenozoic δ¹⁸O history (Fig. 6) that supports our interpretation of the CO₂ source. Since the continental collision, subduction and CO₂ emissions continue at a diminishing rate as the India plate underthrusts the Asian continent and pushes up the Himalayan mountains [104]. We interpret the decline of CO₂ over the past 50 million years as, at least in part, a decline of the metamorphic source from continued subduction of

the Indian plate, but burial of organic matter and increased weathering due to exposure of fresh rock by Himalayan uplift [105] may contribute to CO₂ drawdown. Quantitative understanding of these processes is limited [106], e.g. weathering is both a source and sink of CO₂ [107].

This picture for the broad sweep of Cenozoic CO₂ is consistent with current understanding of the long-term carbon cycle [108], but relative contributions of metamorphism [106] and volcanism [109] are uncertain. Also, emissions from rift-induced Large Igneous Provinces (LIPs) [110, 111] contribute to long-term change of atmospheric CO₂, with two cases prominent in Fig. 6. The Columbia River Flood Basalt at ca. 17–15 MyBP was a principal cause of the Miocene Climatic Optimum [112], but the processes are poorly understood [113]. A more dramatic event occurred as Greenland separated from Europe, causing a rift in the sea floor; flood basalt covered more than a million square kilometers with magma volume 6–7 million cubic kilometers [111]—the North Atlantic Igneous Province (NAIP). Flood basalt volcanism occurred during 60.5–54.5 MyBP, but at 56.1 ± 0.5 MyBP melt production increased by more than a factor of 10, continued at a high level for about a million years, and then subsided (Fig. 5 of Storey et al. [114]). The striking Paleocene-Eocene Thermal Maximum (PETM) δ¹⁸O spike (Fig. 6) occurs early in this million-year bump-up of δ¹⁸O. Svensen et al. [115] proposed that the PETM was initiated by the massive flood basalt into carbon-rich sedimentary strata. Gutjahr et al. [116] developed an isotope analysis, concluding that most of PETM carbon emissions were volcanic, with climate-driven carbon feedbacks playing a lesser role. Yet other evidence [117], while consistent with volcanism as a trigger for the PETM, suggests that climate feedback—perhaps methane hydrate and peat CO₂ release—may have caused more than half of the PETM warming. Berndt et al. [118] describe extensive shallow-water vents that likely released CH₄ as well as CO₂ during the NAIP activity. We discuss PETM warming and CO₂ levels below, but first we must quantify the mechanisms that drove Cenozoic climate change and consider where Earth’s climate was headed before humanity intervened.

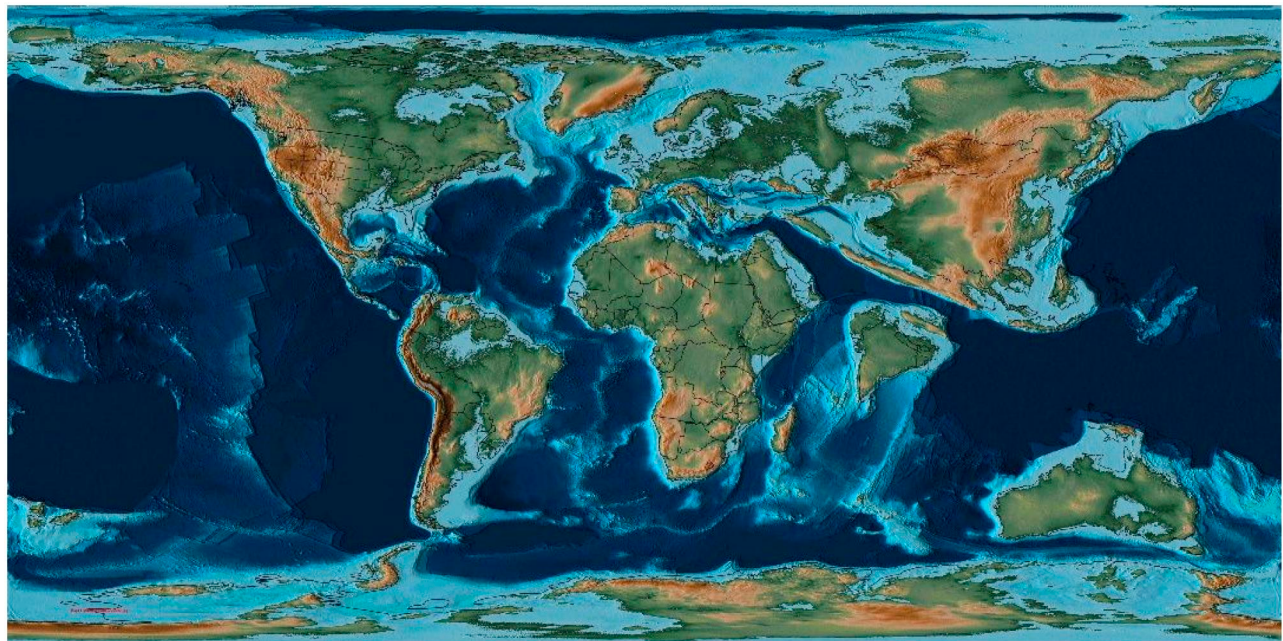


Figure 10. Continental configuration 56 MyBP [97]. Continental shelves (light blue) were underwater as little water was locked in ice. The Indian plate was moving north at about 15 cm per year.

The sum of climate forcings (CO_2 and solar) and slow feedbacks (ice sheets and non- CO_2 GHGs) that maintained EECO warmth was 12.5 W/m^2 (Fig. 11). CO_2 forcing of 9.1 W/m^2 combined with solar forcing of -1.2 W/m^2 to yield a total forcing⁸ 8 W/m^2 . Slow feedbacks were 4.5 W/m^2 forcing (ice albedo = 2 W/m^2 and non- CO_2 GHGs = 2.5 W/m^2). With today's solar irradiance, human-made GHG forcing required for Earth to return to EECO warmth is 8 W/m^2 . Present human-made GHG forcing is 4.6 W/m^2 relative to 7 kyBP.⁹ Equilibrium response to this forcing includes the 2 W/m^2 ice sheet feedback and 25% amplification (of 6.6 W/m^2) by non- CO_2 GHGs, yielding a total forcing plus slow feedbacks of 8.25 W/m^2 . Thus, equilibrium global warming for today's GHGs is 10°C .¹⁰ If human-made aerosol forcing is -1.5 W/m^2 and remains at that level indefinitely, equilibrium warming for today's atmosphere is reduced to 8°C . Either 10°C or 8°C dwarfs observed global warming of 1.2°C to date. Most of the equilibrium warming for today's atmosphere has not yet occurred and need not occur (Earth's energy imbalance section).

Prospects for another snowball Earth

We would be remiss if we did not comment on the precipitous decline of Earth's temperature over the last several million years. Was Earth falling off the table into another Snowball Earth?

Global temperature plummeted in the past 50 million years, with growing, violent, oscillations (Figs 6 and 7). Glacial-interglacial average CO_2 declined from about 325 ppm to 225 ppm in the past five million years in an accelerating decline (Fig. 9a). As CO_2 fell to 180 ppm during recent glacial maxima, an ice sheet covered most of Canada and reached midlatitudes in the U.S. Continents in the current supercontinent cycle [101] are now dispersed, with movement slowing to 2–3 cm/year. Emissions from the last high-speed high-impact tectonic event—collision of the Indian plate with Eurasia—are fizzling out. The

most recent large igneous province (LIP) event—the Columbia River Flood Basalt about 15 million years ago (Fig. 6)—is no longer a factor, and there is no evidence of another impending LIP. Snowball conditions are possible, even though the Sun's brightness is increasing and is now almost 6% greater [69] than it was at the last snowball Earth, almost 600 million years ago [68]. Runaway snowball likely requires only 1–2 halvings [66] of CO_2 from the LGM 180 ppm level, i.e. to 45–90 ppm. Although the weathering rate declines in colder climate [119], weathering and burial of organic matter continue, so decrease of atmospheric CO_2 could have continued over millions of years, if the source of CO_2 from metamorphism and vulcanism continued to decline.

Another factor that may have contributed to cooling in the Pliocene is uplift and poleward movement of Greenland that accelerated about 5 MyBP [120], which likely enhanced glaciation of Greenland and should be accounted for in simulations of Pliocene climate change. We conclude that, in the absence of human activity, Earth may have been headed for snowball Earth conditions within the next 10 or 20 million years, but the chance of future snowball Earth is now academic. Human-made GHG emissions remove that possibility on any time scale of practical interest. Instead, GHG emissions are now driving Earth toward much warmer climate.

Paleocene eocene thermal maximum (PETM)

The PETM event provides a benchmark for assessing the potential impact of the human-made climate forcing and the time scale for natural recovery of the climate system.

Westerhold [90] data have 10°C deep ocean warming at the PETM (Figs 8 and 12a), which exceeds proxy-derived surface warming. Low latitude SST data have 3–4°C PETM warming [121]. Tierney et al. [122] obtain PETM global surface warming 5.6°C (5.4 – 5.9°C , 95% confidence) via analysis of proxy surface temperature data that accounts for patterns of temperature change. Zachos [44] data have a deep ocean warming similar to the proxy-based surface warming. These warming estimates can be reconciled, but first let's note the practical importance of the PETM.

Pre-PETM (56–56.4 MyBP) CO_2 is 910 ppm in our analysis for the most likely ECS (1.2°C per W/m^2). Peak PETM CO_2 required to yield the 5.6°C global surface warming estimate of Tierney et al. [122] is then 1630 ppm if CO_2 provides 80% of the GHG forcing, thus less than a doubling of CO_2 . (In the unlikely case that CO_2 caused 100% of the GHG forcing, required CO_2 is 1780, not quite a doubling.) CO_2 amounts for ECS = 1.0 and 1.4°C per W/m^2 are 1165 and 760 ppm in the pre-PETM and 2260 and 1270 ppm at peak PETM, respectively. In all these ECS cases, the CO_2 forcing of the PETM is less than or about a CO_2 doubling. Our assumed 20% contribution by non- CO_2 GHGs (amplification factor 1.25,

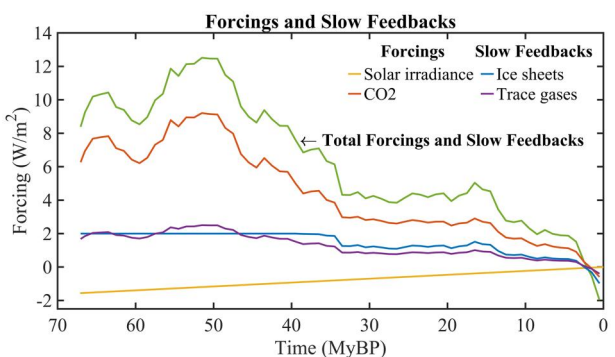


Figure 11. Climate forcings and slow feedbacks relative to 7 kyBP from terms in Equations (21–23).

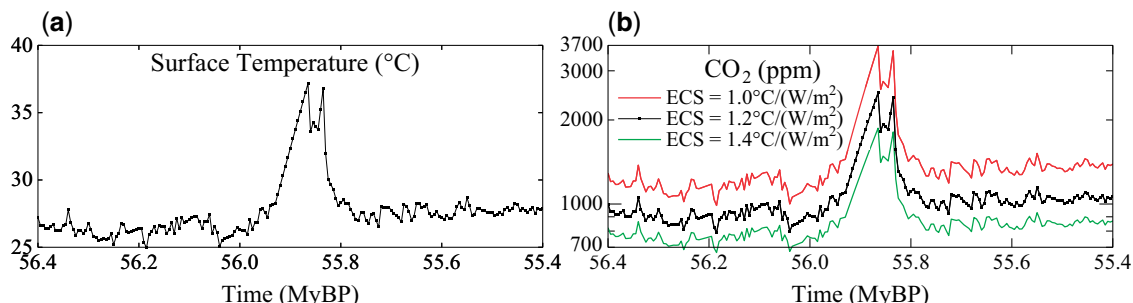


Figure 12. Temperature and CO_2 implied by Westerhold et al. [90] $\delta^{18}\text{O}$, if surface warming equaled deep ocean warming. In reality, the unique PETM event had surface warming $\sim 5.6^\circ\text{C}$, which implies a peak PETM CO_2 of about 1630 ppm (see text).

Climate sensitivity (ECS and ESS) section), is nominal; Hopcroft et al., e.g. estimate a 30% contribution from non-CO₂ GHGs [123], thus an amplification factor 1.43.

Thus, today's human-made GHG forcing (4.6 W/m², growing 0.5 W/m² per decade) is already at least comparable to the PETM forcing, although the net human-made forcing including aerosols has probably not reached the PETM forcing. However, there are two big differences between the PETM and today. First, there were no large ice sheets on Earth in the PETM era. Ice sheets on Antarctica and Greenland today make Earth system sensitivity (ESS) greater than it was during the PETM. Equilibrium response to today's GHG climate forcing would include deglaciation of Antarctica and Greenland, sea level rise of 60 m (200 feet), and surface albedo forcing (slow feedback) of 2 W/m². The second difference between the PETM and today is the rate of change of the climate forcing. Most of today's climate forcing was introduced in a century, which is 10 times or more faster than the PETM forcing growth. Although a bolide impact [124] has been proposed as a trigger for the PETM, the issue is the time scale on which the climate forcing—increased GHGs—occurred. Despite uncertainty in the carbon source(s), data and modeling point to duration of a millennium or more for PETM emissions [121, 125].

Better understanding of the PETM could inform us on climate feedbacks. Gutjahr et al. [116] argue persuasively that PETM emissions were mostly volcanic, yet we know of no other large igneous province that produced such great, temporally-isolated, emissions. Further, Cenozoic orbitally-driven hyperthermal events [126] testify to large CO₂ feedbacks. Northern peatlands today contain more than 1000 Gt carbon [127], much of which can be mobilized at PETM warming levels [128]. The double peak in deep ocean δ¹⁸O (thus in temperature, cf. Fig. 12, where each square is a binning interval of 5000 years) is also found in terrestrial data [129]. Perhaps the sea floor rift occurred in two bursts, or the rift was followed tens of thousands of years later by methane hydrate release as a feedback to the ocean warming; much of today's methane hydrate is in stratigraphic deposits hundreds of meters below the sea floor, where millennia may pass before a thermal wave from the surface reaches the deposits [130]. Feedback emissions, especially from permafrost, seem to be more chronic than catastrophic, but stabilization of climate may require cooling that terminates growth of those feedbacks (Summary section). The PETM provides perhaps the best empirical check on understanding of the atmospheric lifetime of fossil fuel CO₂ [131], but for that purpose we must untangle as well as possible the time dependence of the PETM CO₂ source and feedbacks. If continuing magma flow or a slow-release feedback is a substantial portion of PETM CO₂, the CO₂ lifetime inferred from post-PETM CO₂ recovery may be an exaggeration.

The PETM draws attention to differences between the Westerhold (W) and Zachos (Z) δ¹⁸O data. Zachos attributes the larger PETM response in W data to the shallow (less than 1 km) depth of the Walvis Ridge core in the Southeast Atlantic that anchors the PETM period in the W data (see Supplementary Material SM9). Given that the PETM was triggered by a rift in the floor of the North Atlantic and massive lava injection, it is not surprising that ocean temperature was elevated and circulation disrupted during the PETM. Nunes and Norris [132] conclude that ocean circulation changed at the start of the PETM with a shift in location of deep-water formation that delivered warmer waters to the deep sea, a circulation change that persisted at least 40 000 years. With regard to differences in the early Cenozoic, Zachos notes (Supplementary Material SM9) a likely bias in the Z data with a heavy weighting of data from Southern Ocean sites

(Kerguelan Plateau and Maud Rise), which were intended for study of climate of Antarctica and the Southern Ocean.

Differences between the W and Z data sets have limited effect on our paper, as we apply separate scaling (Equations 7–14) to W and Z data to match observations at the LGM, mid-Holocene, and Oi-1 points. This approach addresses, e.g. the cumulative effect in combining data splices noted by Zachos in SM9. Further, we set the EECO global temperature relative to the Holocene and the PETM temperature relative to pre-PETM based on proxy-constrained, full-field, GCM analyses of Tierney et al. [122] and Zhu et al. [96] Nevertheless, there is much to learn from more precise study of the Cenozoic in general and the PETM in particular.

Policy implications require first an understanding of the role of aerosols in climate change.

Aerosols

The role of aerosols in climate change is uncertain because aerosol properties are not measured well enough to define their climate forcing. In this section we estimate aerosol climate forcing via aerosol effects on Earth's temperature and Earth's energy imbalance.

Aerosol impact is suggested by the gap between observed global warming and expected warming due to GHGs based on ECS inferred from paleoclimate (Fig. 13). Expected warming is from Eq. 5 with the normalized response function of the GISS (2020) model. Our best estimate for ECS, 1.2°C per W/m², yields a gap of 1.5°C between expected and actual warming in 2022. Aerosols are the likely cooling source. The other negative forcing discussed by IPCC—surface albedo change—is estimated by IPCC (Chapter 7, Table 7.8) to be -0.12 ± 0.1 W/m², an order of magnitude smaller than aerosol forcing [12]. Thus, for clarity, we focus on GHGs and aerosols.

Absence of global warming over the period 1850–1920 (Supplementary Fig. S1 of IPCC AR6 WG1 report [12]) is a clue about aerosol forcing. GHG forcing increased 0.54 W/m² in 1850–1920, which causes expected warming 0.3–0.4°C by 1920 for ECS = 1.2°C per W/m² (Equation 5). Natural forcings—solar irradiance and volcanoes—may contribute to lack of warming, but a persuasive case for the required forcing has not been made. Human-made aerosols are the likely offset of GHG warming. Such aerosol

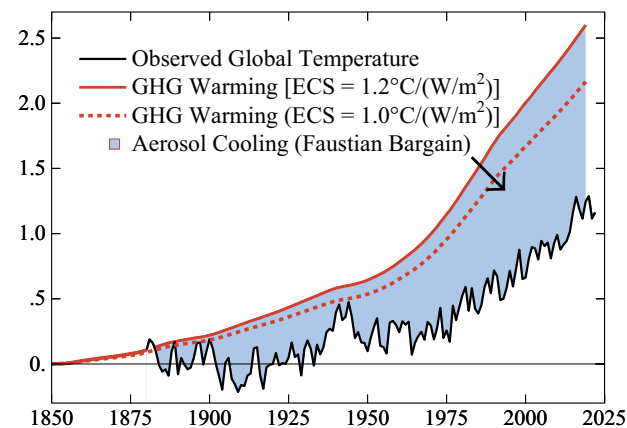


Figure 13. Observed global surface temperature (black line) and expected GHG warming with two choices for ECS. The blue area is the estimated aerosol cooling effect. The temperature peak in the World War II era is in part an artifact of inhomogeneous ocean data in that period [63].

cooling is a Faustian bargain [98] because payment in enhanced global warming will come due once we can no longer tolerate the air pollution. Ambient air pollution causes millions of deaths per year, with particulates most responsible [133, 134].

Evidence of aerosol forcing in the Holocene

In this section we infer evidence of human-made aerosols in the last half of the Holocene from the absence of global warming. Some proxy-based analyses [135] report cooling in the last half of the Holocene, but a recent analysis [50] that uses GCMs to overcome spatial and temporal biases in proxy data finds rising global temperature in the first half of the Holocene followed by nearly constant temperature in the last 6000 years until the last few centuries (Fig. 14). Antarctic, deep ocean, and tropical sea surface data all show stable temperature in the last 6000 years (Supplementary Fig. S6 of reference [60]). GHG forcing increased 0.5 W/m² during those 6000 years (Fig. 15), yet Earth did not warm. Fast feedbacks alone should yield at least +0.5°C warming and 6000 years is long enough for slow feedbacks to also contribute. How can we interpret the absence of warming?

Humanity's growing footprint deserves scrutiny. Ruddiman's suggestion that deforestation and agriculture began to affect CO₂ 6500 year ago and rice agriculture began to affect CH₄ 5000 years ago has been criticized [46] mainly because of the size of proposed sources. Ruddiman sought sources sufficient to offset declines of CO₂ and CH₄ in prior interglacial periods, but such

large sources are not needed to account for Holocene GHG levels. Paleoclimate GHG decreases are slow feedbacks that occur in concert with global cooling. However, if global cooling did not occur in the past 6000 years, feedbacks did not occur. Earth orbital parameters 6000 years ago kept the Southern Ocean warm, as needed to maintain strong overturning ocean circulation [137] and minimize carbon sequestration in the deep ocean. Maximum insolation at 60°S was in late-spring (mid-November); since then, maximum insolation at 60°S slowly advanced through the year, recently reaching mid-summer (mid-January, Fig. 26b of Ice Melt [13]). Maximum insolation from late-spring through mid-summer is optimum to warm the Southern Ocean and promote early warm-season ice melt, which reduces surface albedo and magnifies regional warming [45].

GHG forcing of -0.2 W/m² in 10–6 kyBP (Fig. 15) was exceeded by forcing of +1 W/m² due to ice sheet shrinkage (Supplementary Material in Target CO₂ [60]) for a 40 m sea level rise (Fig. 16). Net 0.8 W/m² forcing produced expected 1°C global warming (Fig. 14). The mystery is the absence of warming in the past 6000 years. Hansen et al. [45] suggested that aerosol cooling offset GHG warming. Growing population, agriculture and land clearance produced aerosols and CO₂; wood was the main fuel for cooking and heating. Nonlinear aerosol forcing is largest in a pristine atmosphere, so it is unsurprising that aerosols tended to offset CO₂ warming as civilization developed. Hemispheric differences could provide a check. GHG forcing is global, while aerosol forcing is mainly in the Northern Hemisphere. Global offset implies a net negative Northern Hemisphere forcing and positive Southern Hemisphere forcing. Thus, data and modeling studies (including orbital effects) of regional response are warranted but beyond the scope of this paper.

Industrial era aerosols

Scientific advances often face early resistance from other scientists [139]. Examples are the snowball Earth hypothesis [140] and the role of an asteroid impact in extinction of non-avian dinosaurs [141], which initially were highly controversial but are now more widely accepted. Ruddiman's hypothesis, right or wrong, is still controversial. Thus, we minimize this issue by showing aerosol effects with and without preindustrial human-made aerosols.

Global aerosols are not monitored with detail needed to define aerosol climate forcing [142, 143]. IPCC12 estimates forcing

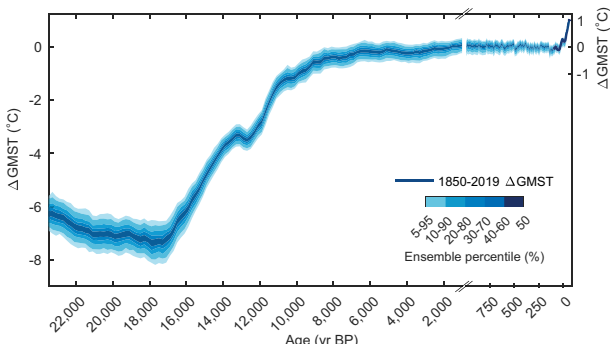


Figure 14. Global mean surface temperature change over the past 24 ky, reproduced from Fig. 2 of Osman et al. [50] including Last Millennium reanalysis of Tardif et al. [136].

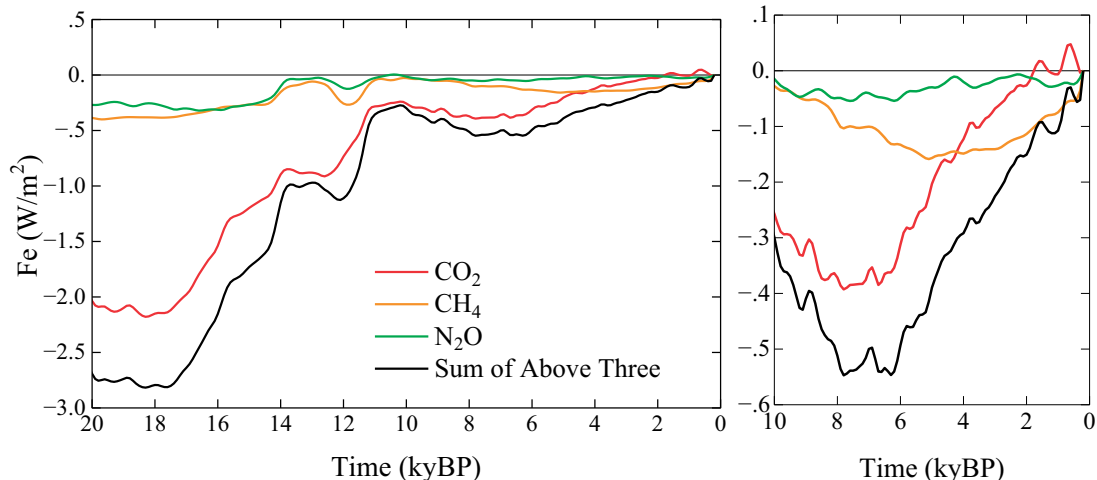


Figure 15. GHG climate forcing in past 20 ky with vertical scale expanded for the past 10 ky on the right. GHG amounts are from Schilt et al. [47]. Formulae for forcing are in Supplementary Material.

(Fig. 17a) from assumed precursor emissions, a herculean task due to many aerosol types and complex cloud effects. Aerosol forcing uncertainty is comparable to its estimated value (Fig. 17a), which is constrained more by observed global temperature change than by aerosol measurements [144]. IPCC's best estimate of aerosol forcing (Fig. 17) and GHG history define the percent of GHG forcing offset by aerosol cooling—the dark blue area in Fig. 17b. However, if human-made aerosol forcing was -0.5 W/m^2 by 1750, offsetting $+0.5 \text{ W/m}^2$ GHG forcing, this forcing should be included. Such aerosol forcing—largely via effects of land use and biomass fuels on clouds—continues today. Thirty million people in the United States use wood for heating [145]. Such fuels are also common in Europe [146, 147] and much of the world.

Figure 17b encapsulates two alternative views of aerosol history. IPCC aerosol forcing slowly becomes important relative to GHG forcing. In our view, civilization always produced aerosols as well as GHGs. As sea level stabilized, organized societies and population grew as coastal biologic productivity increased [148] and agriculture developed. Wood was the main fuel. Aerosols travel great distances, as shown by Asian aerosols in North America [149]. Humans contributed to both rising GHG and aerosol climate forcings in the past 6000 years. One result is that human-caused aerosol climate forcing is at least 0.5 W/m^2 more than usually assumed. Thus, the Faustian payment that will eventually come due is also larger, as discussed in Summary section.

Ambiguity in aerosol climate forcing

In this section we discuss uncertainty in the aerosol forcing. We discuss why global warming in the past century—often used to infer climate sensitivity—is ill-suited for that purpose.

Recent global warming does not yield a unique ECS because warming depends on three major unknowns with only two basic

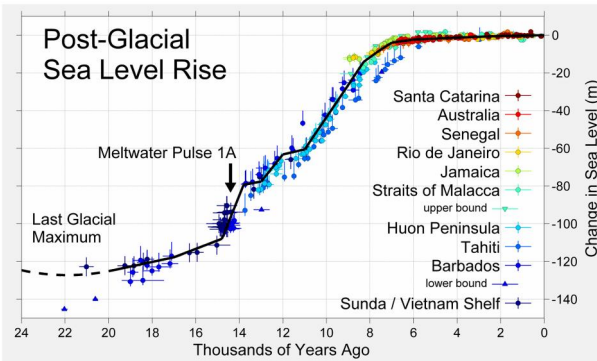


Figure 16. Sea level since the last glacial period relative to present. Credit: Robert Rohde [138].

constraints. Unknowns are ECS, net climate forcing (aerosol forcing is unmeasured), and ocean mixing (many ocean models are too diffusive). Constraints are observed global temperature change and Earth's energy imbalance (EEI) [80]. Knutti [150] and Hansen [75] suggest that many climate models compensate for excessive ocean mixing (which reduces surface warming) by using aerosol forcing less negative than the real world, thus achieving realistic surface warming. This issue is unresolved and complicated by the finding that cloud feedbacks can buffer ocean heat uptake (Climate response time section), affecting interpretation of EEI.

IPCC AR6 WG1 best estimate of aerosol forcing (Table AIII.3) [12] is near maximum (negative) value by 1975, then nearly constant until rising in the 21st century to -1.09 W/m^2 in 2019 (Fig. 18). We use this IPCC aerosol forcing in climate simulations here. We also use an alternative aerosol scenario [151] that reaches -1.63 W/m^2 in 2010 relative to 1880 and -1.8 W/m^2 relative to 1850 (Fig. 18) based on modeling of Koch [152] that included changing technology factors defined by Novakov [153]. This alternative scenario¹¹ is comparable to the forcing in some current aerosol models (Fig. 18). Human-made aerosol forcing relative to several millennia ago may be even more negative, by about -0.5 W/m^2 as discussed above, but the additional forcing was offset by increasing GHGs and thus those additional forcings are neglected, with climate assumed to be in approximate equilibrium in 1850.

Many combinations of climate sensitivity and aerosol forcing can fit observed global warming. The GISS (2014) model ($\text{ECS} = 2.6^\circ\text{C}$) with IPCC AR6 aerosol forcing can match observed warming (Fig. 19) in the last half century (when human-made climate forcing overwhelmed natural forcings, unforced climate variability, and flaws in observations). However, agreement also can be achieved by climate models with high ECS. The GISS (2020) model (with $\text{ECS} = 3.5^\circ\text{C}$) yields greater warming than observed if IPCC

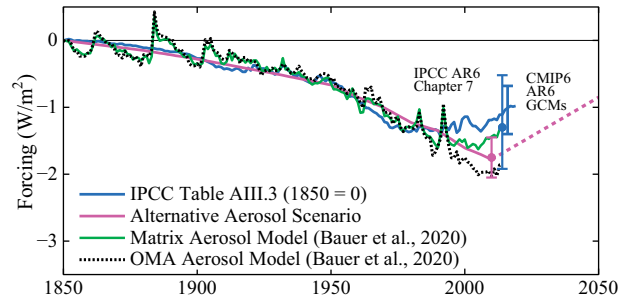


Figure 18. Aerosol forcing relative to 1850 from IPCC AR6, an alternative aerosol scenario [151] two aerosol model scenarios of Bauer et al. [154].

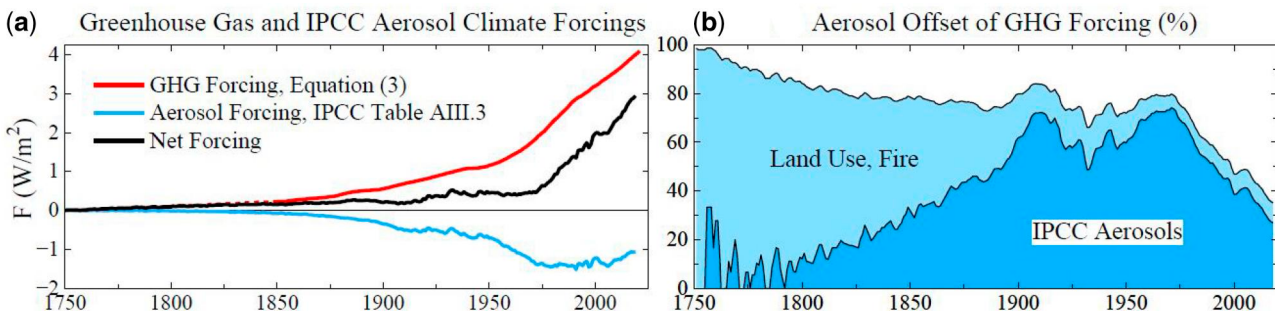


Figure 17. (a) Estimated greenhouse gas and aerosol forcings relative to 1750 values. (b) Aerosol forcing as percent of GHG forcing. Forcings for dark blue area are relative to 1750. Light blue area adds 0.5 W/m^2 forcing estimated for human-caused aerosols from fires, biofuels and land use.

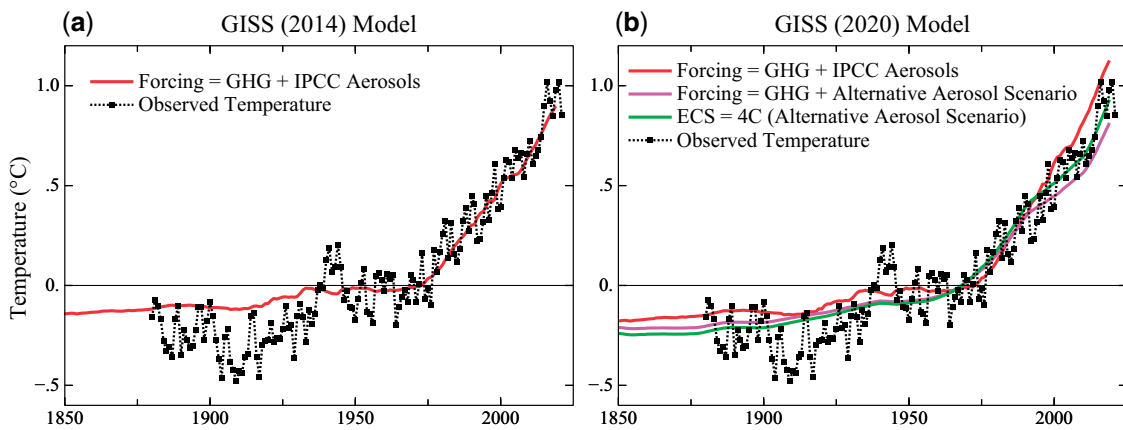


Figure 19. Global temperature change T_G due to aerosols + GHGs calculated with Green's function Equation (5) using GISS (2014) and GISS (2020) response functions (Fig. 4). Observed temperature is the NASA GISS analysis [155, 156]. Base period: 1951–1980 for observations and model.

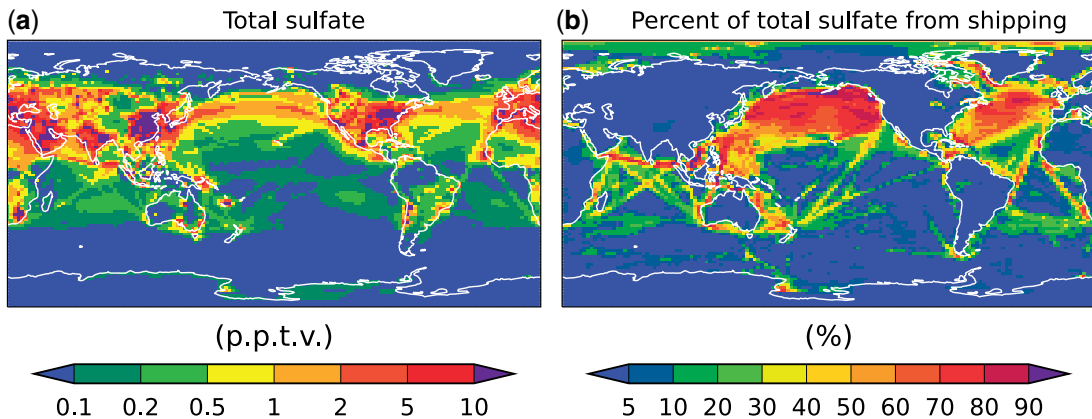


Figure 20. Total sulfate (parts per trillion by volume) and percentage of total sulfate provided by shipping in simulations of Jin et al. [157] prior to IMO regulations on sulfur content of fuels.

aerosol forcing is used, but less than observed for the alternative aerosol scenario (Fig. 19). This latter aerosol scenario achieves agreement with observed warming if ECS $\sim 4^\circ\text{C}$ (green curve in Fig. 19).¹² Agreement can be achieved with even higher ECS by use of a still more negative aerosol forcing.

The issue we raise is the magnitude of the aerosol forcing, with implications for future warming when particulate air pollution is likely to be reduced. We suggest that IPCC reports may have gravitated toward climate sensitivity near 3°C for $2 \times \text{CO}_2$ in part because of difficulty that models have in realistically simulating amplifying cloud feedbacks and a climate model tendency for excessive mixing of heat into the deep ocean. Our finding from paleoclimate analysis that ECS is $1.2^\circ\text{C} \pm 0.3^\circ\text{C}$ per W/m^2 ($4.8^\circ\text{C} \pm 1.2^\circ\text{C}$ for $2 \times \text{CO}_2$) implies that the (unmeasured) aerosol forcing must be more negative than IPCC's best estimate. In turn—because aerosol-cloud interactions are the main source of uncertainty in aerosol forcing—this finding emphasizes the need to measure both global aerosol and cloud particle properties.

The case for monitoring global aerosol climate forcing will grow as recognition of the need to slow and reverse climate change emerges. Aerosol and cloud particle microphysics must be measured with precision adequate to define the forcing [142, 158]. In the absence of such Keeling-like global monitoring, progress can be made via more limited satellite measurements of aerosol and cloud properties, field studies, and aerosol and cloud modeling. As described next, a great opportunity to

study aerosol and cloud physics is provided by a recent change in the IMO (International Maritime Organization) regulations on ship emissions.

The great inadvertent aerosol experiment

Sulfate aerosols are cloud condensation nuclei (CCN), so sulfate emissions by ships result in a larger number of smaller cloud particles, thus affecting cloud albedo and cloud lifetime [144]. Ships provide a large percentage of sulfates in the North Pacific and North Atlantic regions (Fig. 20). It has been suggested that cooling by these clouds is overestimated because of cloud liquid water adjustments [159], but Manshausen et al. [160] present evidence that liquid water path (LWP) effects are substantial even in regions without visible ship-tracks; they estimate a LWP forcing $-0.76 \pm 0.27 \text{ W/m}^2$, in stark contrast with the IPCC estimate of $+0.2 \pm 0.2 \text{ W/m}^2$. Wall et al. [161] use satellite observations to quantify relationships between sulfates and low-level clouds; they estimate a sulfate indirect aerosol forcing of $-1.11 \pm 0.43 \text{ W/m}^2$ over the global ocean. The range of aerosol forcings used in CMIP6 and AR6 GCMs (small blue bar in Fig. 18) is not a measure of aerosol forcing uncertainty. The larger bar, from Chapter 7 [162] of AR6, has negative forcing as great as -2 W/m^2 , but even that does not measure the full uncertainty.

Changes of IMO emission regulations provide a great opportunity for insight into aerosol climate forcing. Sulfur content of fuels was limited to 1% in 2010 near the coasts of North America

and in the North Sea, Baltic Sea and English Channel, and further restricted there to 0.1% in 2015 [163]. In 2020 a limit of 0.5% was imposed worldwide. The 1% limit did not have a noticeable effect on ship-tracks, but a striking reduction of ship-tracks was found after the 2015 IMO regulations, especially in the regions near land where emissions were specifically limited [164]. Following the additional 2020 regulations [165], global ship-tracks were reduced more than 50% [166].

Earth's albedo (reflectivity) measured by CERES (Clouds and Earth's Radiant Energy System) satellite-borne instruments [81] over the 22-years March 2000 to March 2022 reveal a decrease of albedo and thus an increase of absorbed solar energy coinciding with the 2015 change of IMO emission regulations. Global absorbed solar energy is + 1.05 W/m² in the period January 2015 through December 2022 relative to the mean for the first 10 years of data (Fig. 21). This increase is 5 times greater than the standard deviation (0.21 W/m²) of annual absorbed solar energy in the first 10 years of data and 4.5 times greater than the standard deviation (0.23 W/m²) of CERES data through December 2014. The increase of absorbed solar energy is notably larger than estimated potential CERES instrument drift, which is <0.085 W/m² per decade [81]. Increased solar energy absorption occurred despite 2015–2020 being the declining phase of the ~11-year solar irradiance cycle [167]. Nor can increased absorption be attributed to correlation of Earth's albedo (and absorbed solar energy) with the Pacific Decadal Oscillation (PDO): the PDO did shift to the positive phase in 2014–2017, but it returned to the negative phase in 2017–2022 [168].

Given the large increase of absorbed solar energy, cloud changes are likely the main cause. Quantitative analysis [168] of

contributions to the 20-year trend of absorbed solar energy show that clouds provide most of the change. Surface albedo decrease due to sea ice decline contributes to the 20-year trend in the Northern Hemisphere, but that sea ice decline occurred especially in 2007, with minimum sea ice cover reached in 2012; over the past decade as global and hemispheric albedos declined, sea ice had little trend [169]. Potential causes of the cloud changes include: (1) reduced aerosol forcing, (2) cloud feedbacks to global warming, (3) natural variability [170]. Absorbed solar energy was 0.77 W/m² greater in Jan2015-Dec2022 than in the first decade of CERES data at latitudes 20–60°S (Fig. 22), a region of relatively little ship traffic. This change is an order of magnitude larger than the estimate of potential detector degradation [81].

Climate models predict a reduction of cloud albedo in this region as a feedback effect driven by global warming [12] (Sec. 7.4.2.4). Continued monitoring of absorbed energy can confirm the reality of the change, but without global monitoring of detailed physical properties of aerosols and clouds [142], it will be difficult to apportion observed change among candidate causes.

North Pacific and North Atlantic regions of heavy ship traffic are ripe for detailed study of cloud changes and their causes, although unforced cloud variability is large in such sub-global regions. Both regions have increased absorption of solar radiation after 2015 (Fig. 22). The 2014–2017 maximum absorption in the North Pacific is likely enhanced by reduced cloud cover during the positive PDO, but the more recent high absorption is during the negative PDO phase. In the North Atlantic, persistence of increased absorption for several years exceeds prior variability, but longer records plus aerosol and cloud microphysical data are needed for interpretation.

Summary

Climate change is characterized by delayed response and amplifying feedbacks. Delayed response makes human-made climate forcing a threat to today's public and future generations because of the practical difficulty of reversing the forcing once consequences become apparent. Feedbacks determine climate sensitivity to any applied forcing. We find that Earth's climate is very sensitive—more sensitive than the best estimate of the Intergovernmental Panel on Climate Change (IPCC)—which implies that there is a great amount of climate change 'in the pipeline.' Extraordinary actions are needed to reduce the net human-made climate forcing, as is required to reduce global

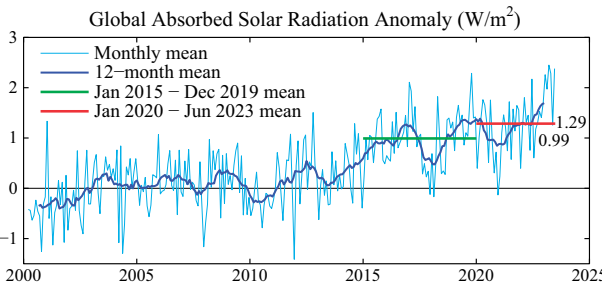


Figure 21. Global absorbed solar radiation (W/m²) relative to mean of the first 120 months of CERES data. CERES data are available at http://ceres.larc.nasa.gov/order_data.php.

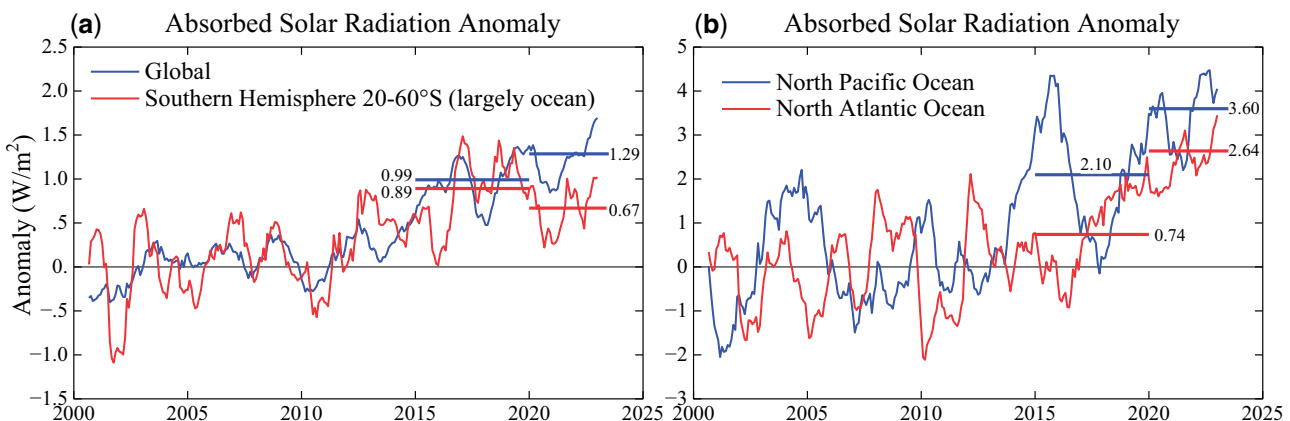


Figure 22. Absorbed solar radiation for indicated regions relative to first 120 months of CERES data. Southern Hemisphere 20–60°S is 89% ocean. North Atlantic is (20–60°N, 0–60°W) and North Pacific is (20–60°N, 120–220°W). Data source: http://ceres.larc.nasa.gov/order_data.php.

warming and avoid highly undesirable consequences for humanity and nature.

Equilibrium climate sensitivity (ECS)

The 1979 Charney study [4] considered an idealized climate sensitivity in which ice sheets and non-CO₂ GHGs are fixed. The Charney group estimated that the equilibrium response to $2 \times \text{CO}_2$, a forcing of 4 W/m^2 , was 3°C , thus an ECS of 0.75°C per W/m^2 , with one standard deviation uncertainty $\sigma = 0.375^\circ\text{C}$. Charney's estimate stood as the canonical ECS for more than 40 years. The current IPCC report [12] concludes that 3°C for $2 \times \text{CO}_2$ is their best estimate for ECS.

We compare recent glacial and interglacial climates to infer ECS with a precision not possible with climate models alone. Uncertainty about Last Glacial Maximum (LGM) temperature has been resolved independently with consistent results by Tierney et al. [49] and Seltzer et al. [51]. The Tierney approach, using a collection of geochemical temperature indicators in a global analysis constrained by climate change patterns defined by a global climate model, is used by Osman et al. [50] to find peak LGM cooling $7.0 \pm 1^\circ\text{C}$ (2σ , 95% confidence) at 21–18 kyBP. We show that, accounting for polar amplification, these analyses are consistent with the $5.8 \pm 0.6^\circ\text{C}$ LGM cooling of land areas between 45°S and 35°N found by Seltzer et al. using the temperature-dependent solubility of dissolved noble gases in ancient groundwater. The forcing that maintained the 7°C LGM cooling was the sum of $2.25 \pm 0.45 \text{ W/m}^2$ (2σ) from GHGs and $3.5 \pm 1.0 \text{ W/m}^2$ (2σ) from the LGM surface albedo, thus $5.75 \pm 1.1 \text{ W/m}^2$ (2σ). ECS implied by the LGM is thus $1.22 \pm 0.29^\circ\text{C}$ (2σ) per W/m^2 , which, at this final step, we round to $1.2 \pm 0.3^\circ\text{C}$ per W/m^2 . For transparency, we have combined uncertainties via simple RMS (root-mean-square). ECS as low as 3°C for $2 \times \text{CO}_2$ is excluded at the 3σ level, i.e. with 99.7% confidence.

More sophisticated mathematical analysis, which has merits but introduces opportunity for prior bias and obfuscation, is not essential; error assessment ultimately involves expert judgment. Instead, focus is needed on the largest source of error: LGM surface albedo change, which is uncertain because of the effect of cloud shielding on the efficacy of the forcing. As cloud modeling is advancing rapidly, this topic is ripe for collaboration of CMIP [53] (Coupled Model Intercomparison Project) with PMIP [54] (Paleoclimate Modelling Intercomparison Project). Simulations should include at the same time change of surface albedo and topography of ice sheets, vegetation change, and exposure of continental shelves due to lower sea level.

Knowledge of climate sensitivity can be advanced further via analysis of the wide climate range in the Cenozoic era (Earth system sensitivity section). However, interpretation of data and models, and especially projections of climate change, depend on understanding of climate response time.

Climate response time

We expected climate response time—the time for climate to approach a new equilibrium after imposition of a forcing—to become faster as mixing of heat in ocean models improved [75]. That expectation was not met when we compared two generations of the GISS GCM (global climate model). The GISS (2020) GCM is improved [32, 33] in its ocean simulation over the GISS (2014) GCM as a result of higher vertical and horizontal resolution, more realistic parameterization of sub-grid scale motions, and correction of errors in the ocean computer program [32]. Yet the time for the model to achieve 63% of its equilibrium response

remained about 100 years. There are two reasons for this: one that is obvious and one that is more interesting and informative.

The surface in the newer model warms as fast as in the older model, but it must achieve greater warming to reach 63% of equilibrium because its ECS is higher, which is one reason that the response time remains long. The other reason is that Earth's energy imbalance (EEI) in the newer model decreases rapidly. EEI defines the rate that heat is pumped into the ocean, so a smaller EEI implies a longer time for the ocean to reach its new equilibrium temperature. Quick drop of EEI—in the first year after introduction of the forcing—implies existence of ultrafast feedback in the GISS (2020) model. For want of an alternative with such a large effect on Earth's energy budget, we infer a rapid cloud feedback and we suggest (Slow, fast and ultrafast feedbacks section) a set of brief GCM runs that define cloud changes and other diagnostic quantities to an arbitrary accuracy.

The Charney report [4] recognized that clouds were a main cause of a wide range in ECS estimates. Today, clouds still cast uncertainty on climate predictions. Several CMIP6 [34] GCMs have ECS of $\sim 4\text{--}6^\circ\text{C}$ for $2 \times \text{CO}_2$ [171, 172] with the high sensitivity caused by cloud feedbacks [84]. As cloud modeling progresses, it will aid understanding if climate models report their $2 \times \text{CO}_2$ response functions for both temperature and EEI (Earth's energy imbalance).

Fast EEI response—faster than global temperature response—has a practical effect: observed EEI understates the reduction of climate forcing required to stabilize climate. Although the magnitude of this effect is uncertain (see Supplementary Material SM6), it makes the task of restoring a hospitable climate and saving coastal cities more challenging. On the other hand, long climate response time implies the potential for educated policies to affect the climate outcome before the most undesirable consequences occur.

The time required for climate to reach a new equilibrium is relevant to policy (Perspective on policy implications section), but there is another response time of practical importance. With climate in a state of disequilibrium, how much time do we have before we pass the point of no return, the point where major climate impacts are locked in, beyond our ability to control? That's a complex matter; it requires understanding of 'slow' feedbacks, especially ice sheets. It also depends on how far climate is out of equilibrium. Thus, we first consider the full Earth system sensitivity.

Earth system sensitivity (ESS)

The Cenozoic era—the past 66 million years—provides an opportunity to study Earth system sensitivity via a consistent analysis for climate ranging from hothouse conditions with Earth 15°C warmer and sea level 60 m higher than preindustrial climate to glacial conditions with Earth 7°C cooler and sea level 120 m lower than preindustrial. Atmospheric CO₂ amount in the past 800 000 years (Fig. 2), confirms expectation that CO₂ is the main control knob [87] on global temperature. We can assume this control existed when CO₂ amount varied due to CO₂ emissions caused by plate tectonics (continental drift). The two-step [91] that the Indian plate executed as it moved through the Tethys (now Indian) ocean left a signature in atmospheric CO₂ and global temperature. CO₂ emissions from subduction of ocean crust were greatest when the Indian plate was moving fastest (inset, Fig. 6) and peaked at its hard collision with the Eurasian plate at 50 MyBP. Diminishing metamorphic CO₂ emissions continue as the Indian plate is subducted beneath the Eurasian plate, pushing up the Himalayan Mountains, but carbon drawdown from

weathering and burial of organic carbon exceeds emissions. Motion of the Indian Plate thus dominates the broad sweep of Cenozoic CO₂, but igneous provinces play a role. The North Atlantic Igneous Province (caused by a rift in the sea floor as Greenland pulled away from Europe) that triggered the Paleocene-Eocene Thermal Maximum (PETM) event about 56 MyBP and the Columbia River Flood Basalt about 15 MyBP (Fig. 6) are most notable.

We infer the Cenozoic history of sea surface temperature (SST) at sites of deepwater formation from the oxygen isotope $\delta^{18}\text{O}$ in shells of deep-ocean-dwelling foraminifera preserved in ocean sediments [44, 90]. High latitude SST change—including a correction term as SST approaches the freezing point—provides an accurate estimate of global surface temperature change. This Cenozoic temperature history and climate sensitivity inferred from the LGM cooling yield an estimate of Cenozoic CO₂ history. We suggest that this whole-Cenozoic approach may define the CO₂ history (Fig. 9a) more accurately than CO₂ proxy measurements. We find CO₂ about 325 ppm in the early Pliocene and 450 ppm at transition to glaciated Antarctica. Global climate models (GCMs) that isolate on the Pliocene tend to use CO₂ levels of order 400 ppm in attempts to match actual Pliocene warmth and ice sheet models use CO₂ of order 700 ppm or greater to achieve ice sheet disintegration on Antarctica, which suggests that the models are not realistically capturing amplifying feedback processes (see Cenozoic CO₂ section).

The Cenozoic provides a perspective on present greenhouse gas (GHG) levels. The dashed line in Fig. 23 is the ‘we are here’ level of GHG climate forcing. Today’s GHG forcing of 4.6 W/m² is relative to mid-Holocene CO₂ of 260 ppm; we present evidence in Cenozoic CO₂ section that 260 ppm is the natural Holocene CO₂ level. Human-caused GHG forcing today is already above the level needed to deglaciate Antarctica, if such forcing is left in place long enough. We do not predict full deglaciation of Antarctica on a time scale people care about—rather we draw attention to how far today’s climate is out of equilibrium with today’s GHG level. This is one measure of how strongly humanity is pushing the climate system. Stabilizing climate requires removing the disequilibrium by reducing human-made climate forcing. A danger is that it will become difficult or implausible to prevent large sea level rise, if deglaciation is allowed to get well underway.

GHGs are not the only large human-made climate forcing. Understanding of ongoing climate change requires that we also include the effect of aerosols (fine airborne particles).

Aerosols

Aerosol climate forcing is larger than the IPCC AR6 estimate and has likely been significant for millennia. We know of no other

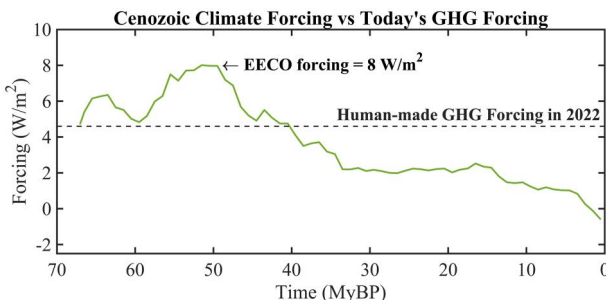


Figure 23. Forcing required to yield Cenozoic temperature for today’s solar irradiance, compared with human-made GHG forcing in 2022.

persuasive explanation for absence of global warming in the last half of the Holocene (Fig. 14) as GHG forcing increased 0.5 W/m² (Fig. 15). Climate models without a growing negative aerosol forcing yield notable warming in that period [173], a warming that, in fact, did not occur. Negative aerosol forcing, increasing as civilization developed and population grew, is expected. As humans burned fuels at a growing rate—wood and other biomass for millennia and fossil fuels in the industrial era—aerosols as well as GHGs were an abundant, growing, biproduct. The aerosol source from wood-burning has continued in modern times [146]. GHGs are long-lived and accumulate, so their forcing dominates eventually, unless aerosol emissions grow higher and higher—the Faustian bargain [98].

Multiple lines of evidence show that aerosol forcing peaked early this century [174]. Emissions from the largest sources, China and India, were increasing in 2000, but by 2010 when the first limits on ship emissions were imposed, China’s emissions were declining. We estimate peak (negative) aerosol forcing as at least 1.5–2 W/m², with turning point at 2010, consistent with Fig. 3 of Bauer et al. [175] GHG plus aerosol forcing grew +0.3 W/m² per decade (GHGs: +0.45, aerosols: -0.15) during 1970–2010, which produced warming of 0.18°C per decade. With current policies, we expect climate forcing for a few decades post-2010 to increase 0.5–0.6 W/m² per decade and produce global warming of at least +0.27°C per decade. In that case, global warming will reach 1.5°C in the 2020s and 2°C before 2050 (Fig. 24). Such acceleration is dangerous in a climate system that is already far out of equilibrium and dominated by multiple amplifying feedbacks.

The sharp change of ship emissions in 2020 (The great inadvertent aerosol experiment section) provides an indirect measure of aerosol effects. Diamond [176] finds a cloud brightness decrease of order 1 W/m² in a shipping corridor. We find a larger effect, increased absorption of about 3 W/m² in regions of heavy ship traffic in the North Atlantic and North Pacific (Fig. 22), but a longer record is needed to define significance. However, the single best sentinel for global climate change is Earth’s energy imbalance.

Earth’s energy imbalance

Earth’s energy imbalance (EEI) is the net gain (or loss) of energy by the planet, the difference between absorbed solar energy and emitted thermal (heat) radiation. As long as EEI is positive, Earth will continue to get hotter. EEI is hard to measure, a small difference between two large quantities (Earth absorbs and emits

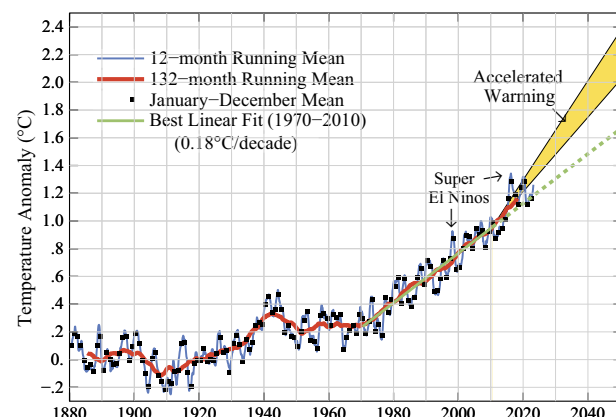


Figure 24. Global temperature relative to 1880–1920. Edges of the predicted post-2010 accelerated warming rate (see text) are 0.36 and 0.27°C per decade.

about 240 W/m² averaged over the entire planetary surface), but change of EEI can be well-measured from space [81]. Absolute calibration is from the change of heat in the heat reservoirs, mainly the global ocean, over a period of at least a decade, as needed to reduce error due to the finite number of places that the ocean is sampled [80]. EEI varies year-to-year (Fig. 25), largely because global cloud amount varies with weather and ocean dynamics, but averaged over several years EEI helps inform us about what is needed to stabilize climate.

The data indicate that EEI has doubled since the first decade of this century (Fig. 25). This increase is one basis for our prediction of post-2010 acceleration of the global warming rate. The EEI increase may be partly due to restrictions on maritime aerosol precursor emissions imposed in 2015 and 2020 (The great inadvertent aerosol experiment section), but the growth rate of GHG climate forcing also increased in 2015 and since has remained at the higher level (Equilibrium warming versus committed warming section).

Reduction of climate forcing needed to reduce EEI to zero is greater than EEI because of ultrafast cloud feedback (Slow, fast and ultrafast feedbacks section), but the magnitude of this effect is uncertain (SM6). Cloud feedbacks are only beginning to be simulated well, but climate sensitivity near 1.2°C per W/m² implies that the net cloud feedback is large and deserves greater attention. Precise monitoring of EEI is essential as a sentinel for future climate change and to assess efforts to stabilize climate and avoid undesirable consequences. Global satellite monitoring of geographical and temporal changes of EEI and ocean in situ monitoring (especially in polar regions of rapid change) are both needed for the sake of understanding ongoing climate change.

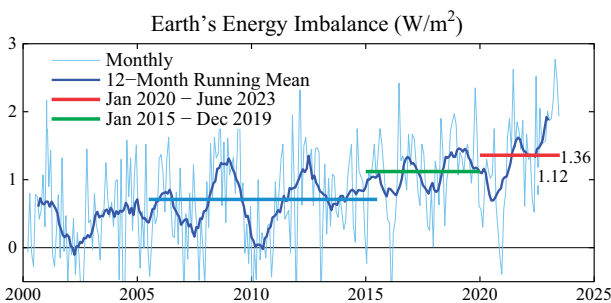


Figure 25. 12-month running-mean of Earth's energy imbalance from CERES satellite data [81] normalized to 0.71 W/m² mean for July 2005–June 2015 (blue bar) from in situ data [80].

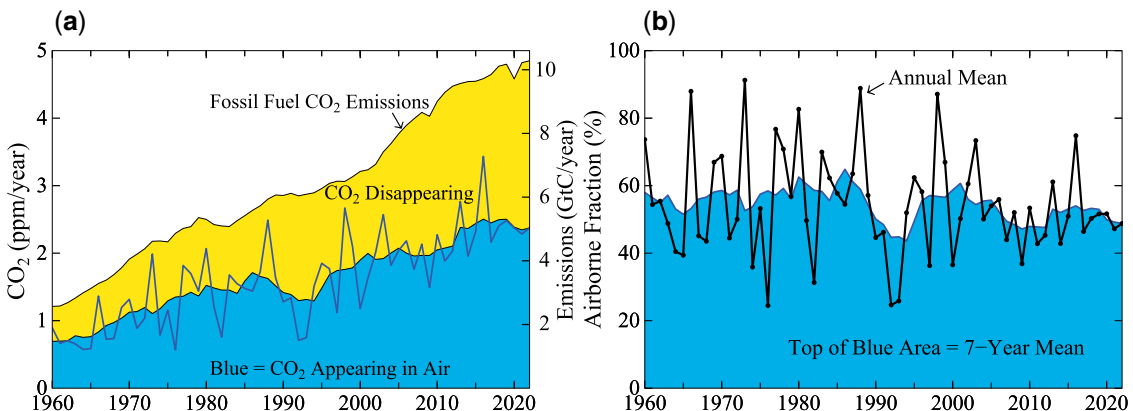


Figure 26. Fossil fuel emissions divided into portions appearing in the annual increase of airborne CO₂ and the remainder, which is taken up by the ocean and land (1 ppm CO₂ ~ 2.12 GtC).

Equilibrium warming versus committed warming

Equilibrium warming for today's climate forcing is the warming required to restore Earth's energy balance if atmospheric composition is fixed at today's conditions. Equilibrium warming is a benchmark that can be evaluated from atmospheric composition and paleoclimate data, with little involvement of climate models. It is the standard benchmark used in definition of the Charney ECS (equilibrium climate sensitivity excluding slow feedbacks) [4] and ESS (Earth system sensitivity, which includes slow feedbacks such as ice sheet size) [71]. GHG climate forcing now is 4.6 W/m² relative to the mid-Holocene (7 kyBP) or 4.1 W/m² relative to 1750. There is little merit in debating whether GHG forcing is 4.6 or 4.1 W/m² because it is still increasing 0.5 W/m² per decade (Perspective on policy implications section). ECS response to 4.6 W/m² forcing for climate sensitivity 1.2°C per W/m² is 5.5°C. The eventual Earth system response (ESS) to sustained 4.6 W/m² forcing is about 10°C (Earth system sensitivity section), because that forcing is large enough to deglaciate Antarctica (Fig. 23). Net human-made forcing today is probably near 3 W/m² due to negative aerosol forcing. Even 3 W/m² may be sufficient to largely deglaciate Antarctica, if the forcing is left in place permanently (Fig. 23).

'Committed warming' is less precisely defined; even in the current IPCC report [12] (p. 2222) it has multiple definitions. One concept is the warming that occurs if human-made GHG emissions cease today, but that definition is ill-posed as well as unrealistic. Do aerosol emissions also cease? That would cause a sudden leap in Earth's energy imbalance, a 'termination shock,' as the cooling effect of human-made aerosols disappears. A more useful definition is the warming that will occur with plausibly rapid phasedown of GHG emissions, including comparison with ongoing reality. However, the required 'integrated assessment models,' while useful, are complex and contain questionable assumptions that can mislead policy (see Perspective on policy implications section).

Nature's capacity for restoration provides hope that future warming can be limited, if humanity moves promptly toward sustainable energy and climate policies. Earth's ability to remove human-made CO₂ emissions from the atmosphere is revealed by Fig. 26. Fossil fuel emissions now total more than 10 GtC/year, which is almost 5 ppm of CO₂, yet CO₂ in the air is only increasing 2.5 ppm/year. The other half is being taken up by the ocean, solid land, and biosphere. Indeed, Earth is taking up even more because deforestation, fires, and poor agricultural and forestry practices are additional human-made CO₂ sources. If human emissions ceased, atmospheric CO₂ would initially decline a few

ppm per year, but uptake would soon slow—it would take millennia for CO₂ to reach preindustrial levels [131]. This underscores the difficulty of restoring Earth's energy balance via emission reductions alone. Furthermore, fossil fuels have raised living standards in most of the world and still provide 80% of the world's energy, which contributes to a policy inertia. As the reality of climate change emerges, the delayed response of climate and amplifying feedbacks assure that the world has already set sail onto even more turbulent climate seas. Scientists must do their best to help the public understand policy options that may preserve and restore a propitious climate for future generations.

Perspective on policy implications

This section is the first author's perspective based on more than 20 years of experience on policy issues that began with a paper [179] and two workshops [180] that he organized at the East-West Center in Hawaii, followed by meetings and workshops with utility experts and trips to more than a dozen nations for discussions with government officials, energy experts, and environmentalists. The aim was to find a realistic scenario with a bright energy and climate future, with emphasis on cooperation between the West and nations with emerging or underdeveloped economies.

Energy, CO₂ and the climate threat

The world's energy and climate path has good reason: fossil fuels powered the industrial revolution and raised living standards.

Fossil fuels still provide most of the world's energy (Fig. 27a) and produce most CO₂ emissions (Fig. 27b). Much of the world is still in early or middle stages of economic development. Energy is needed and fossil fuels are a convenient, affordable source of energy. One gallon (3.8 l) of gasoline (petrol) provides the work equivalent of more than 400 h labor by a healthy adult. These benefits are the basic reason for continued high emissions. The Covid pandemic dented emissions in 2020, but 2022 global emissions were a record high level. Fossil fuel emissions from mature economies are beginning to fall due to increasing energy efficiency, introduction of carbon-free energies, and export of manufacturing from mature economies to emerging economies. However, at least so far, those reductions have been more than offset by increasing emissions in developing nations (Fig. 28).

The potential for rising CO₂ to be a serious threat to humanity was the reason for the 1979 Charney report, which confirmed that climate was likely sensitive to expected CO₂ levels in the 21st century. In the 1980s it emerged that high climate sensitivity implied a long delay between changing atmospheric composition and the full climate response. Ice core data revealed the importance of amplifying climate feedbacks. A climate characterized by delayed response and amplifying feedbacks is especially dangerous because the public and policymakers are unlikely to make fundamental changes in world energy systems until they see visible evidence of the threat. Thus, it is incumbent on scientists to make this situation clear to the public as soon as possible. That task is complicated by the phenomenon of scientific reticence.

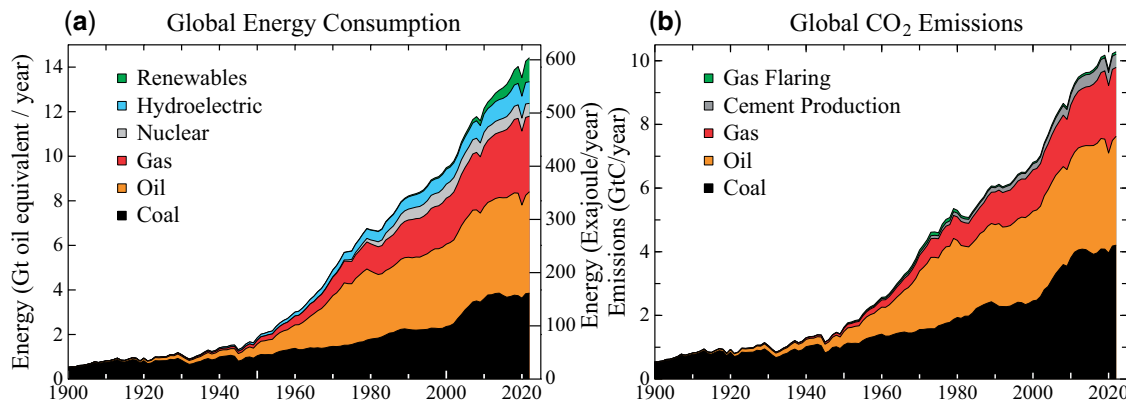


Figure 27. Global energy consumption and CO₂ emissions (Hefner et al. [177] and Energy Institute [178]).

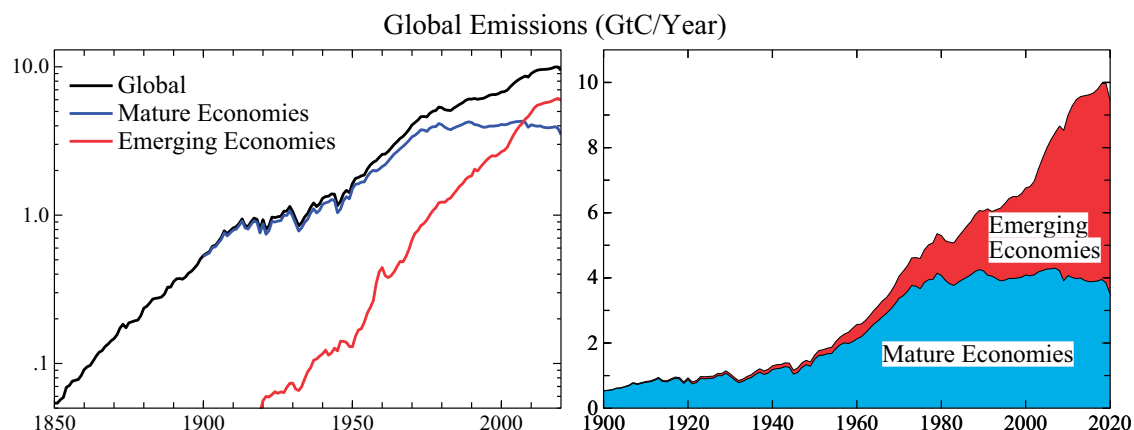


Figure 28. Fossil fuel CO₂ emissions from mature and emerging economies. China is counted as an emerging economy. Data sources as in Fig. 27.

Scientific reticence

Bernard Barber decried the absence of attention to scientific reticence, a tendency of scientists to resist scientific discovery or new ideas [139]. Richard Feynman needled fellow physicists about their reticence to challenge authority [181], specifically to correct the electron charge that Millikan derived in his famous oil drop experiment. Later researchers moved Millikan's result bit by bit—experimental uncertainties allow judgment—reaching an accurate result only after years. Their reticence embarrassed the physics community but caused no harm to society. A factor that may contribute to reticence among climate scientists is ‘delay discounting’: preference for immediate over delayed rewards [182]. The penalty for ‘crying wolf’ is immediate, while the danger of being blamed for ‘fiddling while Rome was burning’ is distant. One of us has noted [183] that larding of papers and proposals with caveats and uncertainties increases chances of obtaining research support. ‘Gradualism’ that results from reticence is comfortable and well-suited for maintaining long-term support. Gradualism is apparent in IPCC’s history in evaluating climate sensitivity as summarized in our present paper. Barber identifies professional specialization—which causes ‘outsiders’ to be ignored by ‘insiders’—as one cause of reticence; specialization is relevant to ocean and ice sheet dynamics, matters upon which the future of young people hangs.

Discussion [184] with field glaciologists¹³ 20 years ago revealed frustration with IPCC’s ice sheet assessment. One glaciologist said—about a photo [185] of a moulin (a vertical shaft that carries meltwater to the base of the Greenland ice sheet)—‘the whole ice sheet is going down that damned hole!’ Concern was based on observed ice sheet changes and paleoclimate evidence of sea level rise by several meters in a century, implying that ice sheet collapse is an exponential process. Thus, as an alternative to ice sheet models, we carried out a study described in *Ice Melt* [13]. In a GCM simulation, we added a growing freshwater flux to the ocean surface mixed layer around Greenland and Antarctica, with the flux in the early 21st century based on estimates from in situ glaciological studies [186] and satellite data on sea level trends near Antarctica [187]. Doubling times of 10 and 20 years were used for the growth of freshwater flux. One merit of our GCM was reduced, more realistic, small-scale ocean mixing, with a result that Antarctic Bottom Water formed close to the Antarctic coast [13], as in the real world. Growth of meltwater and GHG emissions led to shutdown of the North Atlantic and Southern Ocean overturning circulations, amplified warming at the foot of the ice shelves that buttress the ice sheets, and other feedbacks consistent with ‘nonlinearly growing sea level rise, reaching several meters in 50–150 years’ [13]. Shutdown of ocean overturning circulation occurs this century, as early as midcentury. The 50–150-year time scale for multimeter sea level rise is consistent with the 10–20-year range for ice melt doubling time. Real-world ice melt will not follow a smooth curve, but its growth rate is likely to accelerate in coming years due to increasing heat flux into the ocean (Fig. 25).

We submitted *Ice Melt* to a journal that makes reviews publicly available [188]. One reviewer, an IPCC lead author, seemed intent on blocking publication, while the other reviewer described the paper as a ‘masterwork of scholarly synthesis, modeling virtuosity, and insight, with profound implications’. Thus, the editor obtained additional reviewers, who recommended publication. Promptly, an indictment was published [189] of our conclusion that continued high GHG emissions would cause shutdown of the AMOC (Atlantic Meridional Overturning Circulation) this

century. The 15 authors, representing leading GCM groups, used 21 climate projections from eight ‘... state-of-the-science, IPCC class ...’ GCMs to conclude that ‘... the probability of an AMOC collapse is negligible. This is contrary to a recent modeling study [Hansen et al., 2016] that used a much larger, and in our assessment unrealistic, Northern Hemisphere freshwater forcing... According to our probabilistic assessment, the likelihood of an AMOC collapse remains very small (<1% probability) if global warming is below ~ 5K ...’[189]. They treated the ensemble of their model results as if it were the probability distribution for the real world.

In contrast, we used paleoclimate evidence, global modeling, and ongoing climate observations. Paleoclimate data [190] showed that AMOC shutdown is not unusual and occurred in the Eemian (when global temperature was similar to today), and also that sea level in the Eemian rose a few meters within a century [191] with the likely source being collapse of the West Antarctic ice sheet. Although we would not assert that our model corrected all excessive ocean mixing, the higher vertical resolution and improved mixing increased the sensitivity to freshwater flux, as confirmed in later tests [192]. Modern observations showed and continue to add evidence that the overturning Southern Ocean [193, 194] and North Atlantic [195] are already slowing. Growth of meltwater injection onto the Southern [196] and North Atlantic Oceans [197] is consistent with a doubling time of 10–20 years. High climate sensitivity inferred in our present paper also implies there will be a greater increase of precipitation on polar oceans than that in most climate models.

The indictment of *Ice Melt* by Bakker et al. [189] was accepted by the research community. Papers on the same topics ignored our paper or referred to it parenthetically with a note that we used unrealistic melt rates, even though these were based on observations. *Ice Melt* was blackballed in IPCC’s AR6 report, which is a form of censorship [14]. Science usually acknowledges alternative views and grants ultimate authority to nature. In the opinion of our first author, IPCC does not want its authority challenged and is comfortable with gradualism. Caution has merits, but the delayed response and amplifying feedbacks of climate make excessive reticence a danger. Our present paper—via revelation that the equilibrium response to current atmospheric composition is a nearly ice-free Antarctica—amplifies concern about locking in nonlinearly growing sea level rise. Also, our conclusion that CO₂ was about 450 ppm at Antarctic glaciation disparages ice sheet models. Portions of the ice sheets may be recalcitrant to rapid change, but enough ice is in contact with the ocean to provide of the order of 25 m (80 feet) of sea level rise. Thus, if we allow a few meters of sea level rise, we may lock in much larger sea level rise.

Climate change responsibilities

The industrial revolution began in the U.K., which was the largest source of fossil fuel emissions in the 19th century (Fig. 29a), but development soon moved to Germany, the rest of Europe, and the U.S. Nearly half of global emissions were from the U.S. in the early 20th century, and the U.S. is presently the largest source of cumulative emissions (Fig. 29b) that drive climate change [198, 199]. Mature economies, mainly in the West, are responsible for most cumulative emissions, especially on a per capita basis (Fig. 30). Growth of emissions is now occurring in emerging economies (Figs 28 and 29a). China’s cumulative emissions will eventually pass those of the U.S. in the absence of a successful effort to replace coal with carbon-free energy.

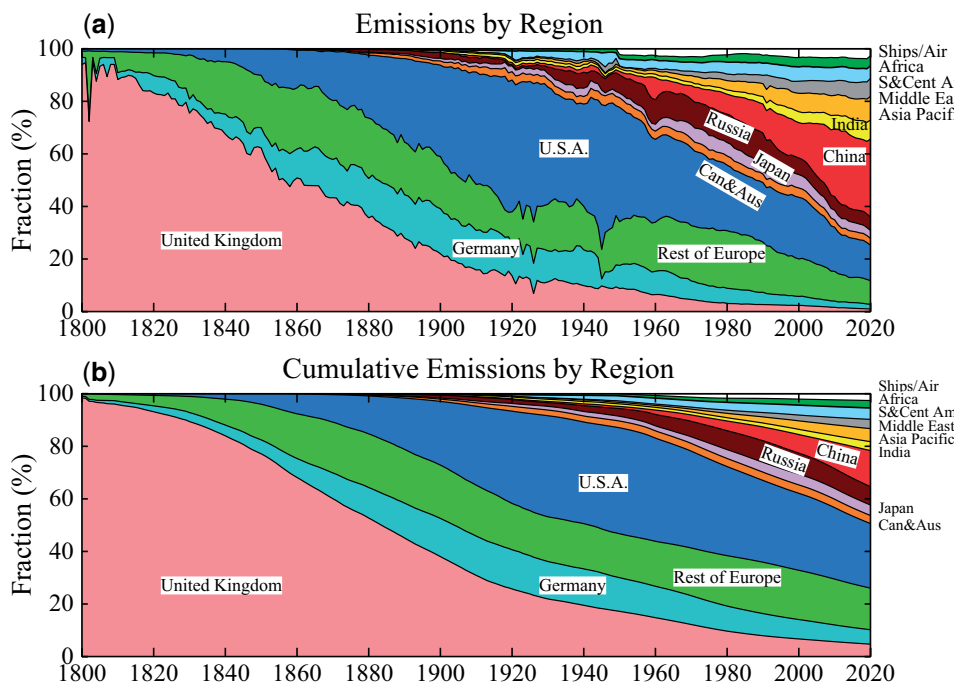


Figure 29. Fossil fuel CO₂ emissions by nation or region as a fraction of global emissions. Data sources as in Fig. 27.

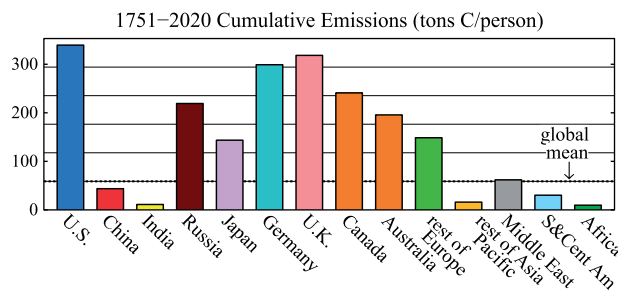


Figure 30. Cumulative per capita national fossil fuel emissions [200].

Greenhouse gas emissions situation

The United Nations uses a target for maximum global warming to cajole progress in limiting climate change. The 2015 Paris Agreement [201] aimed to hold ‘the increase in the global average temperature to well below 2°C above the pre-industrial levels and pursue efforts to limit the temperature increase to 1.5°C above the pre-industrial levels.’ The IPCC AR5 report added a climate forcing scenario, RCP2.6, with a rapid decrease of GHG climate forcings, as needed to prevent global warming from exceeding 2°C. Since then, a gap between that scenario and reality opened and is growing (Fig. 31). The 0.03 W/m² gap in 2022 could be closed by extracting CO₂ from the air. However, required negative emissions (CO₂ extracted from the air and stored permanently) must be larger than the desired atmospheric CO₂ reduction by a factor of about 1.7 [63]. Thus, the required CO₂ extraction is 2.1 ppm, which is 7.6 GtC. Based on a pilot direct-air carbon capture plant, Keith [202] estimates an extraction cost of \$450–920 per tC, as clarified elsewhere [203]. Keith’s cost range yields an extraction cost of \$3.4–7.0 trillion. That covers excess emissions in 2022 only; it is an annual cost. Given the difficulty the UN faced in raising \$0.1 trillion for climate purposes and the growing emissions gap (Fig. 31), this example shows the need to

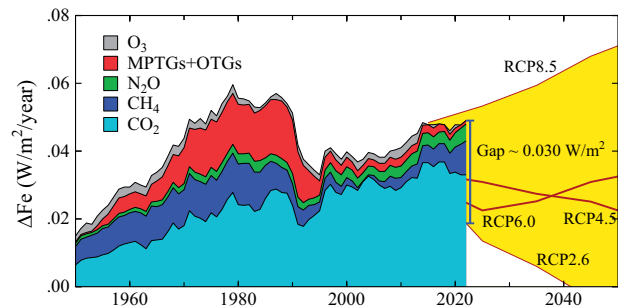


Figure 31. Annual growth of climate forcing by GHGs [38] including part of O₃ forcing not included in CH₄ forcing (Supplementary Material). MPTG and OTG are Montreal Protocol and Other Trace Gases.

reduce emissions as rapidly as practical and shows that carbon capture cannot be viewed as the solution, although it may play a role in a portfolio of policies, if its cost is driven down.

IPCC (Intergovernmental Panel on Climate Change), the scientific body advising the world on climate, has not bluntly informed the world that the present precatory policy approach will not keep warming below 1.5°C or even 2°C. The ‘tragedy of the commons’ [204] is that, as long as fossil fuel pollution can be dumped in the air free of charge, agreements such as the Kyoto Protocol [205] and Paris Agreement have limited effect on global emissions. Political leaders profess ambitions for dubious net-zero emissions while fossil fuel extraction expands. IPCC scenarios that phase down human-made climate change amount to ‘a miracle will occur’. The IPCC scenario that moves rapidly to negative global emissions (RCP2.6) has vast biomass-burning powerplants that capture and sequester CO₂, a nature-ravaging, food-security-threatening [206], proposition without scientific and engineering credibility and without a realistic chance of being deployed at scale and on time to address the climate threat.

Climate and energy policy

Climate science reveals the threat of being too late. ‘Being too late’ refers not only to warning of the climate threat, but also to technical advice on policy implications. Are we scientists not complicit if we allow reticence and comfort to obfuscate our description of the climate situation? Does our training, years of graduate study and decades of experience, not make us well-equipped to advise the public on the climate situation and its policy implications? As professionals with deep understanding of planetary change and as guardians of young people and their future, do we not have an obligation, analogous to the code of ethics of medical professionals, to render to the public our full and unencumbered diagnosis? That is our objective.

The basis for the following opinions of the first author, to the extent not covered in this paper, will be described in a book in preparation [2]. We are in the early phase of a climate emergency. The present huge planetary energy imbalance assures that climate will become less tolerable to humanity, with greater climate extremes, before it is feasible to reverse the trend. Reversing the trend is essential—we must cool the planet—for the sake of preserving shorelines and saving the world’s coastal cities. Cooling will also address other major problems caused by global warming. We should aim to return to a climate like that in which civilization developed, in which the nature that we know and love thrived. As far as is known, it is still feasible to do that without passing through irreversible disasters such as many-meter sea level rise.

Abundant, affordable, carbon-free energy is essential to achieve a world with propitious climate, while recognizing the rights and aspirations of all people. The staggering magnitude of the task is implied by global and national carbon intensities: carbon emissions per unit energy use (Fig. 32). Global carbon intensity must decline to near zero over the next several decades. This chart—not vaporous promises of net zero future carbon emissions inserted in integrated assessment models—should guide realistic assessment of progress toward clean energy. Policy must include apolitical targeting of support for development of low-cost carbon-free energy. All nations would do well to study strategic decisions of Sweden, which led past decarbonization efforts (Fig. 32) and is likely to lead in the quest for zero or negative carbon intensity that will be needed to achieve a bright future for today’s young people and future generations.

Given the global situation that we have allowed to develop, three actions are now essential.

First, underlying economic incentives must be installed globally to promote clean energy and discourage CO₂ emissions.

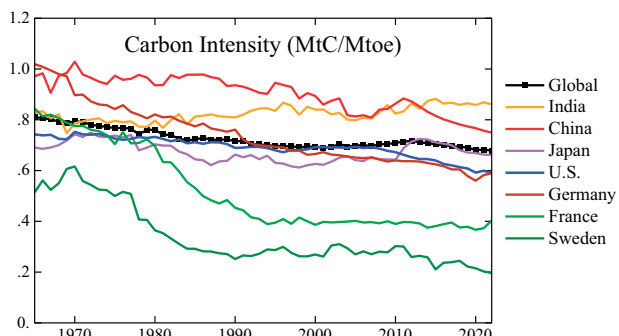


Figure 32. Carbon intensity (carbon emissions per unit energy use) of several nations and the world. Mtoe = megatons of oil equivalent. Data sources as in Fig. 27.

Thus, a rising price on GHG emissions is needed, enforced by border duties on products from nations without a carbon fee. Public buy-in and maximum efficacy require the funds to be distributed to the public, which will also address wealth disparity. Economists in the U.S. support carbon fee-and-dividend [207]; college and high school students join in advocacy [208]. A rising carbon price creates a level playing field for energy efficiency, renewable energy, nuclear power, and innovations; it would spur the thousands of ‘miracles’ needed for energy transition. However, instead, fossil fuels and renewable energy are now subsidized. Thus, nuclear energy has been disadvantaged and excluded as a ‘clean development mechanism’ under the Kyoto Protocol, based on myths about nuclear energy unsupported by scientific fact [209]. A rising carbon price is crucial for decarbonization, but not enough. Long-term planning is needed. Sweden provides an example: 50 years ago, its government decided to replace fossil fuel power stations with nuclear energy, which led to its extraordinary and rapid decarbonization (Fig. 32).

Second, global cooperation is needed. De facto cooperation between the West and China drove down the price of renewable energy. Without greater cooperation, developing nations will be the main source of future GHG emissions (Fig. 28). Carbon-free, dispatchable electricity is a crucial need. Nations with emerging economies are eager to have modern nuclear power because of its small environmental footprint. China-U.S. cooperation to develop low-cost nuclear power was proposed, but stymied by U.S. prohibition of technology transfer [210]. Competition is normal, but it can be managed if there is a will, reaping benefits of cooperation over confrontation [211]. Of late, priority has been given instead to economic and military hegemony, despite recognition of the climate threat, and without consultation with young people or seeming consideration of their aspirations. Scientists can support an ecumenical perspective of our shared future by expanding international cooperation. Awareness of the gathering climate storm will grow this decade, so we must increase scientific understanding worldwide as needed for climate restoration.

Third, we must take action to reduce and reverse Earth’s energy imbalance. Highest priority is to phase down emissions, but it is no longer feasible to rapidly restore energy balance via only GHG emission reductions. Additional action is almost surely needed to prevent grievous escalation of climate impacts including lock-in of sea level rise that could destroy coastal cities world-wide. At least several years will be needed to define and gain acceptance of an approach for climate restoration. This effort should not deter action on mitigation of emissions; on the contrary, the concept of human intervention in climate is distasteful to many people, so support for GHG emission reductions will likely increase. Temporary solar radiation management (SRM) will probably be needed, e.g. via purposeful injection of atmospheric aerosols. Risks of such intervention must be defined, as well as risks of no intervention; thus, the U.S. National Academy of Sciences recommends research on SRM [212]. The Mt. Pinatubo eruption of 1991 is a natural experiment [213, 214] with a forcing that reached [30] –3 W/m². Pinatubo deserves a co-ordinated study with current models. The most innocuous aerosols may be fine salty droplets extracted from the ocean and sprayed into the air by autonomous sailboats [215]. This approach has been discussed for potential use on a global scale [216], but it needs research into potential unintended effects [217]. This decade may be our last chance to develop the knowledge, technical capability, and political will for actions needed to save global coastal regions from long-term inundation.

Politics and climate change

Actions needed to drive carbon intensity to zero—most important a rising carbon fee—are feasible, but not happening. The first author gained perspective on the reasons why during trips to Washington, DC, and to other nations at the invitation of governments, environmentalists, and, in one case, oil executives in London. Politicians from right (conservative) and left (progressive) parties are affected by fossil fuel interests. The right denies that fossil fuels cause climate change or says that the effect is exaggerated. The left takes up the climate cause but proposes actions with only modest effect, such as cap-and-trade with offsets, including giveaways to the fossil fuel industry. The left also points to work of Amory Lovins as showing that energy efficiency plus renewables (mainly wind and solar energy) are sufficient to phase out fossil fuels. Lovins says that nuclear power is not needed. It is no wonder that the President of Shell Oil would write a foreword with praise for Lovins' book, *Reinventing Fire* [218], and that the oil executives in London did not see Lovins' work as a threat to their business.

Opportunities for progress often occur in conjunction with crises. Today, the world faces a crisis—political polarization, especially in the United States—that threatens effective governance. Yet the crisis offers an opportunity for young people to help shape the future of the nation and the planet. Ideals professed by the United States at the end of World War II were consummated in formation of the United Nations, the World Bank, the Marshall Plan, and the Universal Declaration of Human Rights. Progress toward equal rights continued, albeit slowly. The 'American dream' of economic opportunity was real, as most people willing to work hard could afford college. Immigration policy welcomed the brightest; NASA in the 1960s invited scientists from European countries, Japan, China, India, Canada, and those wanting to stay found immigration to be straightforward. But the power of special interests in Washington grew, government became insular and inefficient, and Congress refused to police itself. Their first priority became reelection and maintenance of elite status, supported by special interests. Thousands of pages of giveaways to special interests lard every funding bill, including the climate bill titled 'Inflation Reduction Act'—Orwellian double-speak—as the funding is borrowed from young people via deficit spending. The public is fed up with the Washington swamp but hamstrung by rigid two-party elections focused on a polarized cultural war.

A political party that takes no money from special interests is essential to address political polarization, which is necessary if the West is to be capable of helping preserve the planet and a bright future for coming generations. Young people showed their ability to drive an election—via their support of Barack Obama in 2008 and Bernie Sanders in 2016—without any funding from special interests. Groundwork is being laid to allow third party candidates in 2026 and 2028 elections in the U.S. Ranked voting is being advocated in every state to avoid the 'spoiler' effect of a third party. It is asking a lot to expect young people to grasp the situation that they have been handed—but a lot is at stake. As they realize that they are being handed a planet in decline, the first reaction may be to stamp their feet and demand that governments do better, but that has little effect. Nor is it sufficient to parrot big environmental organizations, which are now part of the problem, as they are partly supported by the fossil fuel industry and wealthy donors who are comfortable with the status quo. Instead, young people have the opportunity to provide the drive for a revolutionary third party that restores democratic ideals

while developing the technical knowledge that is needed to navigate the stormy sea that their world is setting out upon.

Acknowledgements

We thank Eelco Rohling for inviting JEH to describe our perspective on global climate response to human-made forcing. JEH began to write a review of past work, but a paper on the LGM by Jessica Tierney et al. [49] and data on changing ship emissions provided by Leon Simons led to the need for new analyses and division of the paper into two parts. We thank Jessica also for helpful advice on other related research papers, Jim Zachos and Thomas Westerhold for explanations of their data and interpretations, Ed Dlugokencky of the NOAA Earth System Research Laboratory for continually updated GHG data, and David Arthur for pointing out the paper by Steinberger et al. JEH designed the study and carried out the research with help of Makiko Sato and Isabelle Sangha; Larissa Nazarenko provided data from GISS models and helped with analysis; Leon Simons provided ship emission information and aided interpretations; Pushker Kharecha provided critical review of the paper; James Zachos provided critical interpretation of ocean core data needed for interpretation of Cenozoic climate; Norman Loeb and Karina von Schuckmann provided EEI data and insight about implications; Matthew Osman provided paleoclimate data and an insightful review of an early draft paper; Qinjian Jin provided simulations of atmospheric sulfate and interpretations; Eunbi Jeong reviewed multiple drafts and advised on presentation; all authors contributed to our research summarized in the paper and reviewed and commented on the manuscript. Climate Science, Awareness and Solutions, which is directed by JEH and supports MS and PK is a 501(C3) nonprofit supported 100% by public donations. Principal supporters in the past few years have been the Grantham Foundation, Frank Batten, Eric Lemelson, James and Krisann Miller, Carl Page, Peter Joseph, Ian Cumming, Gary and Claire Russell, Donald and Jeanne Keith Ferris, Aleksandar Totic, Chris Arndt, Jeffrey Miller, Morris Bradley and about 150 more contributors to annual appeals.

Supplementary data

[Supplementary data](#) are available at Oxford Open Climate Change online.

Conflict of interest

The authors declare that they have no conflict of interest.

Data availability

The data used to create the Figs in this paper are available in the Zenodo repository, at <https://zenodo.org/record/8419583>.

Authors' contributions

James Hansen (Conceptualization [lead], Data curation [equal], Formal analysis [lead], Funding acquisition [lead], Investigation [lead], Methodology [lead], Project administration [lead], Resources [lead], Software [equal], Supervision [lead], Validation [lead], Visualization [equal], Writing—original draft [lead], Writing—review and editing [lead]), Makiko Sato (Data curation [equal], Formal analysis [supporting], Investigation [supporting], Methodology [supporting], Project administration [supporting]),

Resources [supporting], Software [equal], Supervision [supporting], Validation [supporting], Visualization [equal], Writing—original draft [supporting], Writing—review and editing [supporting]), Leon Simons (Data curation [supporting], Formal analysis [supporting], Investigation [supporting], Methodology [supporting], Resources [supporting], Software [supporting], Supervision [supporting], Validation [supporting], Visualization [supporting], Writing—review and editing [supporting]), Larissa S. Nazarenko (Data curation [supporting], Formal analysis [supporting], Investigation [supporting], Methodology [supporting], Resources [supporting], Software [supporting], Supervision [supporting], Validation [supporting], Visualization [supporting], Writing—review and editing [supporting]), Isabelle Sangha (Formal analysis [supporting], Investigation [supporting], Methodology [supporting], Resources [supporting], Software [supporting], Supervision [supporting], Validation [supporting], Visualization [supporting], Writing—review and editing [supporting]), Pushker Kharecha (Formal analysis [supporting], Investigation [supporting], Methodology [supporting], Resources [supporting], Software [supporting], Supervision [supporting], Validation [supporting], Writing—review and editing [supporting]), James Zachos (Data curation [supporting], Resources [supporting], Writing—review and editing [supporting]), Karina von Schuckmann (Formal analysis [supporting], Investigation [supporting], Methodology [supporting], Resources [supporting], Software [supporting], Supervision [supporting], Validation [supporting], Writing—review and editing [supporting]), Norman G. Loeb (Data curation [supporting], Formal analysis [supporting], Investigation [supporting], Methodology [supporting], Resources [supporting], Software [supporting], Supervision [supporting], Validation [supporting], Visualization [supporting], Writing—review and editing [supporting]), Matthew B. Osman (Data curation [supporting], Formal analysis [supporting], Investigation [supporting], Methodology [supporting], Resources [supporting], Software [supporting], Supervision [supporting], Validation [supporting], Visualization [supporting], Writing—review and editing [supporting]), Qinjian Jin (Data curation [supporting], Formal analysis [supporting], Investigation [supporting], Methodology [supporting], Resources [supporting], Software [supporting], Supervision [supporting], Validation [supporting], Visualization [supporting], Writing—review and editing [supporting]), George Tselioudis (Formal analysis [supporting], Investigation [supporting], Methodology [supporting], Resources [supporting], Software [supporting], Supervision [supporting], Validation [supporting], Visualization [supporting], Writing—review and editing [supporting]), Eunbi Jeong (Formal analysis [supporting], Investigation [supporting], Methodology [supporting], Resources [supporting], Software [supporting], Supervision [supporting], Validation [supporting], Writing—review and editing [supporting]), Andrew Lacis (Formal analysis [supporting], Investigation [supporting], Methodology [supporting], Resources [supporting], Software [supporting], Supervision [supporting], Validation [supporting], Writing—review and editing [supporting]), Reto Ruedy (Formal analysis [supporting], Investigation [supporting], Methodology [supporting], Resources [supporting], Software [supporting], Supervision [supporting], Validation [supporting], Visualization [supporting], Writing—review and editing [supporting]), Gary Russell (Formal analysis [supporting], Investigation [supporting], Methodology [supporting], Resources [supporting], Software [supporting], Supervision [supporting], Validation [supporting], Writing—review and editing [supporting]), Junji Cao (Formal analysis [supporting], Investigation [supporting], Methodology [supporting], Resources [supporting], Software [supporting], Supervision [supporting], Validation [supporting], Writing—review and editing [supporting]), Jing Li (Formal analysis [supporting], Investigation [supporting],

Methodology [supporting], Resources [supporting], Software [supporting], Supervision [supporting], Validation [supporting], Writing—review and editing [supporting]).

Notes

1. Drafts of the chapters of Sophie's Planet relevant to climate sensitivity are available [here](#); criticisms are welcome.
2. David EE Jr later became a global warming denier.
3. GISS (2020) model is described as GISS-E2.1-G-NINT in published papers; NINT (noninteractive) signifies that the models use specified GHG and aerosol amounts.
4. An imbalance of 1 W/m^2 for a millennium is enough energy to melt ice raising sea level 110 m or to raise the temperature of the ocean's upper kilometer by 11°C .
5. Tom Delworth (NOAA Geophysical Fluid Dynamics Laboratory), Gokhan Danabasoglu (National Center for Atmospheric Research), and Jonathan Gregory (UK Hadley Centre) kindly provided long $2 \times \text{CO}_2$ runs of GCMs of these leading modeling groups. All three models had response time as slow or slower than the GISS GCM.
6. The GISS (2014) model is labeled as GISS-E2-R-NINT and GISS (2020) as GISS-E2.1-G-NINT in published papers, where NINT (noninteractive) signifies that the models use specified GHG and aerosol amounts.
7. In Swedish, trapps are stairs. Basalt formations are commonly in layers from multiple extrusions.
8. Small apparent discrepancy is roundoff. CO_2 forcing is 9.13 W/m^2 and solar forcing is -1.16 W/m^2 at 50 MyBP.
9. Forcing = 4.6 W/m^2 assumes that the increase of non- CO_2 GHGs is human-made. This is true for CFCs and most trace gases, but a small part of CH_4 and N_2O growth could be a slow feedback, slightly reducing the GHG forcing.
10. 9.9°C for ECS = 1.2°C per W/m^2 ; 10.1°C for ECS = 1.22°C per W/m^2 (the precise ECS for 7°C LGM cooling).
11. Two significant flaws in the derivation of this 'alternative aerosol scenario' were largely offsetting: (1) the intermediate climate response function employed was too 'fast', but (2) this was compensated by use of a low climate sensitivity of 3°C for $2 \times \text{CO}_2$.
12. In the absence of a response function from a GCM with ECS = 4°C , we use the normalized response function of the GISS (2020) model and put $\lambda = 1^\circ\text{C}$ per W/m^2 in [Equation \(5\)](#).
13. Jay Zwally, Eric Rignot, Konrad Steffen, and Roger Braithwaite.

References

1. Tyndall J. On the absorption and radiation of heat by gases and vapours. *Phil Mag* 1861;**22**:169–194, 273–285.
2. Hansen J. Greenhouse Giants, Chapter 15 in Sophie's Planet. New York: Bloomsbury, 2024.
3. Revelle R, Broecker W, Craig H et al. Appendix Y4 atmospheric carbon dioxide. In: Hornig J, York HF, Branscomb LM et al. (eds.) President's Science Advisory Committee. Restoring the Quality of Our Environment. Washington: The White House, 1965, 111–33.
4. Charney J, Arakawa A, Baker D et al. Carbon Dioxide and Climate: A Scientific Assessment. Washington: National Academy of Sciences Press, 1979.
5. Nierenberg WA. Changing Climate: Report of the Carbon Dioxide Assessment Committee. Washington: National Academies Press, 1983.
6. Hansen JE, Takahashi T (eds). AGU Geophysical Monograph 29 Climate Processes and Climate Sensitivity. Washington: American Geophysical Union, 1984.
7. Hansen J, Lacis A, Rind D et al. Climate sensitivity: analysis of feedback mechanisms. In: Hansen JE, Takahashi T (eds), AGU Geophysical Monograph 29 Climate Processes and Climate Sensitivity. Washington: American Geophysical Union, 1984, 130–63.
8. David EE Jr. Inventing the future: energy and the CO_2 "Greenhouse Effect". In: Hansen JE, Takahashi T (eds). AGU Geophysical Monograph 29 Climate Processes and Climate Sensitivity. Washington: American Geophysical Union, 1984, 1–5.

9. Oreskes N, Conway E. *Merchants of Doubt: How a Handful of Scientists Obscured the Truth on Issues from Tobacco Smoke to Global Warming*. London: Bloomsbury, 2010.
10. Intergovernmental Panel on Climate Change. *History of the IPCC*. <https://www.ipcc.ch/about/history> (date last accessed 7 March 2023).
11. United Nations Framework Convention on Climate Change. *What is the United Nations Framework Convention on Climate Change?* <https://unfccc.int/process-and-meetings/what-is-the-united-nations-framework-convention-on-climate-change> (date last accessed 30 November 2022).
12. IPCC. *Climate Change 2021: The Physical Science Basis*. [Masson-Delmotte V, Zhai P, Pirani A et al. (eds)], Cambridge and New York: Cambridge University Press, 2021.
13. Hansen J, Sato M, Hearty P et al. Ice melt, sea level rise and superstorms: evidence from paleoclimate data, climate modeling, and modern observations that 2 C global warming could be dangerous. *Atmos Chem Phys* 2016; **16**:3761–812.
14. Hansen J. Foreword: uncensored science is crucial for global conservation. In: DellaSala DA (ed), *Conservation Science and Advocacy for a Planet in Peril*. Amsterdam: Elsevier, 2021, 451.
15. Bode HW. *Network Analysis and Feedback Amplifier Design*. New York: Van Nostrand, 1945.
16. Lacis A, Hansen J, Lee P et al. Greenhouse effect of trace gases, 1970–1980. *Geophys Res Lett* 1981; **8**:1035–8.
17. CLIMAP Project Members. Seasonal reconstruction of the Earth's surface at the last glacial maximum. *Geol Soc Amer, Map and Chart Series*, No. 36, Geological Society of America 1981.
18. Manabe S, Stouffer RJ. Sensitivity of a global climate model to an increase of CO₂ concentration in the atmosphere. *J Geophys Res* 1980; **85**:5529–54.
19. Manabe S. Carbon dioxide and climate change. *Adv Geophys* 1983; **25**:39–82.
20. Klein SA, Hall A, Norris JR et al. Low-cloud feedbacks from cloud-controlling factors: a review. *Surv Geophys* 2017; **38**:1307–29.
21. Sherwood SC, Webb MJ, Annan JD et al. An assessment of Earth's climate sensitivity using multiple lines of evidence. *Rev Geophys* 2020; **58**:e2019RG000678.
22. Zelinka MD, Zhou C, Klein SA. Insights from a refined decomposition of cloud feedbacks. *Geophys Res Lett* 2016; **43**:9259–69.
23. Zelinka M, Tan I, Oreopoulos L et al. Detailing cloud property feedbacks with a regime-based decomposition. *Clim Dyn* 2023; **60**:2983–3003.
24. Rind D, Peteet D. Terrestrial conditions at the last glacial maximum and CLIMAP sea-surface temperature estimates: Are they consistent? *Quat Res* 1985; **24**:1–22.
25. Rohling EJ, Marino G, Foster GL et al. Comparing climate sensitivity, past and present. *Ann Rev Mar Sci* 2018; **10**:261–88.
26. IPCC. *Climate Change 2014: Synthesis Report. Contribution of Working Groups I, II and III to the Fifth Assessment Report of the Intergovernmental Panel on Climate Change*. [Core Writing Team, Pachauri RK, Meyer LA (eds)]. Geneva: IPCC, 2014.
27. Andrews T, Gregory JM, Paynter D et al. Accounting for changing temperature patterns increases historical estimates of climate sensitivity. *Geophys Res Lett* 2018; **45**:8490–9.
28. Rugenstein M, Bloch-Johnson J, Abe-Ouchi A et al. LongRunMIP: motivation and design for a large collection of millennial-length AOGCM simulations. *Bull Amer Meteorol Soc* 2019; **100**:2551–70.
29. Myhre G, Shindell D, Bréon F-M et al. Anthropogenic and natural radiative forcing. In: Stocker TF, Qin D, Plattner G-K et al. (eds), *Climate Change 2013: The Physical Science Basis. Contribution of Working Group I to the Fifth Assessment Report of the Intergovernmental Panel on Climate Change*. Cambridge and New York: Cambridge University Press, 2013.
30. Hansen J, Sato M, Ruedy R et al. Efficacy of climate forcings. *J Geophys Res* 2005; **110**:D18104.
31. Lohmann U, Rotstayn L, Storelvmo T et al. Total aerosol effect: radiative forcing or radiative flux perturbation? *Atmos Chem Phys* 2010; **10**:3235–46.
32. Kelley M, Schmidt GA, Nazarenko L et al. GISS-E2.1: configurations and climatology. *J Adv Model Earth Syst* 2020; **12**:e2019MS002025.
33. Miller RL, Schmidt GA, Nazarenko L et al. CMIP6 historical simulations (1850–2014) with GISS-E2.1. *J Adv Model Earth Syst* 2021; **13**:e2019MS002034.
34. Eyring V, Bony S, Meehl GA et al. Overview of the Coupled Model Intercomparison Project Phase 6 (CMIP6) experimental design and organization. *Geosci Model Dev* 2016; **9**:1937–58.
35. Lacis AA, Oinas V. A description of the correlated k distributed method for modeling nongray gaseous absorption, thermal emission, and multiple scattering in vertically inhomogeneous atmospheres. *J Geophys Res* 1991; **96**:9027–63.
36. Rothman L, Rinsland C, Goldman A et al. The HITRAN molecular spectroscopic database and HAWKS (HITRAN Atmospheric Workstation) 1996 edition. *J Quant Spec Rad Trans* 1998; **60**:665–710.
37. Prather M, Ehhalt D. Chapter 4: Atmospheric chemistry and greenhouse gases. In: Houghton JT (ed), *Climate Change 2001: The Scientific Basis*. New York: Cambridge University, 2001, 239–87.
38. Hansen J, Sato M. Greenhouse gas growth rates. *Proc Natl Acad Sci USA* 2004; **101**:16109–14.
39. Columbia University. MPTG and OTG data: www.columbia.edu/~mhs119/GHGs/TG_F.1900-1990.txt and http://www.columbia.edu/~mhs119/GHGs/TG_F.1992-2021.txt (date last accessed 9 August 2023).
40. Jouzel J, Masson-Delmotte V, Cattani O et al. Orbital and millennial Antarctic climate variability over the past 800,000 years. *Science* 2007; **317**:793–6.
41. Lüthi D, Le Floch M, Bereiter B et al. High-resolution carbon dioxide concentration record 650,000–800,000 years before present. *Nature* 2008; **453**:379–82.
42. Hays JD, Imbrie J, Shackleton NJ. Variation in the Earth's orbit: pacemaker of the ice ages. *Science* 1976; **194**:1121–32.
43. Lorius C, Jouzel J, Raynaud D et al. The ice-core record: climate sensitivity and future greenhouse warming. *Nature* 1990; **347**:139–45.
44. Zachos J, Pagani M, Sloan L et al. Trends, rhythms, and aberrations in global climate 65 Ma to present. *Science* 2001; **292**:686–93.
45. Hansen J, Sato M, Kharecha P et al. Climate change and trace gases. *Philos Trans A Math Phys Eng Sci* 2007; **365**:1925–54.
46. Ruddiman WF, Fuller DQ, Kutzbach JE et al. Late Holocene climate: natural or anthropogenic? *Rev Geophys* 2016; **54**:93–118.
47. Schilt A, Baumgartner M, Schwander J et al. Atmospheric nitrous oxide during the last 140,000 years. *Earth Planet Sci Lett* 2010; **300**:33–43.
48. Hansen J, Nazarenko L, Ruedy R et al. Earth's energy imbalance: Confirmation and implications. *Science* 2005; **308**:1431–5.
49. Tierney JE, Zhu J, King J et al. Glacial cooling and climate sensitivity revisited. *Nature* 2020; **584**:569–73.

50. Osman MB, Tierney JE, Zhu J et al. Globally resolved surface temperatures since the Last Glacial Maximum. *Nature* 2021; **599**:239–44.
51. Seltzer AM, Ng J, Aeschbach W et al. Widespread six degrees Celsius cooling on land during the Last Glacial Maximum. *Nature* 2021; **593**:228–32.
52. Schneider T, Teixeira J, Bretherton CS et al. Climate goals and computing the future of clouds. *Nature Clim Change* 2017; **7**:3–5.
53. Pincus R, Forster PM, Stevens B. The radiative forcing model intercomparison project (RFMIP): experimental protocol for CMIP6. *Geosci Model Dev* 2016; **9**:3447–60.
54. Kageyama M, Braconnot P, Harrison SP et al. The PMIP4 contribution to CMIP6 – Part 1: overview and over-arching analysis plan. *Geosci Model Dev* 2018; **11**:1033–57.
55. Hegerl GC, Zwiers FW, Braconnot P et al. Chapter 9: Understanding and attributing climate change. In: Solomon SD (ed), *Climate Change 2007: The Physical Science Basis*. New York: Cambridge University, 2007, 663–745
56. Yoshimori M, Yokohata T, Abe-Ouchi A. A comparison of climate feedback strength between CO₂ doubling and LGM experiments. *J Clim* 2009; **22**:3374–95.
57. Stap LB, Kohler P, Lohmann G. Including the efficacy of land ice changes in deriving climate sensitivity from paleodata. *Earth Syst Dynam* 2019; **10**:333–45.
58. Koppen W. Das geographische system der climate. In: Koppen W, Geiger G (eds), *Handbuch Der Klimatologie* 1(C). Berlin: Boentraeger, 1936.
59. Kohler P, Bintanja R, Fischer H et al. What caused Earth's temperature variations during the last 800,000 years? Data-based evidence on radiative forcing and constraints on climate sensitivity. *Quat Sci Rev* 2010; **29**:129–45.
60. Hansen J, Sato M, Kharecha P et al. Target atmospheric CO₂: where should humanity aim? *Open Atmos Sci J* 2008; **2**:217–31.
61. Rabineau M, Berné S, Olivet J-L et al. Paleo sea levels reconsidered from direct observation of paleoshoreline position during Glacial Maxima (for the last 500,000 yr). *Earth Planet Sci Lett* 2006; **252**:119–37.
62. Rohling EJ, Hibbert FD, Williams FH et al. Differences between the last two glacial maxima and implications for ice-sheet, δ₁₈O, and sea-level reconstructions. *Quat Sci Rev* 2017; **176**:1–28.
63. Hansen J, Sato M, Kharecha P et al. Young people's burden: requirement of negative CO₂ emissions. *Earth Syst Dynam* 2017; **8**:577–616.
64. Hoffman JS, Clark PU, Parnell AC et al. Regional and global sea-surface temperatures during the last interglaciation. *Science* 2017; **355**:276–9.
65. Ruth U, Barnola JM, Beer J et al. EDML1: a chronology for the EPICA deep ice core from Dronning Maud Land, Antarctica, over the last 150 000 years. *Clim Past* 2007; **3**:475–84.
66. Hansen J, Sato M, Russell G et al. Climate sensitivity, sea level, and atmospheric carbon dioxide. *Philos Trans A Math Phys Eng Sci* 2013; **371**:20120294.
67. Russell GL, Miller JR, Rind D. A coupled atmosphere-ocean model for transient climate change studies. *Atmos Ocean* 1995; **33**:683–730.
68. Hoffman PF, Schrag DP. The snowball Earth hypothesis: testing the limits of global change. *Terra Nova* 2002; **14**:129–55.
69. Sackmann J, Boothroyd AI, Kraemer KE. Our Sun. III. Present and future. *Astrophys J* 1993; **418**:457–68.
70. Meraner K, Mauritsen T, Voigt A. Robust increase in equilibrium climate sensitivity under global warming. *Geophys Res Lett* 2013; **40**:5944–8.
71. Lunt DJ, Haywood AM, Schmidt GA et al. Earth system sensitivity inferred from Pliocene modelling and data. *Nature Geosci* 2010; **3**:60–4.
72. Beerling DJ, Fox A, Stevenson DS et al. Enhanced chemistry-climate feedbacks in past greenhouse worlds. *Proc Natl Acad Sci U S A* 2011; **108**:9770–5.
73. Bryan K, Komro FG, Manabe S et al. Transient climate response to increasing atmospheric carbon dioxide. *Science* 1982; **215**:56–8.
74. Hansen J, Russell G, Lacis A et al. Climate response times: dependence on climate sensitivity and ocean mixing. *Science* 1985; **229**:857–9.
75. Hansen J. *Climate Threat to the Planet*, American Geophysical Union, San Francisco, California, 17 December 2008. <http://www.columbia.edu/~jeh1/2008/AGUBjerknes20081217.pdf>. (date last accessed 3 December 2022).
76. Good P, Gregory JM, Lowe JA. A step-response simple climate model to reconstruct and interpret AOGCM projections. *Geophys Res Lett* 2011; **38**:e2010GL0452008.
77. Schmidt GA, Kelley M, Nazarenko L et al. Configuration and assessment of the GISS ModelE2 contributions to the CMIP5 archive. *J Adv Model Earth Syst* 2014; **6**:141–84.
78. Prather MJ. Numerical advection by conservation of second order moments. *J Geophys Res* 1986; **91**:6671–81.
79. Romanou A, Marshall J, Kelley M et al. Role of the ocean's AMOC in setting the uptake efficiency of transient tracers. *Geophys Res Lett* 2017; **44**:5590–8.
80. von Schuckmann K, Cheng L, Palmer MD et al. Heat stored in the Earth system: where does the energy go? *Earth Syst Sci Data* 2020; **12**:2013–41.
81. Loeb NG, Johnson GC, Thorsen TJ et al. Satellite and ocean data reveal marked increase in Earth's heating rate. *Geophys Res Lett* 2021; **48**:e2021GL093047.
82. Hansen J, Johnson D, Lacis A et al. Climate impact of increasing atmospheric carbon dioxide. *Science* 1981; **213**:957–66.
83. Kamae Y, Watanabe M, Ogura T et al. Rapid adjustments of cloud and hydrological cycle to increasing CO₂: a review. *Curr Clim Change Rep* 2015; **1**:103–13.
84. Zelinka MD, Myers TA, McCoy DT et al. Causes of higher climate sensitivity in CMIP6 models. *Geophys Res Lett* 2020; **47**: e2019GL085782.
85. Crowley TJ. Pliocene climates: the nature of the problem. *Marine Micropaleontol* 1996; **27**:3–12.
86. DeConto RM, Pollard D. Rapid Cenozoic glaciation of Antarctica induced by declining atmospheric CO₂. *Nature* 2003; **421**:245–9.
87. Lacis AA, Schmidt GA, Rind D et al. Atmospheric CO₂: principal control knob governing Earth's temperature. *Science* 2010; **330**:356–9.
88. Rae JWB, Zhang YG, Liu X et al. Atmospheric CO₂ over the past 66 million years from marine archives. *Annu Rev Earth Planet Sci* 2021; **49**:609–41.
89. Steinhorsdottir M, Vajda V, Pole M et al. Moderate levels of Eocene pCO₂ indicated by Southern Hemisphere fossil plant stomata. *Geology* 2019; **47**:914–8.
90. Westerhold T, Marwan N, Drury AJ et al. An astronomically dated record of Earth's climate and its predictability over the last 66 million years. *Science* 2020; **369**:1383–7.
91. Yatheesh V, Dyment J, Bhattacharya GC et al. Detailed structure and plate reconstructions of the central Indian Ocean between 83.0 and 42.5 Ma (chrons 34 and 20). *J Geophys Res: Solid Earth* 2019; **124**:4305–22.

92. Cutler KB, Edwards RL, Taylor FW et al. Rapid sea-level fall and deep-ocean temperature change since the last interglacial period. *Earth Planet Sci Lett* 2003; **206**:253–71.
93. Siddall M, Honisch B, Waelbroeck C et al. Changes in deep Pacific temperature during the mid-Pleistocene transition and Quaternary. *Quatern Sci Rev* 2010; **29**:170–81.
94. Rohling EJ, Grant K, Bolshaw M et al. Antarctic temperature and global sea level closely coupled over the past five glacial cycles. *Nature Geosci* 2009; **2**:500–4.
95. Seltzer AM, Blard P-H, Sherwood SC et al. Terrestrial amplification of past, present, and future climate change. *Sci Adv* 2023; **9**:eadf8119.
96. Zhu J, Poulsen CJ, Tierney JE. Simulation of Eocene extreme warmth and high climate sensitivity through cloud feedbacks. *Sci Adv* 2019; **5**:eaax1874.
97. Scotese C. PALEOMAP PaleoAtlas for GPlates, 2016. <https://www.earthbyte.org/paleomap-paleoatlas-for-gplates/> (March 2023, date last accessed).
98. Hansen J. *Storms of My Grandchildren*. New York: Bloomsbury, 2009.
99. Berner RA. *The Phanerozoic Carbon Cycle: CO₂ and O₂*. New York: Oxford University Press, 2004.
100. Rohling EJ. *The Climate Question: natural Cycles, Human Impact, Future Outlook*. New York: Oxford University Press, 2019.
101. Merdith AS, Williams SE, Brune S et al. Rift and plate boundary evolution across two supercontinent cycles. *Global Plan Chan* 2019; **173**:1–14.
102. Peace AL, Phethean JJJ, Franke D et al. A review of Pangea dispersal and large igneous provinces – in search of a causative mechanism. *Earth-Science Rev* 2020; **206**:102902.
103. Baksi AK. Comment on “40Ar/39Ar dating of the Rajahmundry Traps, eastern India and their relationship to the Deccan Traps” by Knight et al. [Earth Planet Sci. Lett. 208 (2003) 85–99]. *Earth Planet Sci Lett* 2005; **239**:368–73.
104. Guo Z, Wilson M, Dingwell D et al. India-Asia collision as a driver of atmospheric CO₂ in the Cenozoic. *Nature Comm* 2021; **12**:3891.
105. Raymo ME, Ruddiman WF. Tectonic forcing of late Cenozoic climate. *Nature* 1992; **359**:117–22.
106. Ramos EJ, Lackey JS, Barnes JD et al. Remnants and rates of metamorphic decarbonation in continental arcs. *Gsat* 2020; **30**:4–10.
107. Bufo A, Hovius N, Emberson R et al. Co-variation of silicate, carbonate and sulfide weathering drives CO₂ release with erosion. *Nat Geosci* 2021; **14**:211–6.
108. Lee CTA, Shen B, Slotnick BS et al. Continental arc-island arc fluctuations, growth of crustal carbonates, and long-term climate change. *Geosphere* 2013; **9**:21–36.
109. McKenzie NR, Horton BK, Loomis SE et al. Continental arc volcanism as the principal driver of icehouse-greenhouse variability. *Science* 2016; **352**:444–7.
110. Petersen KD, Schiffer C, Nagel T. LIP formation and protracted lower mantle upwelling induced by rifting and delamination. *Scientific Rep* 2018; **8**:16578.
111. Eldholm E, Grue K. North Atlantic volcanic margins: dimensions and production rates. *J Geophys Res* 1994; **99**:2955–68.
112. Ji S, Nie J, Lechner A et al. A symmetrical CO₂ peak and asymmetrical climate change during the middle Miocene. *Earth Plan Sci Lett* 2018; **499**:134–44.
113. Babila TL, Foster GL. The Monterey Event and the Paleocene-Eocene Thermal Maximum: two contrasting oceanic carbonate system responses to LIP emplacement and eruption. In: Dickson A, Bekker A (eds), AGU Geographical Monograph 255, Washington: American Geophysical Union, 2021, 403–416.
114. Storey M, Duncan RA, Tegner C. Timing and duration of volcanism in the North Atlantic Igneous Province: implications for geodynamics and links to the Iceland hotspot. *Chem Geol* 2007; **241**:264–81.
115. Svensen H, Planke S, Malthe-Sorensen A et al. Release of methane from a volcanic basin as a mechanism for initial Eocene global warming. *Nature* 2004; **429**:542–5.
116. Gutjahr M, Ridgwell A, Sexton PF et al. Very large release of mostly volcanic carbon during the Palaeocene Thermal Maximum. *Nature* 2017; **548**:573–7.
117. Frielings J, Peterse F, Lunt DJ et al. Widespread warming before and elevated barium burial during the Paleocene-Eocene thermal maximum: evidence for methane hydrate release? *Paleoceanogr Paleoclimatol* 2019; **34**:546–66.
118. Berndt C, Planke S, Alvarez Zarikian CA et al. Shallow-water hydrothermal venting linked to the Palaeocene-Eocene Thermal Maximum. *Nature Geosci* 2023; **16**:803–9.
119. Walker JCG, Hays PB, Kasting JF. A negative feedback mechanism for the long-term stabilization of Earth’s surface temperature. *J Geophys Res* 1981; **86**:9776–82.
120. Steinberger B, Spakman W, Japsen P et al. The key role of global solid-Earth processes in preconditioning Greenland’s glaciation since the Pliocene. *Terra Nova* 2015; **27**:1–8.
121. Foster GL, Hull P, Lunt DJ et al. Placing our current ‘hyperthermal’ in the context of rapid climate change in our geological past. *Phil Trans Roy Soc A* 2018; **376**:200170086.
122. Tierney JE, Zhu J, Li M. Spatial patterns of climate change across the Paleocene-Eocene thermal maximum. *Proc Natl Acad Sci* 2022; **119**:e2205326119.
123. Hopcroft PO, Ramstein G, Pugh TAM et al. Polar amplification of Pliocene climate by elevated trace gas radiative forcing. *Proc Natl Acad Sci U S A* 2020; **117**:23401–7.
124. Schaller MF, Fung MK. The extraterrestrial impact evidence at the Palaeocene-Eocene boundary and sequence of environmental change on the continental shelf. *Phil Trans R Soc A* 2018; **376**:20170081.
125. Turner SK. Constraints on the onset duration of the Paleocene-Eocene Thermal Maximum. *Phil Trans R Soc A* 2018; **376**:20170082.
126. Zachos JC, McCarren H, Murphy B et al. Tempo and scale of late Paleocene and early Eocene carbon isotope cycles: implications for the origin of hyperthermals. *Earth Plan Sci Lett* 2010; **299**:242–9.
127. Nichols JE, Peteet DM. Rapid expansion of northern peatlands and doubled estimate of carbon storage. *Nat Geosci* 2019; **12**:917–21.
128. Hanson PJ, Griffiths NA, Iverson CM et al. Rapid net carbon loss from a whole-ecosystem warmed peatland. *AGU Advan* 2020; **1**:e2020AV000163.
129. Bowen GJ, Maibauer BJ, Kraus MJ et al. Two massive, rapid releases of carbon during the onset of the Palaeocene-Eocene thermal maximum. *Nature Geosci* 2015; **8**:44–7.
130. Archer D, Buffett B, Brovkin V. Ocean methane hydrates as a slow tipping point in the global carbon cycle. *Proc Natl Acad Sci U S A* 2009; **106**:20596–601.
131. Archer D, Eby M, Brovkin V et al. Atmospheric lifetime of fossil fuel carbon dioxide. *Annu Rev Earth Planet Sci* 2009; **37**:117–34.
132. Nunes F, Norris RD. Abrupt reversal in ocean overturning during the Palaeocene/Eocene warm period. *Nature* 2006; **439**:60–3.
133. World Health Organization. *Ambient (Outdoor) Air Pollution*. [https://www.who.int/en/news-room/fact-sheets/detail/ambient-\(outdoor\)-air-quality-and-health](https://www.who.int/en/news-room/fact-sheets/detail/ambient-(outdoor)-air-quality-and-health) (date last accessed 23 June 2022).

134. Vohra K, Vodonos A, Schwartz J et al. Global mortality from outdoor fine particle pollution generated by fossil fuel combustion: results from GEOS-Chem. *Environ Res* 2021; **195**:110754.
135. Marcott SA, Shakun JD, Clark PU et al. A reconstruction of regional and global temperature for the last 11,300. *Science* 2013; **339**:1198–201.
136. Tardif R, Hakim GJ, Perkins WA et al. Last Millennium Reanalysis with an expanded proxy database and seasonal proxy modeling. *Clim Past* 2019; **15**:1251–73.
137. Watson AJ, Garabato ACN. The role of Southern Ocean mixing and upwelling in glacial-interglacial atmospheric CO₂ change. *Tellus* 2006; **58**:73–87.
138. Wikipedia. File:Post-Glacial Sea Level.png. https://commons.wikimedia.org/wiki/File:Post-Glacial_Sea_Level.png (date last accessed 3 December 2022).
139. Barber B. Resistance by scientists to scientific discovery. *Science* 1961; **134**:596–602.
140. Hoffman PF, Kaufman AJ, Halverson GP et al. A Neoproterozoic Snowball Earth. *Science* 1998; **281**:1342–6.
141. Alvarez L, Alvarez W, Asaro F et al. Extraterrestrial Cause for the Cretaceous-Tertiary Extinction. *Science* 1980; **208**:1095–108.
142. Mishchenko MI, Cairns B, Kopp G et al. Accurate monitoring of terrestrial aerosols and total solar irradiance: Introducing the Glory mission. *Bull Amer Meteorol Soc* 2007; **88**:677–92.
143. Hansen J, Rossow W, Fung I. *Long-Term Monitoring of Global Climate Forcings and Feedbacks*. Washington: NASA Conference Publication 3234, 1993.
144. Bellouin N, Quaas J, Gryspeert E et al. Bounding global aerosol radiative forcing of climate change. *Rev Geophys* 2020; **58**:e2019RG000660.
145. Kruzman D. Wood-burning stoves raise new health concerns. *Undark Magazine* 2022, 2 March (6 February 2023, date last accessed).
146. Glojek K, Mocnik G, Alas HDC et al. The impact of temperature inversions on black carbon and particle mass concentrations in a mountainous area. *Atmos Chem Phys* 2022; **22**:5577–601.
147. Rutgard O. *Why is Britain Taking the Axe to Wood-Burning Stoves?* Bloomberg Green, 4 February 2023.
148. Day JW, Gunn JD, Folan WJ et al. Emergence of complex societies after sea level stabilized. *EOS Transactions* 2007; **88**:169–70.
149. VanCuren RA. Asian aerosols in North America: extracting the chemical composition and mass concentration of the Asian continental aerosol plume from long-term aerosol records in the western United States. *J Geophys Res Atmos* 2003; **108**:D20, 4623.
150. Knutti R. Why are climate models reproducing the observed global surface warming so well? *Geophys Res Lett* 2008; **35**:L18704.
151. Hansen J, Sato M, Kharecha P et al. Earth's energy imbalance and implications. *Atmos Chem Phys* 2011; **11**:13421–49.
152. Koch D, Bauer SE, Del Genio A et al. Coupled aerosol-chemistry-climate twentieth-century model investigation: trends in short-lived species and climate responses. *J Clim* 2011; **24**:2693–714.
153. Novakov T, Ramanathan V, Hansen JE et al. Large historical changes of fossil-fuel black carbon aerosols. *Geophys Res Lett* 2003; **30**:1324.
154. Bauer SE, Tsigaridis K, Faluvegi G et al. Historical (1850–2014) aerosol evolution and role on climate forcing using the GISS ModelE2.1 contribution to CMIP6. *J Adv Model Earth Syst* 2020; **12**:e2019MS001978.
155. Hansen J, Ruedy R, Sato M et al. Global surface temperature change. *Rev Geophys* 2010; **48**:RG4004.
156. Lenssen NJL, Schmidt GA, Hansen JE et al. Improvements in the GISTEMP uncertainty model. *JGR Atmospheres* 2019; **124**:6307–26.
157. Jin Q, Grandey BS, Rothenberg D et al. Impacts on cloud radiative effects induced by coexisting aerosols converted from international shipping and maritime DMS emissions. *Atmos Chem Phys* 2018; **18**:16793–808.
158. Hansen J, Rossow W, Carlson B et al. Low-cost long-term monitoring of global climate forcings and feedbacks. *Clim Chan* 1995; **31**:247–71.
159. Glassmeier F, Hoffmann F, Johnson JS et al. Aerosol-cloud-climate cooling overestimated by ship-track data. *Science* 2021; **371**:485–9.
160. Manshausen P, Watson-Parris D, Christensen MW et al. Invisible ship tracks show large cloud sensitivity to aerosol. *Nature* 2022; **610**:101–6.
161. Wall CJ, Norris JR, Possner A et al. Assessing effective radiative forcing from aerosol-cloud interactions over the global ocean. *Proc Natl Acad Sci U S A* 2022; **119**:e2210481119.
162. Forster P, Storelvmo T, Armour K et al. The Earth's energy budget, climate feedbacks, and climate sensitivity. In: Masson-Delmotte V (ed), *Climate Change 2021: The Physical Science Basis*. New York, Cambridge: Cambridge University Press, 2021, 923–1054.
163. International Maritime Organization (IMO). MEPC.176(58). Amendments to the annex of the protocol of 1997 to amend the international convention for the prevention of pollution from ships, 1973, as modified by the protocol of 1978 relating thereto (Revised MARPOL, Annex VI), 2008. [https://wwwcdn.imo.org/localresources/en/OurWork/Environment/Documents/176\(58\).pdf](https://wwwcdn.imo.org/localresources/en/OurWork/Environment/Documents/176(58).pdf) (February 2013, date last accessed).
164. Gryspeert E, Smith TWP, O'Keeffe E et al. The impact of ship emission controls recorded by cloud properties. *Geophys Res Lett* 2019; **46**:547–55.
165. International Maritime Organization. IMO 2020—Cutting Sulphur Oxide Emissions, Lowers Limit on Sulfur Content of Marine Fuels from 3.5% to 0.5%. <https://www.imo.org/en/MediaCentre/HotTopics/Pages/Sulphur-2020.aspx> (date last accessed 5 December 2022).
166. Yuan T, Song H, Wood R et al. Global reduction in ship-tracks from sulfur regulations for shipping fuel. *Sci Adv* 2022; **8**:eabn7988.
167. Columbia University. Data sources, graphs. <http://www.columbia.edu/~mhs119/Solar/> (date last accessed 23 October 2022).
168. Loeb NG, Thorsen TJ, Rose FG et al. Recent variations in EEI, SST & clouds. ERB Workshop, Hamburg, Germany, 12–14 October, 2022 (date last accessed 3 December 2022).
169. Sato M. Sea ice area. Columbia University webpage (date last accessed 5 November 2022).
170. McCoy DT, Burrows SM, Wood R et al. Natural aerosols explain seasonal and spatial patterns of Southern Ocean cloud albedo. *Sci Adv* 2015; **1**:e1500157.
171. Dunne JP, Winton M, Bacmeister J et al. Comparison of equilibrium climate sensitivity estimates from slab ocean, 150-year, and longer simulations. *Geo Res Lett* 2020; **47**:e2020GL088852.
172. Forster PM, Maycock AC, McKenna CM et al. Latest climate models confirm need for urgent mitigation. *Nat Clim Chang* 2020; **10**:7–10.
173. Liu Z, Zhu J, Rosenthal Y et al. The Holocene temperature conundrum. *Proc Natl Acad Sci U S A* 2014; **111**:E3501–E3505.
174. Quaas J, Jia H, Smith C et al. Robust evidence for reversal of the trend in aerosol effective climate forcing. *Atmos Chem Phys* 2022; **22**:12221–39.
175. Bauer SE, Tsigaridis K, Faluvegi G et al. The turning point of the aerosol era. *J Adv Mod Earth Syst* 2022; **14**:e2022MS003070.

176. Diamond MS. Detection of large-scale cloud microphysical changes and evidence for decreasing cloud brightness within a major shipping corridor after implementation of the International Maritime Organization 2020 fuel sulfur regulations. *Atmos Chem Phys* 2023; **23**:8259–69.
177. Hefner M, Marland G, Boden T et al. Global, Regional, and National Fossil-Fuel CO₂ Emissions. Research Institute for Environment, Energy, and Economics, Appalachian State University, Boone, NC, USA. <https://energy.appstate.edu/cdiac-appstate/data-products> (date last accessed 20 August 2023).
178. Energy Institute. 2023 Statistical Review of World Energy (date last accessed 20 August 2023).
179. Hansen J, Sato M, Ruedy R et al. Global warming in the twenty-first century: an alternative scenario. *Proc Natl Acad Sci U S A* 2000; **97**:9875–80.
180. Hansen JE (ed.). Air Pollution as a Climate Forcing: A Workshop. NASA Goddard Institute for Space Studies, 2002.
181. Feynman RP. Surely You're Joking, Mr. Feynman!. New York: WW Norton, 1985.
182. Hariri AR, Brown SM, Williamson DE et al. Preference for immediate over delayed rewards is associated with magnitude of ventral striatal activity. *J Neurosci* 2006; **26**:13213–7.
183. Hansen JE. Scientific reticence and sea level rise. *Environ Res Lett* 2007; **2**:024002. er1246875
184. Hansen JE. A slippery slope: how much global warming constitutes “dangerous anthropogenic interference?”. *Clim Change* 2005; **68**:269–79.
185. Braithwaite RJ. Cover photo for Science 2002;297(5579). Reprinted in Hansen, J. Defusing the global warming time bomb. *Sci Amer* 2004; **290**:68–77.
186. Rignot E, Jacobs S, Mouginot J et al. Ice shelf melting around Antarctica. *Science* 2013; **341**:266–70.
187. Rye CD, Naveira Garabato AC, Holland PR et al. Rapid sea-level rise along the Antarctic margins in response to increased glacial discharge. *Nature Geosci* 2014; **7**:732–5.
188. Hansen J, Sato M, Hearty P et al. Ice Melt, Sea Level Rise and Superstorms: Evidence from Paleoclimate Data, Climate Modeling, and Modern Observations that 2 C Global Warming is Highly Dangerous. *Atmospheric Chemistry and Physics Discussions*. 2015.
189. Bakker P, Schmittner A, Lenaerts JTM et al. Fate of the Atlantic Meridional Overturning Circulation: strong decline under continued warming and Greenland melting. *Geophys Res Lett* 2016; **43**:12252–60.
190. Ivali N, Ninnemann US, Galaasen EV et al. Rapid switches in subpolar hydrography and climate during the Last Interglacial (MIS 5e). *Paleoceanography* 2012; **27**:PA2207.
191. Blanckon P, Eisenhauer A, Fietzke J et al. Rapid sea-level rise and reef back-stepping at the close of the last interglacial high-stand. *Nature* 2009; **458**:881–4.
192. Rye C, Marshall J, Kelley M et al. Antarctic glacial melt as a driver of recent Southern Ocean climate trends. *Geophys Res Lett* 2020; **47**:e2019GL086892.
193. Silvano A, Rintoul SR, Pena-Molino B et al. Freshening by glacial meltwater enhances melting of ice shelves and reduces formation of Antarctic bottom water. *Sci Adv* 2018; **4**:eaap9467.
194. Gunn KL, Rintoul SR, England MH et al. Recent reduced abyssal overturning and ventilation in the Australian Antarctic Basin. *Nat Clim Chang* 2023; **13**:537–44.
195. Ditlevsen P, Ditlevsen S. Warning of a forthcoming collapse of the Atlantic meridional overturning circulation. *Nature Comm* 2023; **14**:4254.
196. Rignot E, Mouginot J, Scheuchl B et al. Four decades of Antarctic ice shelf mass balance from 1979–2017. *Proc Natl Acad Sci U S A* 2018; **115**:1096–103.
197. Otosaka IN, Shepherd A, Ivins ER et al. Mass balance of the Greenland and Antarctic ice sheets from 1992 to 2020. *Earth Syst Sci Data* 2023; **15**:1597–616.
198. Hansen J, Sato M, Ruedy R et al. Dangerous human-made interference with climate: A GISS modelE study. *Atmos Chem Phys* 2007; **7**:2287–312.
199. Matthews HD, Gillett NP, Stott PA et al. The proportionality of global warming to cumulative carbon emissions. *Nature* 2009; **459**:829–32.
200. Hansen J, Sato M. Regional Climate Change and National Responsibilities. *Environ Res Lett* 2016; **11**:034009.
201. Paris Agreement 2015. UNFCCC Secretariat, 2015. https://www.google.com/aclk?sa=l&ai=DChcSEwjrqqAfk2BAxUz2EwCHfzPDPcYABABGj0bQ&gclid=Cj0KCQjw4bipBhCyARIsAFsieCzU7epQQG4ouyspwn7TPYa7IWh2W0OqZJVXr0qbGhLzshwOnCk1YEkaAvzLEALw_wcB&sig=AOD64_3vxA5GjlCwgEGMqI4OhPzk0EBbbQ&q&adurl&ved=2ahUKEwj_a_52Akf2BAxVWsFYBHcL6CYcQ0Qx6BAgJEA (date last accessed 20 August 2023).
202. Keith DW, Holmes G, Angelo D et al. A process for capturing CO₂ from the atmosphere. *Joule* 2018; **2**:1573–94.
203. Hansen J, Kharecha P. Cost of carbon capture: can young people bear the burden? *Joule* 2018; **2**:1405–7.
204. Hardin G. The tragedy of the commons. *Science* 1968; **162**:1243–8.
205. Prins G, Rayner S. Time to ditch Kyoto. *Nature* 2007; **449**:973–5.
206. Creutzig F, Erb KH, Haberl H et al. Considering sustainability thresholds for BECCS in IPCC and biodiversity assessments. *GCB Bioenergy* 2021; **13**:510–5.
207. Economists' Statement on Carbon Dividends. <https://www.historicismade.org/> (date last accessed 28 November 2022).
208. Hansen J. Can Young People Save Democracy and the Planet? https://www.columbia.edu/~jeh1/mailings/2021/20211008_YoungPeople.2021.pdf (date last accessed 28 November 2022)
209. Hayes RB. Nuclear energy myths versus facts support it's expanded use – a review. *Cleaner Ener Sys* 2022; **2**:100009.
210. Cao J, Cohen A, Hansen J et al. China-U.S. cooperation to advance nuclear power. *Science* 2016; **353**:547–8.
211. Ying F. Cooperative competition is possible between China and the U.S. *New York Times*, 24 November.
212. National Academies of Sciences, Engineering, and Medicine. Reflecting Sunlight: Recommendations for Solar Geoengineering Research and Research Governance. <https://doi.org/10.17226/25762> (date last accessed 4 December 2022).
213. Robock A. Volcanic eruptions and climate. *Rev Geophys* 2000; **38**:191–219.
214. Hansen J, Sato M, Ruedy R et al. A Pinatubo climate Modeling investigation. *NATO ASI* 1996; **142**:234–72.
215. Tollefson J. Can artificially altered clouds save the Great Barrier Reef? *Nature* 2021; **596**:476–8.
216. Latham J, Rasch P, Chen CC et al. Global temperature stabilization via controlled albedo enhancement of low-level maritime clouds. *Philos Trans A Math Phys Eng Sci* 2008; **366**:3969–87.
217. Patrick SM. Reflecting sunlight to reduce climate risk: priorities for research and international cooperation. *Council on Foreign Relations*. Special Report No. 93, April 2022 (date last accessed 4 December 2022).
218. Lovins AB. Reinventing Fire. White River Junction, Vermont: Chelsea Green Publishing, 334 p.